Microbial degradation and transformation of the antibiotic sulfamethoxazole under aerobic and anaerobic conditions

vorgelegt von
M. Sc.
Wei-Ying Ouyang

an der Fakultät III – Prozesswissenschaften
der Technischen Universität Berlin
zur Erlangung des akademischen Grades

Doktor der Naturwissenschaften
Dr. rer. nat.

genehmigte Dissertation

Promotionsausschuss:
Vorsitzender: Prof. Dr. Juri Rappsilber
Gutachter: Prof. Dr. Lorenz Adrian
Gutachter: Prof. Dr. Peter Neubauer
Gutachter: PD Dr. Hans-Hermann Richnow

Tag der wissenschaftlichen Aussprache: 04. Juni 2021

Berlin 2021

Declaration

Wei-Ying Ouyang

Declaration for the dissertation with the title:

“Microbial degradation and transformation of the antibiotic sulfamethoxazole under aerobic and anaerobic conditions”

This research was performed at the Helmholtz Centre for Environmental Research-UFZ, Leipzig, Germany between November, 2015 and December, 2019 under the supervision of Prof. Dr. Lorenz Adrian and PD Dr. Hans-Hermann Richnow. I herewith declare that the results of this dissertation were my own research and I also certify that all sentences were written by myself.

Signature _____ Date _____

Acknowledgement

This research work was conducted from November, 2015 to December, 2019 in the research group of Prof. Dr. Lorenz Adrian at the Department of Isotope Biogeochemistry, Helmholtz Centre for Environmental Research Leipzig (UFZ). The research project was funded by the Chinese Scholarship Council, and was also supported by Institute of Urban Environment, Chinese Academy of Sciences.

I would like to express my sincere gratitude to Prof. Dr. Lorenz Adrian for providing me the opportunity to work in his fantastic research group and explore the interesting microbial world. Also many thanks to him for the supervision of my dissertation, productive discussion, constant support and sharing his knowledge. His passion for science and life inspired me in the past years, leading me to be independent and self-confident.

PD Dr. Hans-Hermann Richnow I thank for his supervision in isotope analysis and review of my dissertation. Thanks to Prof. Dr. Peter Neubauer for the review of my dissertation and Prof. Dr. Juri Rappsilber to be the chairperson of the dissertation committee.

I want to thank my colleagues Dr. Rohit Budhraja, Dr. Chang Ding and Dr. Katja Seidel for the working time we spent together, sharing beauty of science and life. Thank Dr. Camelia Algora, Dr. Alba Trueba-Santiso, Dr. Clara Reino-Sanchez and other group members for their creative discussion during the relaxing lunch time. Thanks to Benjamin Scheer together with Danny Frauenstein and Felicitas Ehme for their technical support in the lab work, and organization of many unforgettable group activities. I thank my students Jimmy Köpke, Susiddharthak Chakraborty and Joana Kühnert for their productive work and interesting feedback on my supervision.

Thanks to my collaborators Jan Birkigt and Dr. Steffen Kümmel for their help on method development and data interpretation. I also thank all members in the department of isotope biogeochemistry for their support and advices.

In the end, I would like to thank my parents, Jixing and friends in China for their love and encouragement, making me brave in the past and in the future.

Abstract

Antibiotics discharged in the environment raise concerns in public health and ecological functions. The broad occurrence of antibiotic residues contributes to the development and propagation of antibiotic resistance genes, causing a significant reduction of antibiotics available for treatments of infectious disease. Sulfamethoxazole (SMX) is one of the most frequently detected antibiotics in the environment, especially enriched in manure, sludge, and farm-impacted soil. Microbial degradation is the major sink of SMX in both natural and engineered systems. Aerobic SMX-degraders have been enriched and isolated, whereas identification of in-situ degrading populations is still challenging. Besides, field studies revealed the contribution of anaerobic processes to SMX mitigation, while knowledge about the anaerobic SMX-transforming bacteria is limited and no pure strain was described until now. In addition, a robust assessment method is needed to evaluate attenuation of SMX in complex matrices. In this study, we aimed to identify in-situ aerobic SMX-degraders, characterize anaerobic SMX-transforming cultures, and develop assessment techniques to evaluate removal of SMX in the environment.

We investigated aerobic SMX-degrading bacteria in soil microcosms by culture-independent DNA and protein stable isotope probing (SIP). 0.5% of the carbon from $^{13}C_6$-labeled SMX amended to soil microcosms was transformed to $^{13}CO_2$ demonstrating partial mineralization of the antibiotic. DNA-SIP revealed incorporation of ^{13}C from $^{13}C_6$-labeled SMX into *Actinobacteria* and among them into the families *Intrasporangiaceae, Nocardioidaceae*, and *Gaiellaceae* and the order *Solirubrobacterales.* Protein-SIP demonstrated that the incorporation of ^{13}C from $^{13}C_6$-labeled SMX into proteins of bacteria of the families *Intrasporangiaceae*, *Nocardioidaceae,* and the order *Solirubrobacterales*, which was consistent with the results of DNA-SIP. The ^{13}C abundance of 60 to 80% in several taxonomically relevant proteins indicated that *Intrasporangiaceae* directly acquired carbon from $^{13}C_6$-labeled SMX, acting as primary SMX-degraders in the soil.

Furthermore, we examined how microbial anaerobic transformation contributes to removal of SMX. We enriched SMX-transforming mixed cultures from sediment of a constructed wetland and digester sludge from a wastewater treatment plant. Transformation of SMX was observed in both sulfate-reducing and methanogenic cultures, whereas nitrate-reducing cultures showed no SMX transformation. In sulfate-reducing cultures, up to 90% of an initial SMX concentration of 100-250 µM was removed within 6 weeks of incubation. Our results

demonstrated that the transformation was microbially catalyzed. The transformation products in sulfate-reducing cultures were identified as reduced and isomerized forms of SMX's isoxazole moiety. The transformation products did not spontaneously re-oxidize to SMX after oxygen exposure, and their antibacterial activity significantly decreased compared to SMX. Population analysis in subsequent transfers of the enrichment revealed a community shift towards the genus *Desulfovibrio*. We therefore tested a deposited strain of *Desulfovibrio vulgaris* Hildenborough for its capacity to transform SMX and observed the same transformation products at similar rates. We then investigated the physiology of the mixed SMX-transforming cultures, and found that the mixed cultures did not grow on SMX. Transformation of SMX by *D. vulgaris* Hildenborough was identified as a cometabolic process. Addition of electron donor can promote transformation of SMX by *D. vulgaris* Hildenborough. Intact-cell activity test revealed that anaerobic transformation of SMX was an enzymatic reduction process, and SMX did not induce expression of specific transformation related proteins. Besides, in the intact-cell activity test, exponential phase cells showed higher activity towards SMX transformation compared with stationary phase cells.

Significant carbon and hydrogen isotope fractionations (ε_C=-5.8±0.7‰, ε_H=-33.8±9.2‰) during anaerobic transformation of SMX by *D. vulgaris* Hildenborough was revealed by compound specific isotope fractionation (CSIA). The ε_C (-5.8±0.7‰) is significantly different from the reported values for aerobic degradation (ε_C=-0.6±0.1) and chemical treatments (ε_C=-0.8~-4.8 for photolysis, ε_C=-0.8~-2.2 for oxidation). Mechanism of anaerobic transformation was proposed as reductive transformation, which is different from hydroxylation and oxidation reported for microbial aerobic degradation and chemical treatments (photolysis and oxidation), the fact further verifies the robustness of CSIA to differentiate reaction mechanisms. Good correlation was observed between change of carbon isotopes and change of hydrogen isotopes. The distinctive lambda value ($\Lambda_{\mathrm{bulk}}^{\mathrm{H/C}}$) achieved in our study for anaerobic transformation of SMX can be applied in field study to assess attenuation of SMX.

In sum, our work revealed that *Intrasporangiaceae* as non-cultivable bacteria played key roles in aerobic degradation of SMX in pig-farm impacted soil, and sulfate-reducing bacteria especially *D. vulgaris* transformed and detoxified SMX under anaerobic conditions. Processes for removal of SMX can be differentiated by the robust CSIA method. This study extended the understanding of microbial degradation and transformation of SMX under aerobic and anaerobic conditions, providing suggestions for bioremediation and wastewater treatment.

Zusammenfassung

Die Einführung von Antibiotika in die Umwelt ist nicht nur für die öffentliche Gesundheit sondern auch für die Funktionen von Ökosystemen bedenklich. Deren breites Auftreten trägt zur Entwicklung und Verbreitung von Antibiotika-resistenten Genen bei und verringert die Verfügbarkeit von Antibiotika zur Behandlung von Infektionskrankheiten. Sulfamethoxazol (SMX) ist eines der am häufigsten detektierte Antibiotika in der Umwelt mit besonders hoher Anreicherung in Gülle, Schlamm und agrarwirtschaftlich-beeinflussten Böden. Mikrobielle Degradation ist hierbei die Hauptsenke für SMX in natürlichen wie auch technischen Systemen. Zwar wurden aerobe SMX-degradierende Mikroorganismen angereichert und isoliert, jedoch ist die Identifikation von *in-situ* degradierenden Populationen noch immer herausfordernd. Feldstudien haben den Beitrag von anaeroben Prozessen zur Entschärfung der SMX-Problematik aufgezeigt, jedoch ist das Wissen über anaerobe SMX-transformierende Mikroorganismen limitiert und noch keine Reinkultur beschrieben. Ein robustes Bewertungsverfahren ist nötig, um den SMX-Abbau in komplexer Matrix zu bewerten. In der vorliegenden Studie lag unsere Zielstellung darin, *in-situ* aerobe SMX-Degradierer zu identifizieren, anaerobe SMX-transformierende Kulturen zu charakterisieren und Bewertungsmethoden zu entwickeln, um die Entfernung von SMX aus der Umwelt zu beurteilen.

Wir untersuchten aerobe SMX-degradierende Bakterien in Boden-Mikrokosmen durch Kultivierungs-unabhängige DNS und Protein Stabile-Isotopen-basierte Techniken. Partielle SMX-Mineralisation wurde durch die Kohlenstoff-Transformation von $^{13}C_6$-gelabeltem SMX zu $^{13}CO_2$ um 0.5% in Boden-Mikrokosmen demonstriert. Stabile-Isotopen-basierte Untersuchungen zeigten die Inkorporation von ^{13}C aus $^{13}C_6$-gelabeltem SMX in die DNS von *Actinobacteria*, darunter die Familien *Intrasporangiaceae, Nocardioidaceae* und *Gaiellaceae* sowie die Ordnung *Solirubrobacterales*. Protein stabile-Isotopen-basierte Techniken demonstrierten die Inkorporation von $^{13}C_6$-gelabeltem SMX in bakterielle Proteine der Familien *Intrasporangiaceae*, *Nocardioidaceae* sowie die Ordnung *Solirubrobacterales*. Dies stimmt mit den Ergebnissen der DNS stabilen-Isotopen Untersuchung überein. Die Abundanz von 60-80% des ^{13}C innerhalb einiger taxonomisch relevanter Proteine deutet auf die direkte Aufnahme von ^{13}C-gelabeltem SMX durch *Intrasporangiaceae* und dessen dominante Beteiligung bei der SMX-Degradation im Boden hin.

Zudem untersuchten wir, inwiefern anaerobe Transformation zur Entfernung von SMX beiträgt. Hierbei wurden SMX-transformierende Mischkulturen aus Sediment eines technischen Feuchtgebietes und Faulschlamm einer Kläranlage angereichert. Die SMX-Transformation wurde bei Sulfat-reduzierenden sowie methanogenen, jedoch nicht Nitrat-reduzierenden Kulturen beobachtet. In Sulfat-reduzierenden Kulturen wurden bei einer Initialkonzentration von 100-250 µM SMX bis zu 90% SMX innerhalb von 6 Wochen Inkubation entfernt. Unsere Resultate demonstrierten, dass es sich um eine mikrobiell-katalysierte Transformation handelte. Die Transformationsprodukte unter Sulfat-reduzierenden Bedingungen wurden als reduzierte und isomerisierte Form der SMX Isoxazol-Funktionalität identifiziert und beschrieben. Sie unterlagen bei Sauerstoff-Exposition keiner spontanen Re-Oxidation und ihre antibakterielle Aktivität verringerte sich signifikant im Vergleich zu SMX. Populationsanalysen bei anschließender Übertragung der Anreicherungskulturen zeigten eine Verschiebung der mikrobiellen Gemeinschaft zu der Gattung *Desulfovibrio*. Folglich testeten wir einen hinterlegten Stamm von *Desulfovibrio vulgaris* Hildenborough bzgl. dessen Kapazität SMX zu transformieren und beobachteten bei gleiche Rate die selben Transformationsprodukte. Des Weiteren untersuchten wir die Physiologie der SMX-transformierenden Mischkulturen und zeigten, dass diese nicht auf Basis von SMX wuchsen. Die Transformation von SMX durch *Desulfovibrio vulgaris* Hildenborough wurde als cometabolischer Prozess identifiziert und die Zugabe von Elektronendonor kann die Transformation von SMX durch *D. vulgaris* verstärken. Aktivitäts-Tests mit intakten Zellen zeigten auf, dass die anaerobe Transformation von SMX ein enzymatischer Reduktionsprozess ist und keine Expression spezifischer Transformations-bezogener Proteine induziert wurde. Innerhalb von Aktivitäts-Test mit intakten Zellen wiesen diese in exponentieller Wachstumsphase höhere Aktivität bzgl. SMX-Transformation im Vergleich zu Zellen in stationärer Phase auf.

Signifikante Kohlenstoff- und Wasserstoff-Isotopenfraktionierung (ε_C =-5.8±0.7‰, ε_H =-33.8±9.2‰) wurde während der anaeroben SMX-Transformation durch *D. vulgaris* Hildenborough durch Komponenten-spezifische Isotopen-Fraktionierung (CSIA) aufgedeckt. Der ε_C (-5.8±0.7‰) unterschied sich signifikant im Vergleich zu beschriebenen Werten für die aerobe Degradation (ε_C=-0.6±0.1) und chemische Behandlung (ε_C=-0.8~-4.8 für Photolyse, ε_C =-0.8~-2.2 für Oxidation). Der Mechanismus der anaeroben Transformation wird als reduktive Transformation vorgeschlagen, was sich deutlich von der beschriebenen Hydroxylierung und Oxidation für mikrobielle aerobe Degradation und chemische Behandlung (Photolyse, Oxidation) unterscheidet. Dies bestätigt die Robustheit von CSIA zur

Differenzierung von Reaktionsmechanismen. Eine gute Korrelation konnte zwischen Kohlenstoff- und Wasserstoff-Isotopen beobachtet werden. Die in dieser Studie der anaeroben Transformation von SMX erhaltenen sich unterscheidenden Lambda-Werte ($\Lambda^{H/C}_{bulk}$), können in Feldstudien angewendet werde, um den Abbau von SMX festzustellen.

Zusammengefasst deckte unsere Arbeit auf, dass *Intrasporangiaceae* als nicht-kultivierbare Bakterien eine Schlüsselrolle während der aeroben Degradation von SMX in Schweinezucht-beeinflusstem Boden spielten sowie Sulfat-reduzierende Bakterien, insbesondere *D. vulgaris* Hildenborough, unter anaeroben Bedingungen SMX transformierten und detoxifizierten. Prozesse zur Entfernung von SMX können durch die robuste CSIA-Methode differenziert werden. Diese Studie erweiterte das Verständnis für mikrobielle Transformation von SMX unter aeroben und anaeroben Bedingungen und stellt Vorschläge für Bioremediation und Abwasserbehandlung zur Verfügung.

Major Theses

1. *Intrasporangiaceae* were identified as key SMX-degraders in pig-farm impacted soil by cultivation independent SIP techniques;

2. SMX was transformed and detoxified by sulfate-reducing mixed cultures;

3. Transformation products in sulfate-reducing cultures were identified as reduced and isomerized forms of the SMX's isoxazole moiety;

4. The pure strain *D. vulgaris* transformed SMX but did not use it as a growth electron acceptor;

5. Anaerobic transformation of SMX by *D. vulgaris* is an enzymatic reduction process;

6. Distinct carbon and hydrogen isotope fractionations were observed during transformation of SMX by *D. vulgaris*.

List of publications

Major results of the dissertation have been published in international journals or have been submitted as listed below:

Publication 1:

Wei-Ying Ouyang, Jian-Qiang Su., Hans Hermann Richnow, Lorenz Adrian. (2019) Identification of dominant sulfamethoxazole-degraders in pig farm-impacted soil by DNA and protein stable isotope probing. *Environ. Int.* **126**, 118–126. DOI: 10.1016/j.envint.2019.02.001

Publication 2:

Wei-Ying Ouyang, Jan Birkigt, Hans Hermann Richnow, Lorenz Adrian. (2021) Anaerobic transformation and detoxification of sulfamethoxazole by sulfate-reducing enrichments and *Desulfovibrio vulgaris*. *Environ. Sci. Technol*. 55, (1), 271-282. DOI: 10.1021/acs.est.0c03407

Publication 3:

Wei-Ying Ouyang, Steffen Kümmel, Lorenz Adrian, Hans H. Richnow. (2021) Carbon and hydrogen stable isotope fractionation of sulfamethoxazole during anaerobic transformation by *Desulfovibrio vulgaris* Hildenborough. Prepare to submit it to *Environ. Sci. Technol*.

Publication 4:

Wei-Ying Ouyang, Jimmy Köpke, Susiddharthak Chakraborty, Lorenz Adrian. (2021) Revealing anaerobic transformation of the antibiotic sulfamethoxazole by *Desulfovibrio vulgaris* Hildenborough as an enzymatic reduction process. (in preparation)

Abbreviations

AKIE: Apparent kinetic isotope effect

ANOSIM: Analysis of similarities

APS: Adenosine 5'-phosphosulfate

ARG: Antibiotic resistance gene

ATCC: American Type Culture Collection

BLAST: Basic local alignment search tool

BTEX: Benzene, toluene, ethylbenzene and xylene

CID: Collision-induced dissociation

CSIA: Compound specific isotope analysis

DAD: Diode array detector

DHPS: Dihydropteroate synthase

DSMZ: German Collection of Microorganisms and Cell Cultures

FPLC: Fast protein liquid chromatography

GC: Gas chromatography

HCD: Higher-energy collisional dissociation

IRMS: Isotope ratio mass spectrometry

K_{ow} : The octanol/water partition coefficient

LB: Lysogeny broth

LR: Labeling ratio

MG-RAST: Metagenomics Rapid Annotation using Subsystem Technology

OD: Optical density

OECD: Organization for Economic Co-operation and Development

ORF: Open reading frame

OTU: Operational taxonomic unit

PABA: *p*-aminobenzoic acid

PCA: Principle component analysis

pK_a: Negative base 10 logarithm of the acid dissociation constant ($-\log_{10}K_a$)

QIIME: Quantitative Insights Into Microbial Ecology

RIA: Relative isotope abundance

SDS-PAGE: Sodium dodecyl sulfate polyacrylamide gel electrophoresis

SIP: Stable isotope probing

SMX: Sulfamethoxazole

SPE: Solid phase extraction

SRB: Sulfate-reducing bacteria

TP: Transformation Product

U/HPLC: Ultra/High performance liquid chromatography

VBA: Visual Basic for Applications

VPDB: Vienna PeeDee Belemnite

VSMOW: Vienna Standard Mean Ocean Water

Table of contents

1 Introduction

1.1 Antibiotics in the environment and their impacts

1.1.1 General background of antibiotics and antibiotic resistance

Antibiotics were discovered in the early 20th century to combat infectious disease and dramatically increased the survival rate worldwide.[1] Afterwards in the 1950s the United States Food and Drug Administration approved usage of low dose antibiotics as food-additives in cattle farms. This approach escalated application of antibiotics in daily scenarios apart from clinics.[2] Nowadays, clinical and veterinary antibiotics contribute almost equally to the total consumption in the market.[3,4] Even though governments worldwide devoted efforts to control abuse of antibiotics in clinics and cattle farms, increasing consumption of antibiotics are still reported, especially in developing countries.[5]

Antibiotic resistant pathogens were detected in clinics towards almost all types of antibiotics after the "golden age" of antibiotics, even for the new generation of antibiotics, against which resistance mechanisms were previously considered not to develop.[6] The four fundamental resistance mechanisms include 1) efflux of the antibiotics, 2) alteration of the target, 3) circumvention of the target pathways and 4) inactivation of the antibiotics. According to estimates by "UN Interagency Coordination Group on Antimicrobial Resistance" antibiotic resistance could lead 10 million deaths each year by 2050 and catastrophic damage to the economy as 2008 global financial crisis.[7,8]

1.1.2 Distribution of antibiotics in the environment

Antibiotics are not completely taken up by humans and animals, thus, large amounts (~ 50%) of ingested antibiotics are excreted to the environment and are now considered as emerging trace contaminants in recent years.[9] Cattle farms, aquacultures, hospitals and antibiotic manufacturers are becoming antibiotic hotpots and effluents from them eventually gather in municipal wastewater treatment plants.[10-13] Discharge of antibiotics from hotpots results in widespread distribution of residual antibiotics in natural environments such as surface water, soil, groundwater and sediment, together with abundant antibiotic resistant bacteria (**Figure 1**). Persistent antibiotics can be frequently detected in all environmental compartments and residue concentrations varies from mg kg^{-1} to ng kg^{-1} level.[14-17]

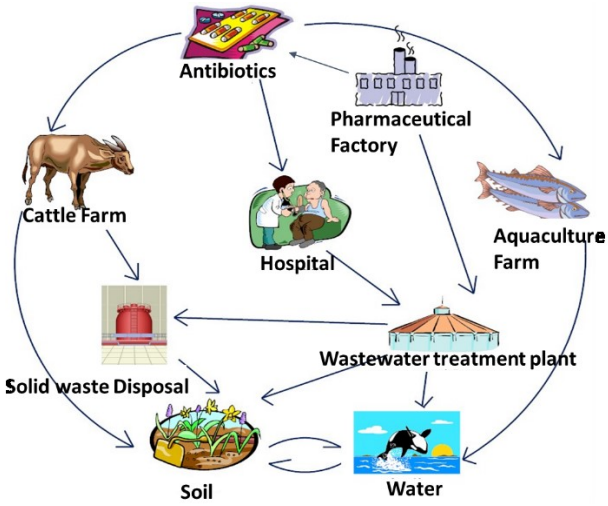

Figure 1. Discharged route of antibiotics from hotspots to the environment, modified from literature.[18] "Solid waste disposal" in this figure represents treatment and disposal of sludge and manure.

1.1.3 Antibiotic resistance on the environmental dimension

Antibiotics in the environment can stimulate the development and propagation of environmental antibiotic resistance genes (ARGs). ARGs were considered as emerging environmental contaminants in 2006,[19] within recent decades more and more ARGs and antibiotic resistant bacteria were detected worldwide, and substantial evidence showed anthropogenic activities significantly increased the diversity and abundance of ARGs in the environment.[20-22] These environmental ARGs shared profiles with the clinic ones,[23] and were considered to be a non-negligible factor for exacerbation of antibiotic resistance crisis. Hence, decreasing the environmental resistance levels could contribute to the solution of global antibiotic threats. Elimination of antibiotic residues in the environment can release the selection pressure on antibiotic resistance genes, and in the meantime also decrease the disturbance of antibiotics on ecological functions.[24]

1.2 The antibiotic SMX in the environment: a model sulfonamide

SMX, used in high amounts as human and veterinary medicine, is prescribed to prevent and treat bacterial infection caused by both gram positive and negative species.[3,25,26] SMX is persistent and one of the most frequently detected antibiotics in the environment.[27-31] Up to 18 mg kg^{-1} SMX was reported in cattle manure.[10,13] Hence, in our study, we selected SMX as a representative sulfonamide antibiotic to investigate microbial degradation of a persistent antibiotic in the environment. Here, we summarized SMX's mode of action, properties, toxicity, and occurrence, transformation products, behavior in the environment.

1.2.1 Mode of action of SMX

SMX is a bacteriostatic antibiotic inhibiting the synthesis of folate in bacterial cells, and has no effect on mammals as they do not synthesize folate. The antibacterial activity of SMX depends on the sulfanilamide moiety as an analog of *p*-aminobenzoic acid (PABA), and PABA is a substrate of dihydropteroate synthase (DHPS) for the formation of dihydropteroate acid. SMX was used in combination with trimethoprim since 1969 to provide sequential and synergistic inhibition of bacterial folate metabolism.[32] SMX and trimethoprim are always detected together in the environment[33] due to their resistance to microbial degradation.

1.2.2 Properties and chemical reactivity of SMX

SMX is polar (log K_{ow} =0.89) and soluble in water (610 mg L^{-1} at 37°C and neutral pH), making it highly mobile among environmental compartments,[34] for example continuously leaching from manure-amended soil to water body.[35] SMX, as a weak acid (pK_{a1}=1.6, pK_{a2}=5.7), exists predominantly as anions under neutral conditions (**Figure 2**), resulting in low levels of adsorption to negatively charged soil particles and reversible desorption from activated sludge.[36,37]

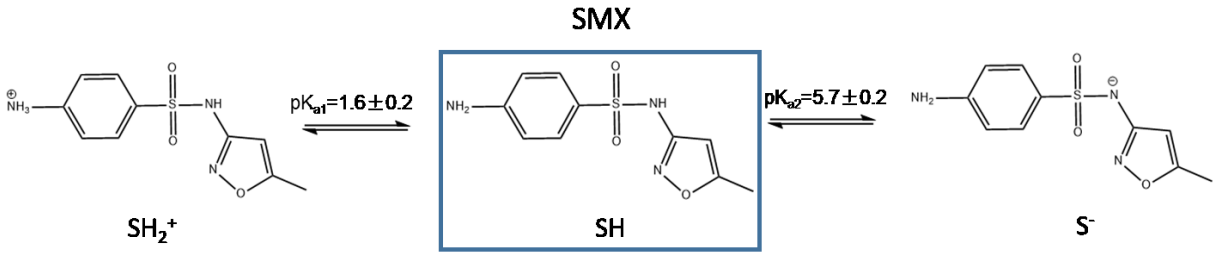

Figure 2. Protonation and deprotonation of SMX based on dissociation constants, showing the cationic form, neutral form and anionic form of SMX.[38]

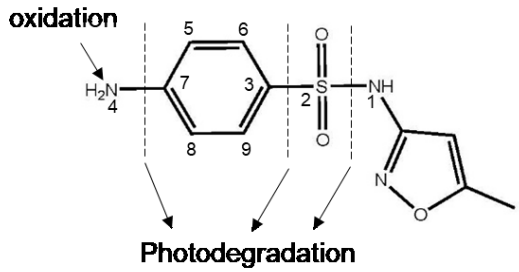

Figure 3. Reactive sites on SMX for chemical reactions including photolysis and oxidation. Numbers on atoms show the conventional usage of atom numbering in sulfonamide antibiotics.

Photolysis: Direct photolysis is the dominant mechanism for photochemical elimination of SMX.[39] The benzene moiety of SMX as a chromophore group can absorb photons and trigger direct photolysis. Photolysis pathways vary depending on pH and irradiation wavelengths.[38,40] Major pathways involve cleavage of the sulfonamide bond, hydroxylation, isomerization and fragmentation of the isoxazole ring (**Figure 3**).[41,42] The acute toxicity of photodegradation products to *Daphnia magna* was higher than that of SMX.[43] Indirect photolysis of SMX was also reported in the presence of Fenton reagents (a solution of hydrogen peroxide with ferrous iron),[44] and addition of nitrate did not promote photolysis of SMX.[42]

Oxidation: Ozone, chlorine dioxide, persulfate and Fenton reagents are often utilized in advanced oxidation to generate highly reactive radicals.[45-47] Both experiments[48] and computation[49] identified the aniline moiety of SMX as the reactive part during oxidation process (**Figure 3**). Both hydroxyl radicals and sulfate radicals attack on the aniline nitrogen of SMX and generate nitro derivatives and dimeric products.[50] Besides, oxidation of SMX by chlorine can induce chlorinated products, which also predominantly occurs on aniline moiety.[51]

1.2.3 Occurrence and toxicity of SMX in the environment

Pharmaceutical factories, livestock farms, hospitals and municipal wastewater treatment plants are considered as contamination sources of SMX. Discharges from these sources result in the occurrence of SMX in various environmental compartments (**Table 1**). The highest SMX residual concentrations were reported in solid waste (manure and activated sludge) up to 18 mg kg^{-1} (**Table 1**).[10] Besides, the SMX concentrations in wastewater from some pharmaceutical manufactories can also reach 1.3 mg L^{-1},[16] whereas the SMX concentrations in wastewater from hospitals, municipal sewage plants are lower and within the range of 0.09-27.8 μg L^{-1}.[10,16,52] No significant differences of SMX concentrations were observed between WWTP influents and effluents, indicating low removal efficiency achieved in municipal sewage treatment plants.[53] On average, SMX residual concentrations in natural water bodies including surface water, ground water and drinking water are lower than that in contamination sources (**Table 1**). High concentrations of SMX in soil were reported up to 671 μg L^{-1} (**Table 1**),[10] as antibiotic-containing manure and activated sludge are applied to soil as fertilizers, thus SMX poses high risks to both agricultural systems and the related water bodies (**Table 1**).

Table 1. A summary of detected frequency and concentrations of SMX in contamination sources and environmental compartments based on studies from different countries (data from literature[52])

Contamination sources or environmental compartments	Detection frequency	Detected concentration (μg L^{-1} for water, μg kg^{-1} for solid)
Pharmaceutical wastewater	40%	24.8-1,340
Livestock wastewater	50%	0.44-8.84
Hospital wastewater	100%	0.2-27.8
WWTP influent	100%	0.36-7.91
WWTP effluent	100%	0.09-9.46
Manure	83%	840-18,000
Activated sludge	100%	0.11-665
Surface water	100%	0.036-4.3
Groundwater	83%	0.009-1.11
Drinking water	100%	0.03-0.116
Soil	100%	0.9-671.5

SMX shows ecotoxicity in the environment as disturbing structures and functions of environmental bacteria, most research on ecotoxicity of SMX was conducted under environmentally relevant concentrations and subtherapeutic concentrations. Toxicity of SMX under low concentrations (1-2 μg L^{-1}) was reported in various studies, only 1.27 μg L^{-1} SMX altered community structures of groundwater bacterial enrichment and inhibited nitrate reduction capabilities,[54] besides, 2 μg L^{-1} SMX changed bacterial population of suspended and granular sludge after 2 months exposure, whereas the 2 μg L^{-1} SMX did not suppress the treatment performance of both sludge.[55] Under higher tested SMX concentrations (0.25-50 mg L^{-1}), within the range of subtherapeutic concentrations and concentrations detected in highly contaminated hotpots like pharmaceutical manufactory and manure, significant shifts of indigenous soil bacteria were reported with reduction of sensitive species[56] and also nitrogen metabolism in the bacterial community was affected.[57] SMX residues also promote the development and dissemination of ARGs on the environmental dimension, showing synergistic effects combined with other contaminants.[58-60] Also, low concentrations of SMX in effluents of wastewater treatment plants enriched antibiotic resistant bacteria in the downstream waterbodies, compared to the levels of unaffected upstream.[61]

1.2.4 Main transformation products in the environment and their toxicity

Apart from SMX, various transformation products and human metabolites of SMX were frequently detected in the environment,[62,63] among which mainly three modification types were reported: derivatization, conjugation and bond cleavage (**Table 2**). Derivatization and conjugation predominantly occur on N^4 and N^1. N^4-acetyl-SMX and N^4-glucuronide-SMX are the two major human metabolites excreted into the environment, and they can be re-converted to SMX in wastewater treatment plants, resulting in an increase of SMX concentrations in effluents.[64,65] Similarly, pterin-conjugates formed in wastewater treatment plants lead to reversible generation of SMX in the environment.[66] Transformation products modified at the *para* amino group still have antibacterial effects, especially 4-NO_2- and 4-OH-SMX even show higher antibacterial activity than SMX. In contrast, N^4-acetyl- and N^4-hydroxy-acetyl-SMX exhibit much less toxicity than SMX. Breakdown products via bond cleavage always lose their biological activities.[62] The structure of *R'* in **Table 2** represents the key structure of SMX (**Figure 4**).

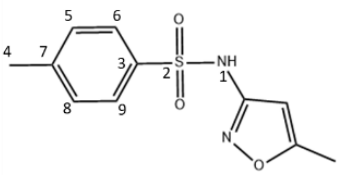

Figure 4. Structure of R' described in **Table 2** representing the key structure of SMX.

Table 2. Structures of main SMX transformation products and human metabolites. This is a modified table from literature[62-63]. Note that *N4*- means the modification is attached on the amine group at the position 4 of SMX, and 4- means the amine group at the position 4 of SMX is substituted by other functional groups.

Derivative/Conjugative products (*R'*-)		Breakdown products	
4-hydroxy-SMX	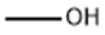	Sulfanilamide	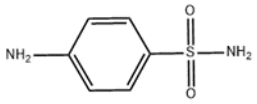
4-nitroso-SMX	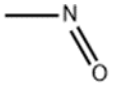	3-amino-5-methylisoxazole	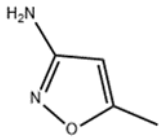
4-nitro-SMX	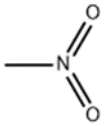	Sulfanilic acid	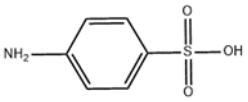
N4-hydroxy-SMX	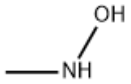	Benzensulfonamide	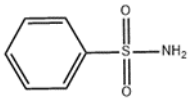
N4-acetyl-SMX	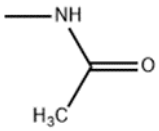	Aniline	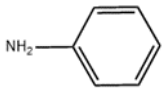
N4-hydroxy-acetyl-SMX	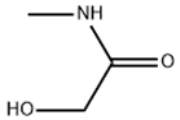		
N4-Glucuronide-SMX	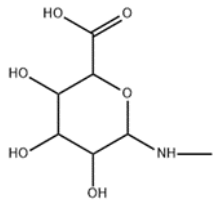		
N4-Glucoside-SMX	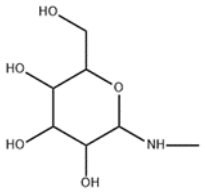		
N4-Pterin-SMX	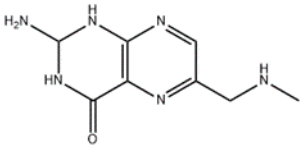		

1.2.5 Removal of SMX in the environment

Removal of SMX in the environment under aerobic and anaerobic conditions were investigated in various studies.[37,67,68] In aerobic environmental compartments, fast attenuation of SMX was reported in soil and surface water microcosm.[67-69] In wastewater treatment plants, elimination of SMX was observed in biological treatments using different techniques, including conventional activated sludge systems, fixed-bed reactors and membrane reactors.[70,71] Besides, mixed cultures and pure strains aerobically degrading SMX were enriched and isolated from environmental samples.[72] Even though anaerobic transformation is considered to be slower than aerobic degradation, removal of SMX under anaerobic conditions was also observed and reported in literature. Incubation experiments showed that river sediment not only removed SMX, but also two major human metabolites of SMX (N^4-acetyl-SMX and N^1-glucuronide-SMX). Besides, transformation of SMX was detected in other anaerobic compartments like groundwater and during anaerobic processes like bank filtration.[73-75]

The main factors affecting the transformation of SMX in the environment are: **1)** initial concentrations of SMX, as no degradation process could happen if SMX concentration is below the threshold for induction of transformation related genes, while longer lag phase is needed if SMX concentration exceeds inhibition level; **2)** functions and structures of microbial communities in the environment, e.g. it was reported that in a wastewater treatment plant digester sludge had much higher anaerobic SMX transformation activity than that of effluent;[76] **3)** presence of other carbon sources, transformation of SMX could be boosted if additional carbon sources induce cometabolism, whereas transformation is suppressed if the additional carbon sources have higher priority than SMX;[77] **4)** physical conditions of the system.[70] Thus, microbial related factors primarily caused discrepancies of SMX's fates in different scenarios.

1.3 Microbial transformation and degradation of SMX

Almost every naturally occurring substance and many synthetic xenobiotics can be converted by some specific groups of bacteria.[78] Based on changes occurring on structures of substance, four fundamental terms are used in microbiology to describe the fate of contaminants: transformation, degradation, assimilation and mineralization. The main difference between transformation and degradation is whether the compound is cleaved to smaller moieties. The pair assimilation/mineralization refers to the fact whether the compound's atoms are incorporated into microbial biomass or released as mineral forms. There are overlaps between

these two pairs of terminology, in this dissertation these terms will be used based on the definition and aspects I would like to emphasize on.

Transformation: A→ A variant, modification without breakdown

Degradation: A→B+C, cleaved to smaller moieties

Assimilation: A→ microbial biomass

Mineralization: A→ CO_2 or CH_4, NH_3

1.3.1 Microbial metabolic and cometabolic process for removal of SMX

Degradation/transformation of contaminants by bacteria can be metabolic processes, cometabolic processes, and microbially mediated abiotic processes. Bacteria use contaminants as sole energy source (electron acceptor or electron donor) or/and carbon source in metabolic processes, as bacteria can obtain carbon, energy and reducing equivalents via metabolic processes to live and reproduce. In contrast, in cometabolic processes bacteria simultaneously degrade two compounds and the degradation of the second compound relies on the presence of the first compound, meaning the second compound is not a growth supporting substrate. In a microbially mediated abiotic process, contaminants chemically react with metabolites released by bacteria. The main difference between metabolic degradation/transformation of contaminants and cometabolic degradation/transformation of contaminants is whether bacteria can take up contaminants and transform them to metabolically useful compounds.

SMX was reported to be degraded or transformed in metabolic processes, cometabolic processes, and microbially mediated abiotic processes.[79-82] All metabolic processes for SMX degradation were reported under aerobic conditions, flavin-dependent monooxygenases were proposed to be responsible for the degradation and present in aerobic SMX-degrading cultures. Besides, cometabolic processes were reported under both aerobic and anaerobic conditions, especially in complex environmental compartments, removal of SMX was enhanced by addition of cosubstrates including glucose, humic acid, acetate and methanol.[37,64,77,80,83] Both metabolic and cometabolic processes for removal of contaminants have potentials for bioremediation but with different strategies (e.g. add cosubstrates or not).[84,85]

1.3.2 Biodegradability of SMX

As elimination of SMX by routine wastewater treatment is not efficient causing prevalence of SMX in the environment, SMX was considered as a recalcitrant contaminants by some researchers.[86] Therefore, biodegradability of SMX was evaluated by defined standard tests in previous studies. The well accepted biodegradability test is OECD (Organization for Economic Co-operation and Development) closed bottle test (OECD 301) based on aerobic respiration with organic compounds, in which oxygen consumption or carbon dioxide evolution is measured to estimate the degradation levels of tested compounds by acclimated bacteria. The acclimated bacteria could be derived from activated sludge, sewage effluents, surface waters and soils but without strict selecting rules. According to the OECD test, compounds are defined as readily degradable if the degradation levels exceed 60% based on initially amended compounds within 10 days after 10% degradation is reached.[87] Meanwhile, anaerobic degradability of compounds is also investigated based on production of carbon dioxide and methane in a digester system (OECD 311 or ISO 11734).[88,89]

SMX was found not to be aerobically readily degradable as a sole carbon source by using OECD 301 closed bottle test, and only low degradation was observed after a defined incubation period of 28 days.[90-92] Besides, an anaerobic test (ISO 11734) also showed poor anaerobic degradability of SMX.[89] Even though SMX is not readily degradable under both aerobic and anaerobic conditions according to the standard tests, still fast microbial degradation and transformation of SMX under aerobic and anaerobic conditions were reported in both natural and engineered systems.[64,71,92] Thus, the biodegradability of SMX revealed by standard tests was biased by the selected acclimated bacteria and analysis methods, for example fermentation of SMX to small organic acids could not be detected by measuring evolution of carbon dioxide or methane, similarly, transformation of SMX could also not be detected by only measuring gas evolution. Therefore, anaerobic transformation and fermentation of SMX are overlooked by standard biodegradability tests, and instructions for selecting acclimated bacteria are ambiguous which resulted in discrepancies in different studies.

1.3.3 Aerobic degradation of SMX

Even though SMX is not aerobically readily biodegradable based on standard biodegradability tests, still wide ranges of bacteria were identified as SMX-degraders in various studies. Enrichment cultivation and isolation were widely used to identify key players from

environmental samples, mainly from activated sludge and bioreactors (**Table 3**). SMX concentrations range from 6 mg L^{-1} to 2,530 mg L^{-1} in the tested SMX-degrading cultures (**Table 3**), which is higher than the detected environmental concentrations (**Table 1**). The reported SMX-degrading cultures can degrade and mineralize SMX, SMX either acted as sole carbon source or/and sole nitrogen source, or was cometabolized with cosubstrates like glucose (**Table 3**). The removal percentage of SMX ranged from 20% to 100% in the reported SMX-degrading cultures (**Table 3**). Apart from enrichment cultivation and isolation, population analysis of SMX-degrading communities was also applied to postulate SMX-degraders (**Table 4**), but the evidence is not strong enough for the proposed SMX-degraders, as the community shift caused by SMX could also be attributed to resistance of SMX.

Table 3. SMX-degrading bacteria in enrichment cultures or isolates

Taxa of cultures	Sources of inoculum	Initial concentration of SMX and conditions of enrichment cultivation	Removal type	Removal percentage and rate	References
Microbacterium sp., *Rhodococcus* sp., *Achromobacter* sp., *Ralstonia* sp.	1.5 liter MBR continuously operating for 10 months with 100 μg L^{-1} of SMX	Initial concentration of mineralization test was not mentioned; 0.5 mM (126.5 mg L^{-1}) SMX in the mineral salts medium and subculture each month	Mineralization	*Microbacterium* sp.: 40% , *Rhodococcus* sp.: 35%, *Achromobacter* sp.: 41%, *Ralstonia* sp.: 44%, mineralization occurred after 300 hours incubation	[93]
Acinetobacter sp.	Activated sludge from a wastewater treatment plant in Beijing	5-240 mg L^{-1} SMX, 25°C and pH=7.0. Inoculum on solid medium containing 50 mg L^{-1} SMX, transfer the colonies to liquid medium containing 200 mg L^{-1} SMX	Degradation and mineralization	100% degradation within 1-7 hours and 95% mineralization within 48 hours	[94]
*Pseudomonas psychrophila (*cold-adapted bacterium*)*	Activated sludge from a Harbin Taiping municipal wastewater treatment plant	100 mg L^{-1} SMX; Enrich in mineral salts medium containing 100 mg L^{-1} SMX for two months	Degradation (SMX as sole carbon source and energy source)	34.3% degradation after 192 hours at 10°C	[79]

Rhodococcus rhodochrous	Pure strains bought from American Type Culture Collection (ATCC)	40 mg L^{-1} SMX	Degradation, co-metabolism with glucose, cannot grow on SMX	20% degradation after 36 days incubation	[80]
Rhodococcus equi, Pseudomonas. aeruginosa (only 5.6% removal but metabolite was detected)	Pure strains obtained from Cedarlane® Canada	6 mg L^{-1} SMX	Degradation, co-metabolism with glucose	29% removal with glucose for *R. equi* after 120 h, when mixed with other organisms the removal was 5%	[72]
Achromobacter Denitrificans	Activated sludge from a wastewater treatment plant	0.6-10 mM (152.0-2532.8 mg L^{-1}) SMX, Enrich in medium containing 250 mg L^{-1} SMX and 1 g L^{-1} yeast extract.	Degradation, SMX as sole carbon, nitrogen and energy source	99% (0.6 mM after 6 days, 5 mM after 103 days and 10 mM after 188 days)	[95]
Pseudomonas sp., *Brevundimonas* sp., *Variovorax* sp., *Microbacterium* sp.	SMX-acclimated activated sludge	10 mg L^{-1}	Degradation, SMX as sole carbon and nitrogen source	*Pseudomonas* sp: 56.5%-97.7%, *Brevundimonas* sp.:100% , *Variovorax* sp.: 64.7%, *Microbacterium* sp.: 100% after 10 days	[96]

Shewanella sp.	Pure strains provided by the Soil Microbiology Laboratory of Northwest Agriculture and Forestry University	10 mg L^{-1}	Degradation	59.88-63.89% was removed after 5 days incubation	[97]

Table 4. SMX-degrading bacteria in environmental samples or reactors revealed by population analysis

Taxa of cultures	Description of environmental samples or reactors	Initial concentration of SMX and conditions in the system	Degradation type	Removal percentage	References
Bacillus firmus, *Bacillus cereus* (prevalent resistant bacteria in the system)	Water-sediment system in a natural river	1-100 mg L^{-1}, the degradation is concentration independent, addition of humic acid facilitate the removal of SMX in water	Cometabolism	82.9% at 25°C within 35 days incubation, 90.1% with 30 mg L^{-1} humic acid within 35 days	[83]
Rhodopirellula baltica and *Methylibium petroleiphilum* sp.	Biofilm in an internal loop photobiodegradation reactor. Inoculum for the reactor was activated sludge from municipal wastewater treatment plants and acclimated with SMX	10-120 mg L^{-1}	Degradation	20%-100% degradation within 8 hours with addition of nitrogen source	[98]
Acinetobacter, Alcaligenes, Brevundimonas	Sewage sludge from a wastewater treatment plant in Taipei	20 mg L^{-1}, sludge in bioreactor with or without spent	Degradation and mineralization	99% removal after 45 days incubation	[99]

and *Pseudomonas* sp.		mushroom compost and soil-sludge mixture			

The general principle of aerobic degradation depends on oxidation via oxygenase for destructuring structures of compounds. For SMX, and also for other sulfonamides, the breakdown of C-S bond, S-N bond and N-C bond was widely reported during microbial aerobic degradation (**Figure 5**).[79,94,100-102] . The initial attack is accomplished by hydrolysis at different sites of SMX (**Figure 5**), among which attacking at aromatic ring was confirmed by Ricken et. al as *ipso*-hydrolysis pathway.[100] Detected degradation products were mainly the aromatic moiety (aniline, sulfanilamide and sulfanilic acid) and the isoxazole moiety (3-amino-5-methylisoxazole). It is considered that the aromatic products could further undergo mineralization steps while the isoxazole moiety is released into the environments as a dead-end product.[79,94,100-102] Aerobic degradation of SMX by *Microbacterium* sp. was well studied, both Ricken and Kim proposed that $FMNH_2$-dependent monooxygenases initiated SMX degradation, as upregulation of flavin-dependent monooxygenase and flavin reductase were observed in response to SMX, and further expression of these two enzymes in *E. coli* increased its resistance level to SMX.[100,102,103] Other proteomics analysis also proposed enzyme candidates responsible for SMX degradation, for example, urethanase which hydrolyze N-acetylated compounds like anilides and N-acetyl-phenyl-ethylamine hydrolase could cause the generation of 4-OH-SMX.[72]

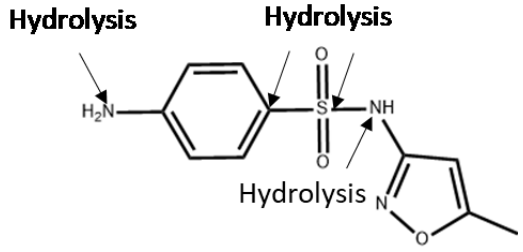

Figure 5. Initial attacking sites on SMX by aerobic degraders via hydrolysis.

1.3.4 Anaerobic transformation of SMX

Anaerobic transformation has high potentials to treat aerobically recalcitrant compounds.[84] Conditions with different electron acceptors are classified as anoxic or anaerobic regarding redox potentials: denitrification>manganese reduction>iron reduction (anoxic)>sulfate reduction (anaerobic) >methanogenesis (**Figure 6**). Anaerobic/anoxic transformation of organic contaminants are widely observed under manganese/iron reducing, sulfate-reducing, methanogenic, and nitrate reducing conditions.[104] These redox gradients are nicely presented in natural environments like soil-aquifers and bank filtration, and constructed vertical wetlands (column experiments). Behavior of SMX in natural soil-aquifer showed that SMX was

sensitive to redox conditions and better removed under lower redox potentials, in the layer where iron reduction prevailed high degradation of SMX (> 50%) was observed, while in the denitrifying layer with significantly higher redox potentials no degradation of SMX was detected.[105] The similar results were reported in various bank filtration studies, showing that the removal of SMX under anaerobic or strictly anaerobic conditions was higher than that under aerobic and denitrifying conditions.[106-108] However, contradictory results were also reported: a long-term column experiment showed that degradation of SMX in the aerobic layer (half-life: 1-9 days) was faster than that in the anaerobic layer (half-life: 16 days), and the slowest degradation of SMX was observed in the anoxic layer (half-life: 49 days).[73] Even though there exist discrepancies on SMX degradation under different redox conditions especially under aerobic conditions, preferential degradation of SMX under low redox potentials (lower than denitrifying) was always reported in both natural and laboratory-scale systems.

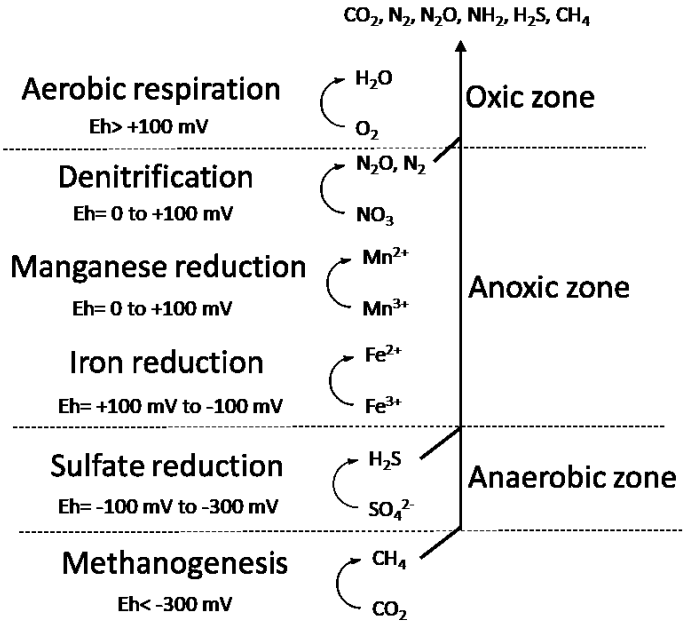

Figure 6. Redox potentials of various conditions with different electron acceptors.[104]

Laboratory-scale incubation tests further revealed that anaerobic samples harbored strong potentials to fast and efficiently eliminate SMX when electron acceptors (bicarbonate, sulfate and nitrate) were added.[74] Anaerobic transformation of SMX under denitrifying and iron reducing conditions was investigated and proposed as microbially mediated abiotic process. Under denitrifying conditions, generated nitrite from nitrate reducing bacteria reacts with SMX to form 4-nitro-SMX, and 4-nitro-SMX can reversibly produce SMX which could contribute to contradictory results mentioned above under anaerobic conditions.[82,109,110] Similar

interaction between SMX and nitrite was also observed with the presence of ammonia oxidizing bacteria, 4-nitro SMX, desamino-SMX and N^4-acetyl-SMX were detected as transformation products.[81] Besides, in soil under iron reducing conditions rapid transformation of SMX was attributed to interaction between SMX and Fe(II) generated from iron reducing bacteria, the transformation products were identified as modification of the isoxazole ring of SMX.[111] Similarly, in a sulfate-reducing bioreactor spiked with SMX, the SMX transformation products with modified isoxazole moiety were also detected,[112] the fact indicated that sulfate-reducing bacteria could play a role in anaerobic transformation of SMX. In summary, anaerobic conditions with low redox potentials were reported to be suitable for SMX transformation, while relevant key players and transformation pathways were not investigated and identified.

1.4 Physiology of the sulfate-reducing bacteria and *Desulfovibrio vulgaris* Hildenborough

1.4.1 Distribution of sulfate-reducing bacteria in natural and engineered systems

Sulfate is one of the most abundant anions in natural water bodies,[113] especially ubiquitous in groundwater and seawater. Geochemical recycling of sulfur contributes to redox distribution in many environmental compartments. Sulfate-reducing bacteria (SRB) distribute widely in both natural environment and engineered systems, including marine sediment, rice field, deep-sea hydrothermal vents, oil fields environments and so on.[114-116] SRB have successfully adapted to almost all the ecosystems by being phylogenetically and metabolically versatile. In subsurface environment sulfate-reducing zones and methanogenic zones are generated based on competition for acetate and H_2.[117] Additional organic electron donors can support diverse SRB in reactors to treat metal- and sulfate-containing wastewater.[118]

1.4.2 Metabolism of SRB

Dissimilatory sulfate reduction is a widely present and well-studied central metabolic process in SRB. The process is comprised of several activation and reduction steps in cytoplasm for energy conservation (**Figure 7**). Sulfate is energetically stable and need to be first activated by sulfate adenylyl transferase (Sat) and ATP to adenosine 5'-phosphosulfate (APS). APS is metabolically active and can be reduced to sulfite by APS reductase (AprBA), further reduction of sulfite to DsrC trisulfide is catalyzed by DsrAB/DsrC, and the final step is reduction of the DsrC trisulfide to sulfide and reduced DsrC by the membrane-bound DsrMKJOP complex

(**Figure 7**).[119] The four electrons in the last step of sulfite reduction is likely to originate from the menaquinol pool, which could couple proton gradient across the membrane with sulfite reduction and energy conservation.[119] In the dissimilatory sulfate reduction, a net energetic benefit is obtained due to more ATP is generated via ATPase than that is used to activate sulfate to APS. Apart from sulfate, nitrate and other forms of sulfur including organic sulfur can also be utilized as alternative electron acceptors by SRB.[120,121] Besides, formate cycling was proposed to be also important for SRB's energy conservation.[122]

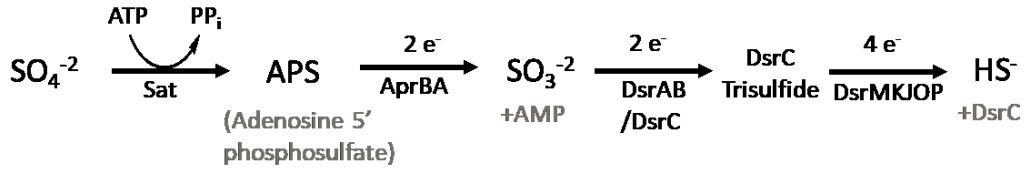

Figure 7. Dissimilatory sulfate reduction mechanism in SRB

SRB can oxidize wide ranges of organic compounds including amino acids (e.g. glycine, serine), sugars (e.g. fructose, glucose), monocarboxylic acids (e.g. acetate, propionate, butyrate), dicarboxylic acids (e.g. fumarate, succinate, malate), alcohols (e.g. methanol, ethanol), and aromatic compounds (e.g. benzoate, phenol) as electron donors,[123,124] indicating versatile metabolic potentials of SRB. Some SRB are lithotrophic and can use hydrogen gas or phosphite (e.g. *Desulfotignum phosphitoxidans*) as electron donors.[125] Besides, another group of SRB (e.g. *Desulfovibrio sulfodismutans*, *Desulfocapsa thiozymogenes*, *Desulfocapsa sulfoexigens*) can disproportionate sulfur compounds to conserve energy, such as elemental sulfur (S_0), sulfite (SO_2^{-3}) or thiosulfate ($S_2O_2^{-3}$) can be used as electron donor and electron acceptor simultaneously and split into hydrogen sulfide and sulfate.[126]

D. vulgaris Hildenborough is a type strain of SRB with completely sequenced genome.[127] Energy conservation by *D. vulgaris* linking electron flow from lactate oxidation to sulfate reduction is extensively investigated, as grown with lactate as an electron and carbon source provides robust proliferation of *D. vulgaris*. Instead of mineralization, *D. vulgaris* can only incompletely oxidize lactate to acetate stoichiometrically. Primary oxidation of lactate occurs in the cytoplasm of *D. vulgaris,* lactate is mainly converted to pyruvate by a membrane-bound lactate dehydrogenase delivering electrons directly to the membrane menaquinone pool; secondly, decarboxylation of pyruvate is catalyzed by pyruvate dehydrogenase; and then acetyl-CoA is subsequently converted to CoA and acetate.[128] Like other SRB, *D. vulgaris* is metabolically versatile, reflected by the presence of multiple energy conservation associated

proteins, for example, periplasmic hydrogenases ([Fe]-, [NiFe]-, [NiFeSe] hydrogenases),[127] membrane-bound electron-transferring complexes (e.g. Dsr, Qmo, Hmc, Tmc, Rnf, etc.)[129] and electron carriers (e.g. cytochromes, ferredoxin, etc.).[129,130] *D. vulgaris* contains various c-type cytochromes creating a vast network of interconnected hemes for intermolecular electron transfer and storage, as this network could provide electrical wiring for connecting multiple periplasmic redox proteins and also serve as a storage for low-potential electrons.[131] Furthermore, it is reported that the electrons stored in cytochrome network can be used for external reduction, for example reduction of toxic metals Cr(VI) and U(VI).[132-134]

1.4.3 The role of SRB in bioremediation of xenobiotics

SRB have a large spectrum of energy source, enabling them to use complex organic molecules as electron donors or electron acceptors. Besides, SRB play an important role in immobilization of toxic metals including precipitation as metal sulfides and reduction of toxic metals. Large amounts of organic contaminants were reported to be oxidized by SRB as electron donors, among these are monoaromatic hydrocarbons like benzene, toluene, ethylbenzene and xylene from petroleum contamination,[135,136] polycyclic aromatic hydrocarbons like naphthalene and anthracene,[137,138] and alkanes.[139] The activation steps in transformation process were reported as 1) carboxylation, 2) fumarate addition, 3) hydroxylation, 4) methylation.[135,140-142] Besides, SRB have the capacity for reductive dehalogenation and also play a role in reduction of azo dyes by generated sulfide.[143,144] Apart from organic compounds, generated sulfide by SRB can also precipitate various toxic metals for detoxification.[145] Reduction of toxic metals including uranium, arsenic and chromium can also be achieved enzymatically by SRB,[146-148] and proteins associated with metal reduction were proposed as cytochromes, hydrogenase and ferredoxin.[134,149]

1.5 Experimental approaches

In addition to conventional cultivation methodology, we also applied cutting-edge microbiological technology to investigate microbial degradation of SMX under aerobic and anaerobic conditions, especially for non-cultivable bacteria, and evaluating attenuation of SMX in the environment. Laboratory-scale cultivation is the most straightforward method to study bacteria of interest, active mixed cultures and pure strains can be cultivated in defined chemical medium for various research aims. Cultivation was widely applied in environmental microbiology for decades to enrich and isolate key players responsible for biotransformation

processes.[101,150] However, more and more research revealed that large amounts of non-cultivable environmental bacteria overlooked by current cultivation technology played key roles in various scenario,[151] therefore, development of cultivation-independent approaches is essential. Apart from identification of key players by means of cultivation and cultivation-independent approaches, we also need other specific and robust experimental approaches to better understand the mechanism of the microbial process and further evaluate the process on the environmental dimension.

Enrichment cultivation and isolation

Enrichment cultivation is a conventional method for screening functional bacteria, by means of using chemically defined medium with target substrates to enrich bacteria preferentially relying on the substrate. Even though enrichment cultivation is a low-throughput method for identification of functional bacteria in the environment compared to molecular methods, it can be used to confirm functions of the selected bacteria, which is more precise than the predictions based on database, furthermore, new functions and new bacteria identified from enrichment cultivation are also used to update database. Both batch cultures and reactors are widely used in enrichment cultivation, especially in the research on degradation of micropollutant and removal of nitrogen.[152-154] In most cases, mixed cultures containing key players as dominant bacteria are achieved from enrichment cultivation, further isolation steps could be applied to obtain a functional pure strain, among which the most common technique is series dilution on the surface (aerobic bacteria) of or in (anaerobic bacteria) the solid medium,[96,101] besides, other sorting techniques like flow-cytometry and atomic force microscope also show high potentials in isolation.[155,156]

Stable isotope probing (SIP)

SIP as a cultivation-independent method complements enrichment cultivation for identification of uncultivable bacteria from the environment. SIP can provide direct evidence for the involvement of specific microbial populations under more natural conditions without cultivation, if the bacteria can assimilate carbon or nitrogen from the labeled substrate.[157,158] In SIP approaches microorganisms are cultivated with an isotopically labeled substrate (only with stable isotopes) and molecules with phylogenetic information such as DNA (DNA-SIP),[159] RNA (RNA-SIP)[160] or proteins (protein-SIP)[158] are analyzed for the integration of heavy stable isotopes to identify assimilation of the substrate. Labeled nucleic acids can be physically separated in density gradients via ultracentrifugation,[159] and the metabolic

incorporation into proteins can be identified by mass spectrometry[161,162]. In protein-SIP studies two values are often described assuming that each protein is present in a labeled and an unlabeled state: the abundance of ^{13}C isotopes in the labeled version of a given protein, $X(^{13}C)_{LP}$ ("Relative Isotope Abundance-RIA" from MetaProSIP), and the abundance of the labeled version of a protein among the sum of the labeled and unlabeled version of this protein, $X(LP)_{\Sigma P}$ ("Labeling Ratio-LR" from MetaProSIP).[163,164] Isotopically labeled proteins and nucleotides contain taxonomic information of key players. Apart from the taxonomic affiliation of active microbial members of a consortium, SIP can also elucidate metabolic pathways when stable isotope incorporation is traced into proteins with annotated functions.[161,165,166] Protein-SIP can detect much lower relative isotope abundance than nucleotide SIP.[158] All sequences identified in nucleotide-SIP can be phylogenetically evaluated, e.g., by using BLAST, whereas in protein-SIP proteins can only be identified if the encoding genes were previously determined by a metagenomic approach.[167,168] Therefore, DNA- and protein-SIP have different advantages and their results can be complementary.

Intact-cell activity assay

Intact-cell activity assay is used in the study of bacteria-catalyzed process to investigate biochemical mechanisms and evaluate the activity of the process in the environment. In biochemical experiments, an established biochemical enzyme activity test can be used to isolate enzymes responsible for the activity and search for the encoding genes in the genome, e.g. dehalogenation enzyme activity test, which was working well in identification of a multi-protein reductive dehalogenase complex in *Dehalococooides mccartyi* CBDB1.[169] Besides, activity assay related to biogeochemical process played important roles in ecological research, for example, denitrification enzyme activity assay was used to measure how environmental factors drive the shift of denitrification potentials.[170] In our study, intact-cell activity assay can be established to investigate how bacteria transform SMX and identify related key factors influencing the transformation process.

Compound-specific-isotope-analysis (CSIA)

CSIA has become a robust method to assess natural attenuation of contaminants in the environment,[171] tracing in-situ biodegradation in fields over time or spatially. This method utilizes slightly different reaction kinetics of isotopologues in the first rate-limiting steps where bond cleavage/transformation occurs (compounds that have a lighter isotope at the reactive position may react faster). This slight preferential transformation of lighter isotopologues can

be precisely measured by isotope ratio mass spectrometry (IRMS), in which compounds are separated by GC (GC-IRMS) or HPLC (HPLC-IRMS) and online converted into a simple analyte gas (e.g. CO_2 or H_2) for isotope composition analysis. The extent of isotope fractionation for degradation of contaminants can be quantified by using the Rayleigh equation and expressed as isotope enrichment factor (ε). Pronounced isotope fractionation was observed in selected enzymatic reactions and abiotic transformation (e.g. photolysis).).[40,172] Also often differences between aerobic and anaerobic transformation were identified by CSIA for many compounds including hydrocarbons,[173,174] chlorobenzenes[175] and chlordecone,[176] as distinct isotope fractionations were observed in the activation steps for these transformation process. A recent application of CSIA for emerging micropollutant bromoxynil[177] was reported, where nitrogen fractionation was much larger in the aerobic degradation compared to anaerobic transformation. The isotope fractionation data obtained from lab model strains with known transformation pathways can be applied in field studies to characterize the in-situ biodegradation.[178]

However, isotope fractionation in biological systems can be influenced by cellular mass transfer, as cross-membrane transfer as rate-limiting step prior to bond cleavage mask the real extend of isotope effects in the reaction.[179,180] In order to overcome these masking effects, multi-element isotope fractionation concepts (e.g. C, H) were developed relying on lambda (Λ) values expressing the slope of changing hydrogen and carbon isotope signatures during biodegradation.[178,181,182] Previously, method for carbon isotope analysis of SMX was established on HPLC-IRMS, whereas by applying this method other elements like H, N and S cannot be detected.[183] Hence, carbon isotope fractionation of SMX by microbial aerobic degradation, photolysis and oxidation was investigated, showing low to moderate isotope effects.[38,40,46] To our best knowledge, no data on isotope fractionation for anaerobic transformation of SMX is available. Furthermore, two-dimensional isotope fractionation of SMX during transformation process are also not available.

1.6 Aim of the study

This study focused on microbial degradation and transformation of SMX under aerobic and anaerobic conditions. Environmental samples from hotspots including pig-farm impacted soil, digester sludge from a wastewater treatment plant and sediment from a constructed wetland were taken as representative aerobic and anaerobic samples, high concentrations of SMX were detected in the above mentioned samples, posing risk on development and dissemination of

ARGs and antibiotic resistant bacteria. We aimed to identify key players responsible for aerobic degradation and anaerobic transformation of SMX, filling the knowledge gaps that in-situ aerobic SMX-degraders especially non-cultivable bacteria were not thoroughly investigated, and potentials of anaerobic bacteria on transformation of SMX were previously overlooked. Therefore, in-situ aerobic SMX-degraders in pig-farm impacted soil were identified by means of DNA- and protein-SIP, and anaerobic SMX-transforming cultures were enriched from digester sludge and sediment. Upon the obtainment of anaerobic SMX-transforming cultures, we tried to characterize the transformation process and explore the transformation mechanisms. Furthermore, carbon and hydrogen isotope fractionation during anaerobic transformation of SMX were investigated in laboratory-scale by means of CSIA, attenuation of SMX in the environment could be assessed with the distinct laboratory-scale fractionation data. Together the research gave insight into removal of SMX by microbial activities and provided theoretical support for bioremediation of SMX in the environment.

2 Materials and Methods

2.1 Chemicals

SMX (4-amino-N-(5-methyl-1,2-oxazol-3-yl)benzenesulfonamide), ^{13}C-benzyl-SMX, sulfanilic acid and sulfanilamide were purchased from Sigma-Aldrich at analytical quality. Methanol and formic acid used for UPLC mobile phases were of HPLC grade. All other chemicals used for culture media were obtained from Merck with a purity of at least 98%. Chemicals used in our study were reagent level and above.

2.2 Collection and pre-treatment of environmental samples and pure strains

2.2.1 Pig-farm impacted soil

Surface soils (0-15 cm) were collected from a vegetable garden in Xiamen, Fujian Province, China, which had been regularly irrigated with effluents from a pig farm containing veterinary antibiotics. Soil samples were immediately transferred to the laboratory and air-dried at room temperature. The air-dried soil was thoroughly mixed and sieved through a 2 mm mesh to remove plant debris and stones. Soils were moistened with sterile water to adapt to the original humidity and incubated at 30°C in the dark for two weeks to activate the soil microorganisms. No further substrates were added for this incubation.

2.2.2 Anaerobic samples for enrichment cultivation

Two anaerobic samples from antibiotic hotspots were collected as inocula for establishment of SMX-transforming cultures. One is sediment from a constructed wetland treating pharmaceutical containing waste water (Institute of urban environment, Chinese Academy of Sciences, Xiamen), and another one is digester sludge from a municipal waste water treatment plant (Xiamen, China). Besides, the sediment from the constructed wetland and another digester sludge taken from biogas reactor in Chinese Academy of Agricultural Sciences, Beijing, China were used for enrichment of sulfanilamide/sulfanilic acid-transforming cultures. All samples were stored in 50 mL sterile Falcon tubes (Fisher Scientific, USA) without headspace at 4^{o}C until subsequent operation.

2.2.3 Pure strains

D. vulgaris Hildenborough (DSMZ No. 644) was obtained from German Collection of Microorganisms and Cell Cultures (DSMZ) as a freeze-dried strain.

2.3 Establishment of enrichment cultures and cultivation of pure strains

2.3.1 Establishment of aerobic SMX-degrading cultures from pig-farm impacted soil

One gram of the pig-farm impacted soil (described in 2.2.1) was transferred to 40 mL SMX containing medium (**Table 5**) to enrich aerobic SMX-degrading cultures. The medium for enrichment cultivation was comprised of mineral salts, trace elements (**Table 6**) and vitamin mixture (Vit10, **Table 7**). Either $(NH_4)_2SO_4$ or $NaNO_3$ was provided as nitrogen source (**Table 5**). SMX was added from acetone stock solution accordingly and the final concentrations of SMX in the medium ranged from 350 nM to 200 μM. All the cultivation bottles were closed with cotton septum and incubated on shakers at 250 rpm for the access of oxygen. The SMX concentrations in cultures were monitored via UPLC (described in 2.7.2). The mixed cultures were transferred every three weeks with 10% inoculum. Overall, five passages were established and 16S rRNA gene sequencing was done for the fifth passage. Details on DNA extraction from the cultures and 16S rRNA gene sequencing are described in 2.8.1 and 2.8.2.

Table 5. Components of the medium for enrichment of aerobic SMX-degraders in 1 liter, pH was adjusted to 7.2.

Chemicals	Amounts
Na_2HPO_4	800 mg
KH_2PO_4	200 mg
$MgSO_4 \cdot 7H_2O$	200 mg
$CaCl_2 \cdot 2H_2O$	100 mg
$(NH_4)_2SO_4$/ $NaNO_3$	1000 mg/640 mg
Trace elements (**Table 6**)	1 mL 1000× stock
Vitamin mixture (**Table 7**)	1 mL 1000× stock
SMX	Adding accordingly

Table 6. Components of the 1000x concentrated trace elements in 1 liter, pH was adjusted to 7.0. The solution was sterilized by autoclaving at 121°C for 20 minutes. Note that the following compounds were dissolved in small amount of water separately, except that $FeCl_2$ was dissolved in 300-500 mL water with nitrilotriacetic acid and pH was adjusted to 7.0 by adding NaOH.

Chemicals	Amounts
$ZnCl_2$	70 mg
$MnCl_2 \cdot 2H_2O$	80 mg
H_3BO_3	6 mg
$CoCl_2 \cdot 6H_2O$	190 mg
$CuCl_2 \cdot 2H_2O$	2 mg
$NiCl_2 \cdot 6H_2O$	24 mg
$Na_2MoO_4 \cdot 2H_2O$	36 mg
$FeCl_2$	2 g
Nitrilotriacetic acid	12.8 g

Table 7. Components of the 1000x concentrated vitamin mixture (Vit10) in 1 liter, pH was adjusted to 7.0. The solution was sterilized by filtration with 0.2 µm filters.

Chemicals	Amounts
D(+)Biotin	20 mg
Folic acid	20 mg
Pyridoxine dihydrochloride monohydrate	252 mg
(-)-Riboflavin	50 mg
Thiamine chloride hydrochloride	50 mg
Nicotinic acid	50 mg
Calcium-D(+)-pantothenate	50 mg
p-aminobenzoic acid	50 mg
DL-α-Lipoic acid	50 mg
Vitamin B12	50 mg

2.3.2 Establishment of anaerobic SMX-transforming cultures from sediment and digester sludge

Anaerobic sediment from a constructed wetland set up for treatment of pharmaceuticals including SMX,[184] and digester sludge from wastewater treatment plants with the occurrence of SMX were used as inocula for enrichments. Defined anaerobic medium (**Table 8**) containing mineral salts (**Table 9**) trace elements (**Table 6**), vitamin mixture (**Table 7**), 10 mM $NaHCO_3$ as pH buffer and 0.1% resazurin as a redox indicator was used for enrichment cultivation. 1 mM sulfate or 1 mM nitrate was added as electron acceptors, or 10 mM $NaHCO_3$ in the medium as pH buffer was also used as electron acceptor. The anaerobic medium was prepared by flushing with N_2 for 60 min, and 4 mM cysteine was added as reducing agent (except in nitrate treatments). One gram of sediment or 1 mL of digester sludge was transferred to 100 mL anaerobic medium in an anaerobic glovebox (Coy, USA) to establish mixed cultures. The headspace of cultures was 97% N_2 plus 3% H_2 from the gas phase in the glovebox. SMX was added at a final concentration of 700 nM from a 200 µM acetone stock solution. Subculture were established when half of the added SMX was removed, by transferring a 10% inoculum to fresh SMX-amended medium, and incubation time for one passage lasted two to three weeks. After two passages, particle-free cultures were obtained under methanogenic and sulfate-reducing conditions. All cultures were incubated at 30°C in the dark without shaking. Abiotic 'no-cell controls' (NCC) and 'no-substrate control' cultures (NSC) were set up in parallel and stored as mentioned above. Adsorption of SMX to sludge and sediment was examined in autoclaved biomass treatments (NCC ST and NCC DS) under the same incubation conditions. Cell density was quantified by cell counting after SYBR-Green staining on agarose-coated slides using epifluorescence microscopy.[185]

In the following experiments on characterizing sulfate-reducing mixed cultures, the defined anaerobic medium described in **Table 8** was used for cultivation with some modifications according to the purpose of the experiments. In the results section, we only describe the modified components in each experiment referring to **Table 8**.

Table 8. Components of the defined medium for enrichment of anaerobic SMX-transforming cultures in 1 liter. All the solutions were sterilized separately.

Chemical/solution	Amounts/concentrations
Widdel solution (**Table 9**)[1]	20 mL 50x stock
Trace elements (**Table 6**)[1]	1 mL 1000x stock
Se/W solution[1]	1 mL 1000x stock
Vitamin mixture (**Table 7**)[1]	1 mL 1000x stock
Resazurin (redox indicator)[1]	0.25 mL 0.1% stock
$NaHCO_3$ (pH buffer)[1]	10 mM
Reducing agent (cysteine)[2]	4 mM (except in nitrate treatments)
Electron acceptors[2]	1 mM K_2SO_4 or 1 mM KNO_3 or no additional
Substrate (SMX)[2]	Adding accordingly

[1]are unchanged components in the medium for different experimental set ups (for different mixed cultures and the pure strain *D. vulgaris* Hildenborough).

[2]are variable components (reducing agent, electron acceptors, and substrate) can be changed according to the purpose of experiments).

Table 9. Mineral salts stock solution Widdel solution (50x) to 1 liter.[186] The solution was sterilized by autoclaving at 121°C for 40 minutes.

Chemical	Amounts
KH_2PO_4	10 g
NH_4Cl	13.5 g
NaCl	50 g
$MgCl_2 \cdot 6\ H_2O$	20.5 g
KCl	26 g
$CaCl_2 \cdot 2\ H_2O$	7.5 g

2.3.3 Establishment of sulfonamide/sulfanilic acid-transforming cultures from digester sludge and sediment

Digester sludge and sediment described in 2.2.2 were used as inocula for establishment of sulfonamide/sulfanilic acid-transforming cultures. Defined anaerobic medium (**Table 8**) was prepared as described in 2.3.2 for enrichment cultivation, but no additional electron acceptors

or SMX were added in the medium referring to **Table 8**. Instead, we added 1 mM sulfanilic acid or 0.5 mM sulfanilamide in the medium from acetone stock solution as electron acceptors. One gram of sediment or 0.5 mL digester sludge was added in the defined medium in an anaerobic glovebox (Coy, USA). In addition, 0.3 bar H_2 was gassed in the headspace as electron donor once per week. Samples were taken from each bottle to monitor the concentrations of sulfanilic acid or sulfanilamide via UPLC, details of the measurement method are described in 2.7.5.

2.3.4 Cultivation of *D. vulgaris* Hildenborough

D. vulgaris Hildenborough (DSM 644) was obtained from DSMZ as a freeze-dried strain. Cultivation was done according to DSMZ instructions using *Desulfovibrio* (Postgate) medium (DSMZ No. 63). Inoculation was done under anaerobic conditions within a glove box. Cultures were incubated at 30°C in the dark until the precipitation of black particles (FeS) was observed, indicating sulfate reduction. The active strain (10% v/v inoculum) was then transferred to the medium described in **Table 8** amended with 1 mM sulfate as electron acceptors and 2 mM cysteine as reducing agent. Cell growth was monitored via epifluorescence microscopy.[185] When growth was observed, 100 µM SMX was spiked to the medium. We then monitored SMX concentrations and transformation products in the medium to investigate the role of *Desulfovibrio* in anaerobic transformation of SMX in the sulfate-reducing mixed cultures.

To achieve higher cell density and transformation activity, *D. vulgaris* was then cultivated and maintained in the defined anaerobic medium (**Table 8**) with 21 mM sulfate as electron acceptor, 17.8 mM lactate as electron donor and carbon source, and spiked with 100 µM SMX for more in-depth investigation.

2.4 SIP experiments

2.4.1 Incubation of pig-farm impacted soil with $^{13}C_6$-SMX

This moistened and activated pig-farm impacted soil (described in 2.2.1) was amended either with SMX labeled on all six carbon atoms of the phenyl ring ($^{13}C_6$-SMX) or unlabeled SMX to a final concentration of 20 mg kg^{-1}. For this amendment we prepared SMX stock solution of 2 g L^{-1} with either $^{13}C_6$-labeled or unlabeled SMX in acetone and spread 1 mL of the stock solution to 1 g of dried soil. Then, 1 g of the SMX-amended dry soil was well mixed with 99 g of activated soil. Finally, 10 g of this mixture were distributed to 120 mL brown serum bottles.

Eight replicate bottles with ^{12}C-SMX, eight replicate bottles with ^{13}C-SMX, and six replicate bottles without SMX were incubated at 30°C in the dark (in the following referred to as ^{13}C-SMX, ^{12}C-SMX and control-treatment, respectively). On days 14 and 28, four replicate bottles of each treatment were sacrificed and the soil was stored at -20°C until DNA and protein were extracted.

2.4.2 Density gradient fractionation of DNA from stable isotope labeled soil

CsCl density centrifugation was applied for separation of DNA from stable isotope labeled soil. Approximately 5 µg extracted DNA was applied to a 15 mL sterile plastic screw cap tube containing 1 mL gradient buffer (0.1 M Tris-HCl, 0.1 M HCl, 1.0 mM EDTA, pH=8.0) and 4.9 mL 7.163 M CsCl solution. The refractive index of the solution was determined with a refractometer and adjusted to 1.4029±0.0002, equivalent to a density of around 1.725 g mL^{-1}. The solution was transferred to a polyallomer bell-top ultracentrifuge tube and sealed. Ultracentrifugation was done at 45 000 rpm for 40 h at 20°C (Hitachi CP80WX, rotor type: P65VT2). Then the ultracentrifuge tube was smoothly taken out of the instrument and fixed on a pedestal. A needle connected to a syringe pump was injected into the top part of the tube and a small hole was pierced to the bottom of the tube. Fractions with different buoyant densities were retrieved from the bottom by pumping ink-stained sterile water to the top with a flow of 200 µL min^{-1}. Each fraction (200 µL) was collected in a 1.5 mL sterile Eppendorf tube and the buoyant density was measured with a refractometer to confirm the density distribution. Twenty six fractions were collected and DNA was precipitated from each fraction by adding 400 µL of polyethylene glycol (PEG6000) solution.[187] Then the pellet was washed with 70% ethanol and dissolved in Tris-EDTA buffer for subsequent analysis.

2.4.3 Identification of ^{13}C-labled OTUs in DNA-SIP data

We then compared relative OTU abundances in the corresponding density gradient fractions of the ^{13}C-SMX and the ^{12}C-SMX amended microcosms. A "shifted OTU" was defined as an OTU for which we found different distributions of the relative OTU abundances in the two SMX treatments. The hypothesis was that OTUs incorporating ^{13}C from SMX would be shifted from lighter to heavier fractions in the ^{13}C-SMX treatment. The significance of determined shifts was tested with the G-test[188] algorithm using the "***group_significance.py***" script in QIIME (Quantitative Insights Into Microbial Ecology), which compares the ratio of OTU frequencies in the sample groups according to an extrinsic hypothesis that all sample groups

have equal OTU frequencies. Benjamini-Hochberg FDR adjusted P-values were used (FDR-P) for multiple comparisons.[189]

2.4.4 Metagenome sequencing and construction of a database for mass spectrometric protein identification

Total DNA from the original extraction was handed over to Novogene Bioinformatics Technology (Beijing, China) for shearing and metagenome sequencing on an Illumina Hiseq 2000 platform. From the raw pair-end reads (average of 125 bp) we removed low-quality reads (quality score below 20), reads with more than 10% ambiguous nucleotides, adapter sequences and artificial duplications using cutadapt 1.8.1. Filtered reads were assembled using SOAPdenovo 2.21 and contigs with less than 300 bp were removed. Then the assembly contained a total of 61,954,654 base pairs organized in 97,370 contigs with an average length of 636 bp. Open reading frames (ORFs) were identified and annotated using the Metagenomics Rapid Annotation using Subsystem Technology (MG-RAST) server.[190] The constructed metagenome-based protein database had a total size of 19.1 million amino acids containing 117,003 ORFs with a mean size of 163 amino acids per ORF.

2.4.5 Protein-SIP analysis

For protein identification we converted mass spectrometric raw-data files to mzML format using msconvert (ProteoWizard). The OpenMS MetaProSIP tool[164] was adopted to calculate ^{13}C incorporation into proteins. For this, unlabeled peptides were identified with the OpenMS OMSSA search engine and transferred as featureXML-files to MetaProSIP. MetaProSIP used our translated metagenome database together with centroided mass spectrometric data containing scans from labeled and unlabeled peptides and compared mz values and charges of detected features to calculate the relative amount of incorporated ^{13}C atoms within each labeled peptide (denominated in MetaProSIP as RIA). For each peptide RIA a confidence value 'Cor' is calculated[164] . From the calculated intensities of labeled and non-labeled peaks MetaProSIP also calculates the relative abundance of the labeled peptides (labeled peptide / (labeled peptide + non-labeled peptide), denominated in MetaProSIP as LR). If several peptides of a protein are found to be labeled MetaProSIP calculates the median RIA for a protein (median relative abundance of labeled isotopes within a protein) here referred to as $X(^{13}C)_{LP}$ and the median LR (median relative abundance of a labeled protein forms among all its forms (labeled + non-

labeled)) here referred to as $X(LP)_{\Sigma P}$. We used VBA (Visual Basic for Applications) scripts to export MetaProSIP data to Microsoft Excel to proceed with standard spreadsheet analysis.

For each labeled protein we retrieved the encoding gene from the metagenome nucleotide database. Nucleotide sequences of the identified ORFs were then used for a BLASTn search in the NCBI nucleotide databases to identify the phylogenetic affiliation and closely related sequences. We picked the best BLASTn hit to affiliate a phylogenetic origin to the labeled protein. If a taxonomic family contained at least two labeled proteins with a BLAST score $\geqslant$ 200 it was considered as incorporating ^{13}C. Other labeled proteins with BLAST scores $\geqslant$ 200 that hit a family for which only this single hit was found, the hits were summarized in the overarching phylum. Proteins were functionally classified by BLASTp searching the Gene Ontology protein database.

2.5 Intact-cell activity test for SMX transformation by SRB

Intact-cell activity test with artificial electron donor methyl viologen was established for SMX transformation by SRB. The test was conducted in closed 2 mL glass vials containing reaction mix described in **Table 10**, colorless methyl viologen can be stoichiometrically reduced by titanium (II) citrate to blue radicals as electron mediators. Either concentrated intact cells or cell crude extracts were added in the reaction mix under anaerobic conditions, and the closed vials were incubated at 30°C in the dark until subsequent analysis. Concentrated (50×) intact cells were harvested via three steps centrifugation at 6000 rcf, and cells were washed by phosphate buffer before being added to the reaction mix. Cell crude extracts were obtained by bead-beating for 20 seconds, the procedure was repeated for three times and cooling step was conducted in between to avoid high temperature, the bead-beating tubes were tightly closed until they were transferred to glovebox to avoid interference of oxygen on transformation activities. SMX and transformation products (TPs) in the glass vials were measured on UPLC described in 2.7.2.

Table 10. Composition of reaction mix for intact-cell activity test for SMX transformation by SRB

Ingredients	Final concentration
Anaerobic sterile water	Fill up to the final volume
Potassium phosphate buffer (1 M, pH 6.5)	200 mM
Methyl viologen	1 mM
Ti(III) Citrate	1 mM
Substrate (SMX in acetone)	50 μM/100 μM

2.6 CSIA experiment

2.6.1 Development of a detection method for SMX on GC-MS

An Agilent 7890 series GC (Agilent Technologies, USA) equipped with a 5975C mass spectrometer (Agilent Technologies, USA) and a CombiPAL autosampler (CTC Analytics AG, Switzerland) was used to set up the separation method for SMX. For chromatographic separation, a Zebron ZB-1 column (60 m × 0.32 mm × 0.25 μm; Phenomenex, Germany) with a constant carrier gas flow of 2.0 mL min^{-1} was used. The temperature program was as set as: 40°C for 5 min, then increase to 330°C at the rate of 10°C/min, and hold for 20 min. The injector temperatures was tested from 180°C to 260°C in steps of 20 degrees. Samples were injected in split mode (1:10) with injection volumes of 1 μL.

2.6.2 Analysis of carbon and hydrogen stable isotopes ratios on GC-IRMS

Carbon and hydrogen stable isotope ratios of SMX were measured by GC-IRMS. SMX was separated via an Agilent 7890 series GC (Agilent Technologies, USA) on a Zebron ZB-1 column using the same temperature program as described for GC-MS analysis, and further converted to either CO_2 or H_2 in a GC IsoLink interface (Thermo Fisher, Germany). A combustion reactor was held at 1000°C with a CuO/NiO catalyst for carbon conversion[176] and a pyrolysis reactor was held at 1400°C with chromium catalyst for hydrogen conversion.[191] The combustion reactor or the pyrolysis reactor was connected via a ConFlo IV open split system to a MAT 253 IRMS (Thermo Fisher, Germany) for carbon or hydrogen isotopes analysis respectively. Samples were injected into the GC via split/splitless injection mode.

The combustion reactor was oxidized by flushing with O_2 after several times analysis. Injection volumes were 1-5 μL adapting to SMX concentrations in samples. A EuroEA3000 elemental analyzer (EA, HEKAtech) was used to analyze the bulk stable isotope ratios of SMX.[192] Bulk

carbon isotope ratios were measured via a combustion reactor converting carbon to CO_2, and hydrogen isotope ratios were measured via a pyrolysis reactor converting hydrogen to H_2. The elemental analyzer conditions were set as: reactor temperature as 1050°C, carrier gas flow rate as 75 mL min^{-1} and purge flow rate as 50 mL min^{-1}.

Isotope ratios were defined as delta notation ($\delta^{13}C$ or $\delta^{2}H$) based on equation (1)

$$\delta^{13}C \text{ or } \delta^{2}H = \frac{R_{sample}}{R_{standard}} - 1 \quad (1)$$

R_{sample} and $R_{standard}$ are the ratios of $^{13}C/^{12}C$ or $^{2}H/^{1}H$ of the sample or the international standard, respectively. The international standard for carbon isotopes is Vienna Dee Belemnite (VPDB) and the one for hydrogen isotopes is Vienna Standard Mean Ocean Water (VSMOW). The delta notations are expressed in Ur (Urey) according to recent IUPAC recommendations (1 mUr = 1‰). The detection precision is determined by less abundant isotopes.

2.6.3 Quantification of isotope fractionation (ε and Λ)

The linearized Rayleigh equation (2) was used to express the quantitative relationship between isotopic composition and degree of degradation.

$$\ln \frac{\delta_t + 1000}{\delta_0 + 1000} = \varepsilon \times \ln \frac{C_t}{C_0} \quad (2)$$

δ_t and δ_0 are the isotope ratios at one time point t and at the beginning of the degradation; c_t and c_0 are the corresponding concentrations of SMX at time point t and 0. ε is the enrichment factor deciphering the relationship between the change of isotope ratios and degradation induced decreases in concentrations.

The lambda value ($\Lambda^{H/C}_{bulk}$) was introduced for dual isotope (C-H) analysis, the hydrogen versus carbon isotope signatures were plotted and the $\Lambda^{H/C}_{bulk}$ was derived from the slope of linear regression according to equation (3).

$$\Lambda^{H/C}_{bulk} = \frac{\Delta\delta^{2}H_{bulk}}{\Delta\delta^{13}C_{bulk}} \quad (3)$$

The uncertainty of the enrichment factors and the $\Lambda^{H/C}_{bulk}$ value were given as the 95% confidence interval, derived from linear regression. Qualities of the enrichment factors and the

$\Lambda^{H/C}_{bulk}$ value were evaluated by the correlation parameter in linear regression (R^2), the respective isotope fractionation was regarded as significant if R^2 is higher than 0.8.

The AKIE (apparent kinetic isotope effect) values were introduced to link observable bulk stable isotope fractionation to transformation pathways.[193] In this case, isotope fractionation factors were adjusted based on number of atoms located at reactive positions responsible for bond changes. Therefore, bulk isotope ratios (δ_{bulk}) were converted to bulk isotope ratios of reactive positions ($\delta_{\text{reactive position}}$) in equation (4), and the enrichment factor of the reactive position ($\varepsilon_{\text{reactive position}}$) was calculated based on the corrected $\delta_{\text{reactive position}}$ and linearized Rayleigh equation.

$$\delta_{reactive\ position}=\delta_{bulk} \times \frac{n}{x} \quad (4)$$

Here, *n* is the total number of atoms for one element and *x* is the number of atoms at the reactive positions.

Apart from the correction for enrichment factors of the reactive position ($\varepsilon_{\text{reactive position}}$), the calculation of AKIE values was also based on a second correction due to the location of nondiscriminable atoms of one element at the reactive position in equation (5).

$$\text{AKIE}=\frac{1}{1+z \times \varepsilon_{\text{reactive position}}/1000} \quad (5)$$

Here, z is the number of nondiscriminable atoms of one element at the reactive positions

The uncertainties of AKIE values were calculated by error propagation in equation (6).

$$error\ of\ AKIE = \left|\frac{\partial AKIE}{\partial \varepsilon_{reactive\ position}}\right| \times error\ of\ \varepsilon_{reactive\ position} \quad (6)$$

2.6.4 Extraction of SMX from cultures

In order to reach the detection limit of SMX on GC-IRMS, SMX was extracted from cultures via solid phase extraction (SPE) and concentrated in acetone for analysis. The SPE cartridge (Waters HLB OASIS 6cc/500 mg) contains a universal polymeric reversed-phase sorbent often used for pharmaceutical analysis. Cultures were centrifuged at 2,000 rcf (Eppendorf 5424R) for 10 min to remove particles and avoid interference on cartridge's filling. For pre-conditioning and equilibration, SPE cartridges were rinsed with 6 mL acetone, 6 mL methanol and 6 mL MQ water sequentially at the flow rate of 2 mL min^{-1} (drop by gravity). 180 mL (or 120 mL, depending on the SMX's residual concentration) of cultures were loaded on SPE

cartridge at the flow rate of 2 mL min^{-1} by applying vacuum pump. After sample loading, 12 mL of 5% methanol in water was added to wash the cartridge. Elution of SMX from the cartridge was performed by adding 9 mL methanol. The eluate was collected, concentrated under a continuous nitrogen stream until dryness and dissolved in 200 µM acetone. The concentrated samples were stored at -20°C for subsequent UPLC and GC-IRMS measurement.

2.7 Analytical methods

2.7.1 Gas measurement

Headspace CO_2 concentrations were measured by GC with thermal conductivity detection (GC-TCD, Agilent 7890A, USA) connected to a custom-designed robotized incubation system composed of a water bath incubator and an autosampler. Headspace samples were taken every three days. The average soil respiratory activity was calculated as CO_2 production per kilogram dry soil per day. Gas samples were manually collected every three days for $^{13}CO_2$ measurement using GC-IRMS (Thermo Finnigan Delta V Advantage, Germany). After each measurement, the headspace was completely replaced with sterile fresh air to avoid inhibition from CO_2 accumulation.

2.7.2 Sample preparation and SMX analysis by UPLC

SMX is water soluble and can be analyzed directly from the medium without extraction. For that, 1 mL culture sample was centrifuged at 10,000 rcf for 10 min to remove particles and bacterial cells, and 750 µL of the supernatant was transferred to a 2 mL glass vial. UPLC analysis was done at room temperature by injecting 10 µL of the sample to an UltiMate 3000 UPLC system (ThermoFisher) equipped with a C_{18} column (LiChrospher 100 RP-18, endcapped, 5 µm; Merck) and a diode array detector (DAD). The flow rate was set as 0.6 mL min^{-1}. The mobile phase was composed of solution A (0.1% formic acid in Milli-Q water) and solution B (HPLC grade methanol) and the following gradient was used: 0-1.25 min: 95% solution A and 5% solution B, 1.25 min to 8 min: 95% to 2% solution A and 5% to 98% solution B, 8 min to 10 min: 2% to 95% solution A and 95% to 5% solution B, 10 min to 17 min: 95% solution A and 5% solution B. The column equilibrated in the last 7 minutes of this program. We collected absorbance data from 190 to 400 nm and SMX was quantified at 270 nm against external analytical standards.

2.7.3 Identification of TPs by mass spectrometry

For product identification we coupled the effluent line of our UPLC-DAD system with the heated electron spray ionization chamber (HESI-II, Thermo Fisher) of an Orbitrap Fusion high-resolution mass spectrometer (Thermo Fisher). Separation was done using a Hypersil Gold C_{18} column (150 x 2.1 mm, 3 µm; Thermo Fisher). With the coupled system, peaks of SMX and SMX transformation products were monitored simultaneously on a DAD and the Orbitrap mass analyzer. Ionization was done in positive mode. To avoid salt contamination of the ionization source, we directed the effluent within the first 5 min of each analysis to a waste bottle using a valve in the connection line. Peaks in the precursor mass spectra were correlated with peaks in the DAD signals. Target peaks were then isolated by the embedded quadrupole in the Orbitrap Fusion and fragmented using higher-energy collisional dissociation (HCD, 30% Thermo units) fragmentation.

2.7.4 Measurement of sulfate and sulfide in cultures

Sulfate and sulfide concentrations were measured to monitor metabolic status of sulfate-reducing bacteria. One mL sample was taken from cultures and centrifuged at 10,000 rcf for ten minutes at room temperature, then 0.5 mL supernatant was transferred to vials with filtered caps. Dionex-120 Ion chromatograph equipped with an IonPac AS4A-SC (4 mm×250 mm) column was used for sulfate analysis, the composition of isocratic mobile phase was 4.5 mM Na_2CO_3 and 4.5 mM $NaHCO_3$ with a constant flow rate of 1.0 mL min^{-1}. The linear response was confirmed in a range between 10 and 1000 µM, the retention time of sulfate was 30 min. Sulfide in cultures were quantified photometrically as fresh colloidal CuS,[194] 0.5 mL sample was withdrawn from cultures and mixed with 4 mL acidic $CuSO_4$ solution (5 mM CuSO4 and 50 mM HCl) in a 12 mL reagent tube, the content was transferred in a cuvette and measured absorption at 480 nm, besides, the background absorption of acidic $CuSO_4$ solution was also measured.

2.7.5 Measurement of sulfanilic acid and sulfanilamide in cultures

Sample preparation from cultures is described in 2.7.2. UPLC system (ThermoFisher) equipped with a C_{18} column (LiChrospher 100 RP-18, endcapped, 5 µm; Merck) and a diode array detector (DAD) was used for measurement of sulfanilic acid and sulfanilamide. Both sulfanilic acid and sulfanilamide are hydrophilic compounds, and can be eluted easily as the retardation of C18 column is weak. The same gradient was used for both compounds, gradient buffer

composing of solution A (0.1% formic acid in Milli-Q water) and solution B (HPLC grade pure methanol) was set as: 0-1.25 min: 90% solution A and 10% solution B, 8 min: 70% solution A and 30% solution B, 10 min: 90% solution A and 10% solution B, 17 min: 90% solution A and 10% solution B. The flow rate was constant as 0.6 ml min^{-1} and the injection volume was 10 µL. The absorbance wavelength for sulfanilic acid was 250 nm and for sulfanilamide was 260 nm.

2.7.6 Measurement of lactate and acetate in the cultures

Sample preparation from cultures is described in 2.7.2. UPLC system (UltiMate 3000, ThermoFisher) equipped with a Rezex ROA organic acid column (Phenomenex, H+ 8%, 150 × 7.8 mm) and a diode array detector (DAD) was used for lactate and acetate measurement. The detection range for lactate and acetate was from 0.5 µM to 50 mM. Isocratic program was applied here with 2.5 mM H_2SO_4 as mobile phase, running with the flow rate as 0.5 mL min^{-1} for 15 minutes for one sample. The injection volume was 10 µL. The peak of lactate was detected at 10.52 min, and the retention time for acetate peak was 12.80 min. Both lactate and acetate were quantified at 210 nm against an external analytical standard curve.

2.8 Biological methods

2.8.1 DNA extraction from soil and cultures

The soil in incubation experiment was thoroughly mixed by shaking flasks and DNA was extracted from 0.5 g soil using FastDNA® SPIN Kit (MP Bio, USA) according to the manufacturer's instructions. DNA of enrichment cultures was extracted from 1 mL cultures by using NucleoSpin Tissue kit (Genomic DNA from tissue, MACHEREY-NAGEL). The concentration and quality of extracted DNA were evaluated with a UV-VIS spectrophotometer (ND-1000, NanoDrop, USA) and DNA was then stored at -20°C for subsequent analysis.

2.8.2 Quantification of 16S rRNA gene and sequencing of 16S rRNA gene amplicon

DNA samples from density gradient fractionation treatment were screened before sequencing. The abundance of total 16S rRNA genes was analyzed in each fraction by qPCR with universal primers[20] using a LightCycler® 480 (Roche, Pleasanton, CA, USA). The seven fractions with the highest abundance of 16S rRNA genes were selected for Illumina sequencing. For each

OTU the relative abundance in a fraction was calculated by relating the number of curated paired reads within the OTU to the overall number of curated paired reads in a fraction.

Both DNA extracted from soil samples and enrichment cultures were sequenced. The V4/V5 region of 16S rRNA gene[195] were amplified, purified and sequenced using an Illumina Hiseq2500 platform (Novogene Bioinformatics Technology, Beijing, China). An average of 50,000 reads were produced for all DNA samples. Raw paired-end reads were assembled after filtering adaptor sequences and removing low-quality reads, ambiguous nucleotides and barcodes to generate clean sequences. The resulting high quality sequences were analyzed for their phylogenetic affiliation using QIIME,[189] resulting in a set of operational taxonomic units (OTU) for each DNA sample.

2.8.3 Protein extraction, separation, digestion and mass spectrometric analysis

Protein was extracted from 5 g of soil using the MOBIO NoviPure™ soil protein kit (QIAGEN, Germany) according to the manufactures' protocol. The protein pellet was re-suspended in 100 µL of rehydration buffer (7 M urea, 2 M thiourea and 2% CHAPS) and proteins were quantified using a 2-D Quant kit (GE Healthcare, UK). The protein extract was then separated by sodium dodecyl sulfate polyacrylamide gel electrophoresis (SDS-PAGE) and Coomassie stained to estimate its size range. The extract was stored at -20°C until mass spectrometric analysis was done.

For mass spectrometric analysis soil protein extracts from labeled and unlabeled samples were first applied to a short run on an SDS-PAGE (4% stacking gel and 12% running gel) to remove contaminants. The protein containing gel part (~2 cm) was cut into four slices. Gel slices were then washed in 50 mM ammonium bicarbonate and reduced with 10 mM dithiothreitol in 50 mM ammonium bicarbonate for 30 min at room temperature. Then, cysteine residues were alkylated by incubation with 100 mM iodoacetamide in 50 mM ammonium bicarbonate for 30 min at room temperature in the dark. Subsequent in-gel digestion was performed by adding 0.1 µg of porcine trypsin (Proteomic Sequencing Grade, Promega, US) and incubating at 37°C overnight. Then peptides were extracted twice by incubation in 50% (v/v) acetonitrile and 5% (v/v) formic acid for 10 min. Extracted peptide samples were desalted using C18 Zip Tip columns (Millipore) before they were analyzed via nLC-MS/MS using an Orbitrap Fusion mass spectrometer (Thermo Fisher Scientific, Germany) coupled with a nanoHPLC system (nanoAcquity, Waters, US) via an TriVersa NanoMate (Advion, Ltd., Harlow, UK).[196] Peptides were separated at 35°C on a 15 cm analytical column (Acclaim PepMap RSLC, 2 µm

C18 particles, Thermo Scientific) using a 90 min linear gradient from 4% to 55% solvent A (0.1% formic acid) to solvent B (80% acetonitrile, 0.08% formic acid). Precursor ions were measured in the Orbitrap analyzer at a resolution of 120, 000; fragmentation was done at 30% CID (collision-induced dissociation) and measured in the ion trap at a resolution of 15, 000.

2.8.4 Toxicity test of SMX transformation products

For toxicity tests we used the SMX-susceptible strain *E. coli* K-12 (DSM 498). It was cultivated on LB-plates and then stored at 4°C. One day before inoculation it was transferred into liquid LB medium and incubated overnight at 37°C. Initial SMX toxicity tests were set up in mineral medium with 1 mM sulfate, 20 mM glucose and 3-100 µM SMX that was inoculated with 3% (v/v) *E. coli* and incubated at 37°C on a rotary shaker. Growth was monitored by spectrophotometer at the wavelength of 600 nm (OD600).

Because we could not commercially obtain SMX transformation products, we set up further toxicity tests in spent medium. For this we used a batch of SMX-transforming mixed cultures initially set up with different initial SMX concentrations (100, 150, 250, 400, 600 and 750 µM) and 1 mM sulfate that had been incubated for 14 months. After this time SMX was transformed and we filtered the cultures to obtain the sterile supernatant with the SMX transformation products through 2 µM filters. As a comparison we used medium of negative controls in which no transformation of SMX occurred during the 14 months incubation period. All tests were done in duplicates. The filtered media were then amended with 20 mM glucose, inoculated with 3% (v/v) fresh *E. coli* K12 and incubated at 30°C under agitated aerobic conditions. Growth was monitored by spectrophotometer at the wavelength of 600 nm (OD600). Concentrations of SMX and transformation products were monitored by UPLC-DAD.

3 Results

3.1 Key players in aerobic SMX degradation in pig-farm impacted soil

SMX is persistent in different environmental compartments and enriched in agricultural soil contaminated by manure.[197] Microbial degradation contributes to depletion of SMX in soil while isolated degraders based on cultivation technique could not be a real representative of in-situ degrading populations. Therefore, we applied SIP techniques along with conventional cultivation to identify in-situ SMX-degraders in agricultural soil. The agricultural soil was collected from a vegetable garden associated with a pig farm in Fujian Province (China). The vegetable garden was regularly fertilized with SMX-containing pig manure and irrigated with the effluents from the pig farm. Aerobic SMX-degrading mixed cultures were enriched from the agricultural soil. Besides, we hypothesized that we would be able to trace ^{13}C from $^{13}C_6$-labled SMX into specific microbial populations, assuming that strongly ^{13}C-incorporating populations play a major role in SMX degradation. To address this hypothesis, we incubated soil microcosms with 20 mg kg^{-1} SMX for 30 days, and monitored the shift of the soil microbial community, respiration of the soil microorganisms, mineralization of SMX, and integrated DNA- and protein-SIP to obtain complementary results on the identification of SMX-degrading microorganisms. The added concentration of SMX was a compromise between natural conditions and the detection limit of SIP. Identification of key players in SMX degradation in hotspots is crucial for better understanding the fate of SMX and remediation of contaminated sites.

3.1.1 Enrichment of aerobic SMX-degrading cultures from pig farm impacted soil

To enrich cultivable SMX-degraders, the pig-farm impacted soil was used as inocula and incubated with 350 nM SMX in mineral salts medium described in **Table 5**. We established five passages and each passage lasted for 3-4 weeks, and the added SMX concentrations increased from 350 nM to 200 µM along the five passages. Degradation of SMX was observed in each passage. In the passage one with 350 nM SMX, no significant degradation of SMX was observed for the first 7 days, but after 16 days incubation 90% of the spiked SMX was degraded (**Figure 8**). For the following passages, similar trends on the lag phase and the degradation ratio were recorded with higher SMX concentrations up to 200 µM (data not shown here). To investigate the bacterial composition of the aerobic SMX-degrading cultures, 16S rRNA gene sequencing was conducted for the passage 5 of the aerobic SMX-degrading cultures. The genus

Sediminibacterium dominated the community accounting for 34% of the population, besides, the genera *Phyllobacterium* and *Mycobacterium* with the family *Alcaligenaceae* also accounted for more than 10% of the population (**Figure 9**). However, none of these above-mentioned dominant bacteria were previously reported as isolated SMX-degraders in the literature.

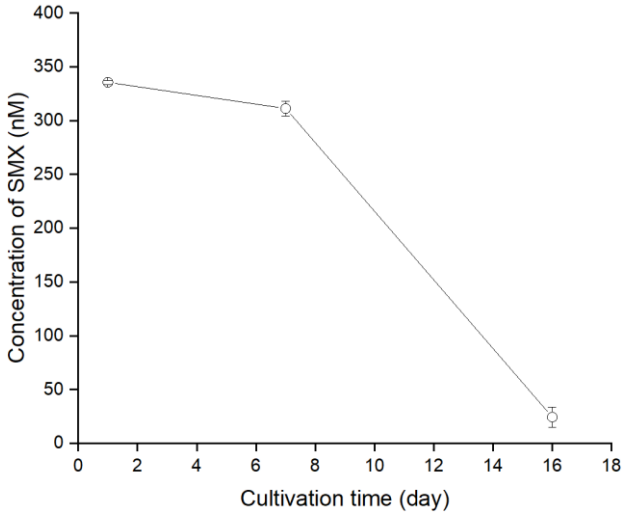

Figure 8. Degradation of SMX in the aerobic mixed cultures enriched from pig-farm impacted soil. The passage one is shown here.

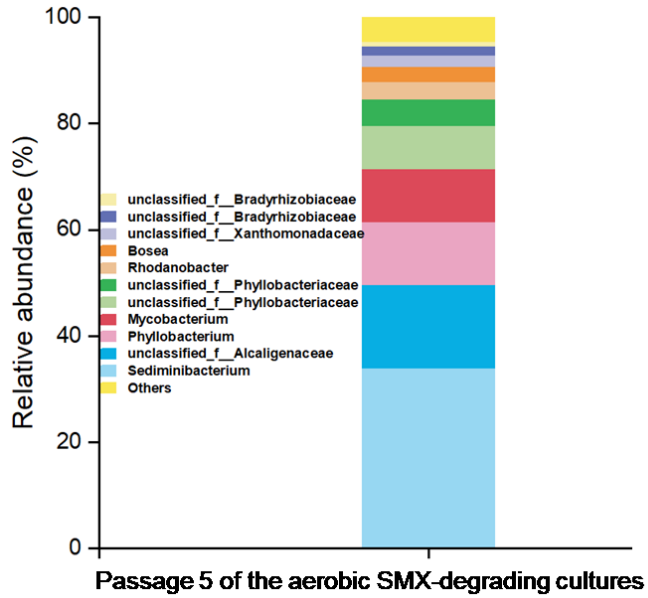

Figure 9. Population analysis of the aerobic SMX-degrading cultures enriched from pig-farm impacted soil, analyzed by 16S rRNA gene amplicon sequencing. The passage 5 is shown here. Only the 10 most abundant taxa are shown individually, all others are summarized as "Others". For the unclassified genera their family is also indicated in the legend.

3.1.2 Effects of SMX on bacterial respiratory activities and community structures in soil

In parallel with enrichment of aerobic SMX-degrading cultures from the soil, we also incubated the soil either with ^{13}C labeled SMX or unlabeled SMX to identify the aerobic in-situ SMX-degraders in soil, as well as to monitor the effects of SMX on soil microorganisms and mineralization of SMX in soil. For the effects of SMX on soil microorganisms, we focused on bacterial respiratory activities by monitoring the evolution of CO_2, and bacterial community structures by population analysis. In soil microcosm incubations, SMX significantly decreased the production of CO_2 compared to control soil without SMX within the first 21 days (**Figure 10**a) In all samples the bacterial communities were dominated by *Actinobacteria* (21.9%-30.8%) (**Figure 11**b), *Chloroflexi* (19.8%-21.4%), *Gemmatimonadetes* (9.4%-13.4%), *Proteobacteria* (11.0%-12.7%), *Acidobacteria* (5.2%-8.5%) and *Firmicutes* (2.5%-8.3%) (**Figure 11**a). No strong changes of the bacterial community compositions at phylum level were observed within the incubation time or after the addition of SMX (**Figure 11**a). Only a principal component analysis of the bacterial community at OTU level revealed that the original sample and the control samples without SMX from two different time points separated into well separated clusters (**Figure 10**b). All SMX-amended samples together formed a fourth well-separated cluster, demonstrating that SMX addition significantly changed the structure of the bacterial community in soil (ANOSIM test, R=0.81, P<0.001).

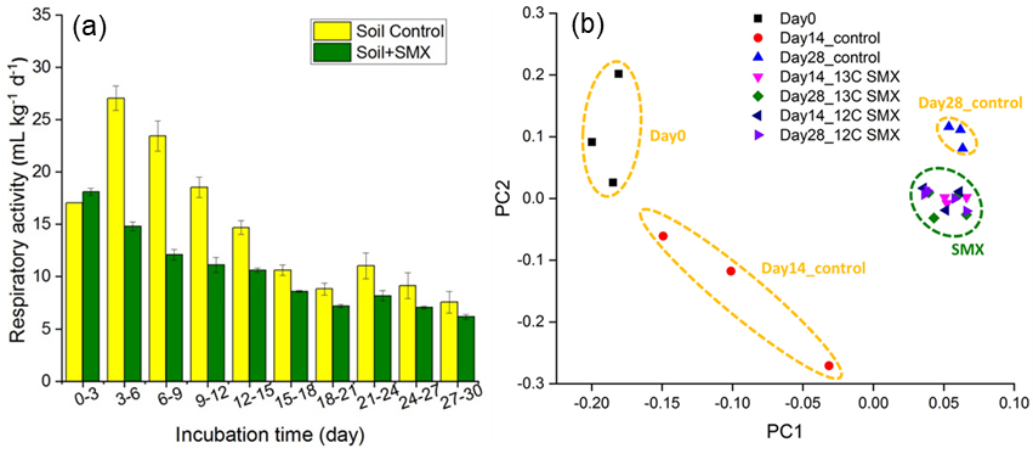

Figure 10. Effects of SMX on soil bacterial community. **a)** Respiratory activity in soil microcosms. Soil respiratory activity with ^{12}C-SMX (shown here as "Soil+SMX") or without SMX was measured as CO_2 production per kg of soil per day. The shown data represents the average of quadruplicate bottles ± SD within the indicated three days. **b)** Principle Component Analysis (PCA) showing the difference of microbial community structures at OTU level depending on incubation time and presence or absence of SMX.

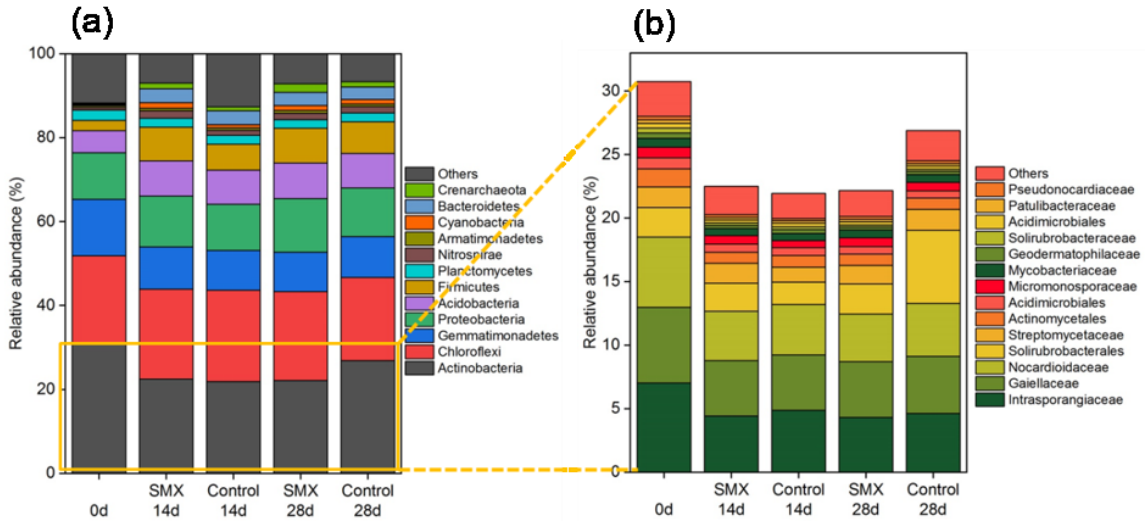

Figure 11. Population analysis of the microbial community after different incubation times with ^{12}C-SMX and in controls without SMX. Incubation times of 0, 14 and 28 days are shown. Shown are average values of four replicates. **a)** Total population analysis on phylum level; **b)** members of the phylum *Actinobacteria* classified on the family level.

3.1.3 Mineralization of SMX in soil

To evaluate the mineralization of SMX in soil, the evolution of $^{13}CO_2$ was measured for 30 days during the incubation period. In $^{13}C_6$-SMX-amended soil incubations, an increase of the $\delta^{13}C$ value of $^{13}CO_2$ in the gas phase demonstrated that partial $^{13}C_6$-SMX mineralization occurred. The amount of evolved $^{13}CO_2$ during each successive 3-day period gradually increased over time to a value higher than 20‰ after about one-month of incubation (**Figure 12**). Such a continuous increase of $^{13}CO_2$ production per time unit from $^{13}C_6$-SMX indicated an enrichment of SMX-mineralizing microorganisms. However, the total amount of carbon released from $^{13}C_6$-SMX as ^{13}C-CO_2 was low and estimated to be at around 0.5% of the added SMX-carbon.

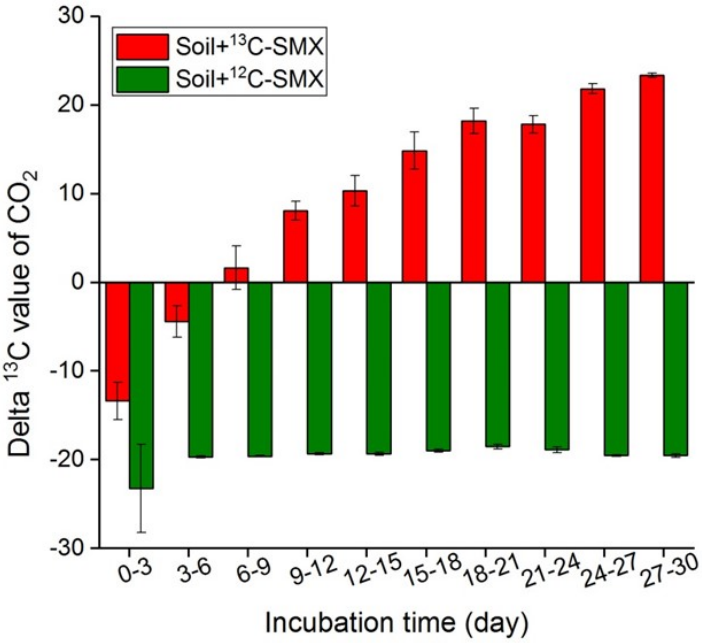

Figure 12. Production of ^{13}C-labeled CO_2 within 3-day periods in soil microcosm amended with ^{13}C-SMX or ^{12}C-SMX during 30-day incubation. The data is given in δ-notation as the difference of carbon isotope ratios relative to the VPDB standard of CO_2 from the headspace. Each bar shows the ^{13}C-CO_2 value for every 3 days during incubation. After each measurement the gas phase was completely exchanged with sterile fresh air to avoid inhibition of CO_2 to soil microorganisms. δ-notation values of the ^{12}C-SMX treatment are consistent with natural abundance.

3.1.4 Identification of potential in-situ SMX-degraders by DNA-SIP

The assimilation of ^{13}C from ^{13}C-SMX to bacterial biomass was traced in bacterial DNA to identify the phylogeny of in-situ SMX-degraders. DNA was extracted from the soil in ^{12}C- and $^{13}C_6$-SMX treatments and labeled DNA was separated from non-labeled DNA by CsCl density centrifugation. Seven DNA-containing fractions were selected from each treatment (**Figure 13**) and the identity and the relative abundance of OTUs were determined for each fraction. OTUs with significantly different distribution of the relative abundances across the fractions in $^{13}C_6$-SMX treatments compared to ^{12}C-SMX treatment are defined as "shifted OTUs". The total number of such shifted OTUs ranged from 7 to 86 for the different fractions, representing 0.1-0.6% of all detected OTUs (**Table S1**). In the three lighter fractions (fraction 5 to 7) the numbers of significantly enriched and the numbers of significantly diminished OTUs in the $^{13}C_6$-SMX treatment were almost identical. In contrast, in the heavier fractions most shifted OTUs (70-90%) were enriched in the ^{13}C-treatment (**Table S1**). Looking at overall shifting patterns, 13 OTUs showed clear light-to-heavy shifting and they were all affiliated to the phylum *Actinobacteria.* Among them there were OTUs affiliated to the families

Nocardioidaceae, *Intrasporangiaceae* and *Gaiellaceae* and OTUs affiliated to the order *Solirubrobacterales* (**Figure 14**). Eight of these 13 OTUs showed the expected shifting pattern for bacteria incorporating ^{13}C from $^{13}C_6$-SMX by being diminished in the lighter fractions and enriched in heavier fractions. The other five shifted OTUs were preferentially enriched in the heavier fractions but contained some irregularities by being enriched across all fractions or not being enriched in the heaviest fraction. In addition to these 13 OTUs with clear light-to-heavy shifting pattern, other OTUs were detected to be significantly shifted, but their pattern was so irregular that incorporation of ^{13}C from $^{13}C_6$-SMX was ambiguous. These OTUs were affiliated to the class *Ktedonobacteria*, order *Xanthomonadales* and family *Streptomycetaceae*. In summary, bacterial species belonging to the families *Nocardioidaceae, Intrasporangiaceae and Gaiellaceae* and bacteria belonging to the order *Solirubrobacterales* were inferred as potential SMX-degrading populations, among which the families *Intrasporangiaceae* and *Nocardioidaceae* showed the strongest shifts in population abundance (**Figure 14**).

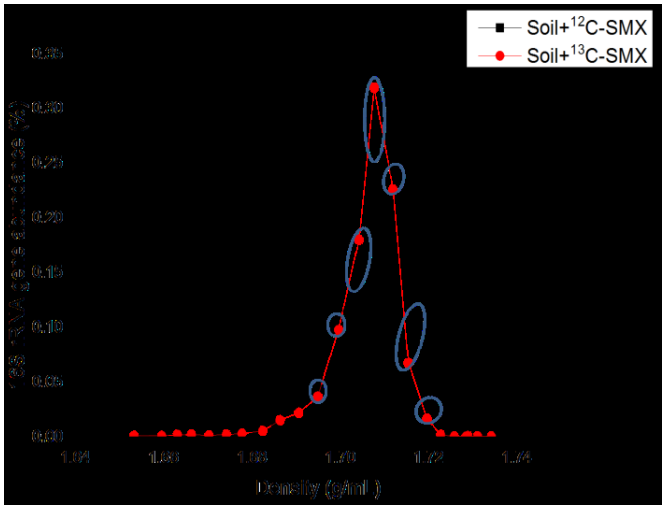

Figure 13. The abundance of 16S rRNA genes relative to all detected 16S rRNA genes in one treatment in 26 eluent fractions for the ^{12}C-SMX treatment (black line) and the ^{13}C-SMX treatment (red line) after 14 days of incubation. The blue circles indicate the seven fractions selected for population analysis (fraction 1 to fraction 7).

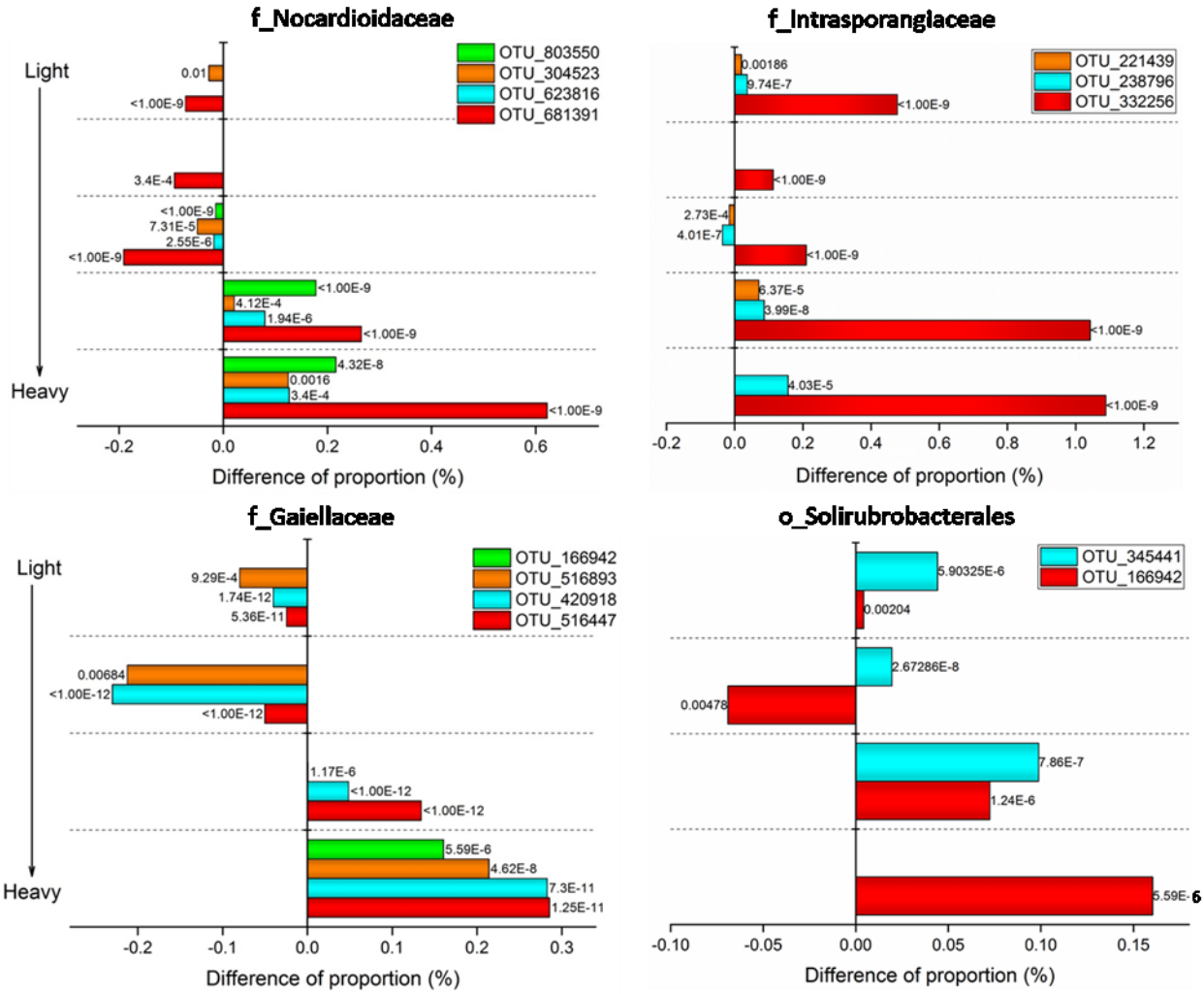

Figure 14. Distribution patterns of OTUs showing clear shift of their occurrence from light-to-heavy gradient fractions after growing in ^{13}C-SMX-amended soil. OTUs were affiliated to the families *Nocardioidaceae*, *Intrasporangiaceae* and *Gaiellaceae* and the order *Solirubrobacterales*. The x-axis represents the absolute difference of proportion of OTUs from ^{13}C-SMX treatments compared with that in the ^{12}C-SMX treatment; the y-axis represents different buoyant density fractions. Numbers on data bars indicate FDR p-values generated from the G-test (describe in 2.6.3). OTUs affiliated to the same taxonomy entity were grouped together in one panel and only OTUs with $p<0.05$ are shown. Significant light-to-heavy shifts were concluded if significant ($p<0.05$) opposite changes in light and in heavy fractions were obtained. Shown are fractions 1, 2, 3, 4, 7 for *Nocardioidaceae*, fractions 1, 2, 3, 4, 7 for *Intrasporangiaceae*, fractions 1, 2, 3, 7 for *Gaiellaceae*, and fractions 1, 2, 3, 7 for *Solirubrobacterales*.

3.1.5 Taxonomic affiliation of ^{13}C-labeled proteins

Protein-SIP was done with the SMX-degrading community to independently evaluate the DNA-SIP results. Total proteins were extracted from the incubated soils for the identification of ^{13}C labeled proteins. From the samples collected after 14 days of incubation, a total of 185 labeled proteins were identified applying a threshold of 10% for both values $X(^{13}C)_{LP}$ and

$X(LP)_{\Sigma P}$, reflecting significant isotope incorporation.[164] We clustered these 185 labeled proteins into four categories based on the quality of the taxonomic affiliation as judged by the BLASTn scores against the NCBI nt database (**Figure 15**a): 69 labeled proteins were highly reliably affiliated with BLASTn scores of ⩾ 200, 28 labeled proteins were medium reliably affiliated with a BLASTn scores of 80-200, 16 labeled proteins were weakly reliably affiliated with BLASTn scores between 50 and 80, and 72 of these labeled proteins were matching our metagenome database but could not be affiliated to any taxon by comparison with the NCBI databases. All the 113 identified taxonomic affiliations (high, medium and low score affiliations together) were among the phyla *Proteobacteri*a, *Actinobacteria* or *Bacteroidetes,* 40 of the 69 high score affiliations (=61%) were to the family *Intrasporangiaceae* within the phylum *Actinobacteria* whereas other high-score affiliations were to the *Conexibacteraceae* (7%), *Nocardioidaceae* (6%) and *Sphaerobacteraceae* (6%) (**Figure 15**a).

We then compared the 113 taxonomic affiliations obtained from protein SIP with those from DNA-SIP. Only seven protein categories were shared by different organisms, the rest could be affiliated to one single bacterial group. Three out of four organism groups identified by DNA-SIP to incorporate ^{13}C from SMX were also detected as host of labeled proteins (red diamonds in **Figure 15**b). These three groups were the families *Intrasporangiaceae*, *Nocardioidaceae* and the order *Solirubrobacterales* with its subfamilies *Conexibacteraceae* and *Patulibacteraceae*. Indeed, 90% of the communities labeled by both DNA- and protein-SIP were contained within the group of high-score affiliated proteins during protein-SIP (green highlighted boxes in **Figure 15**a).

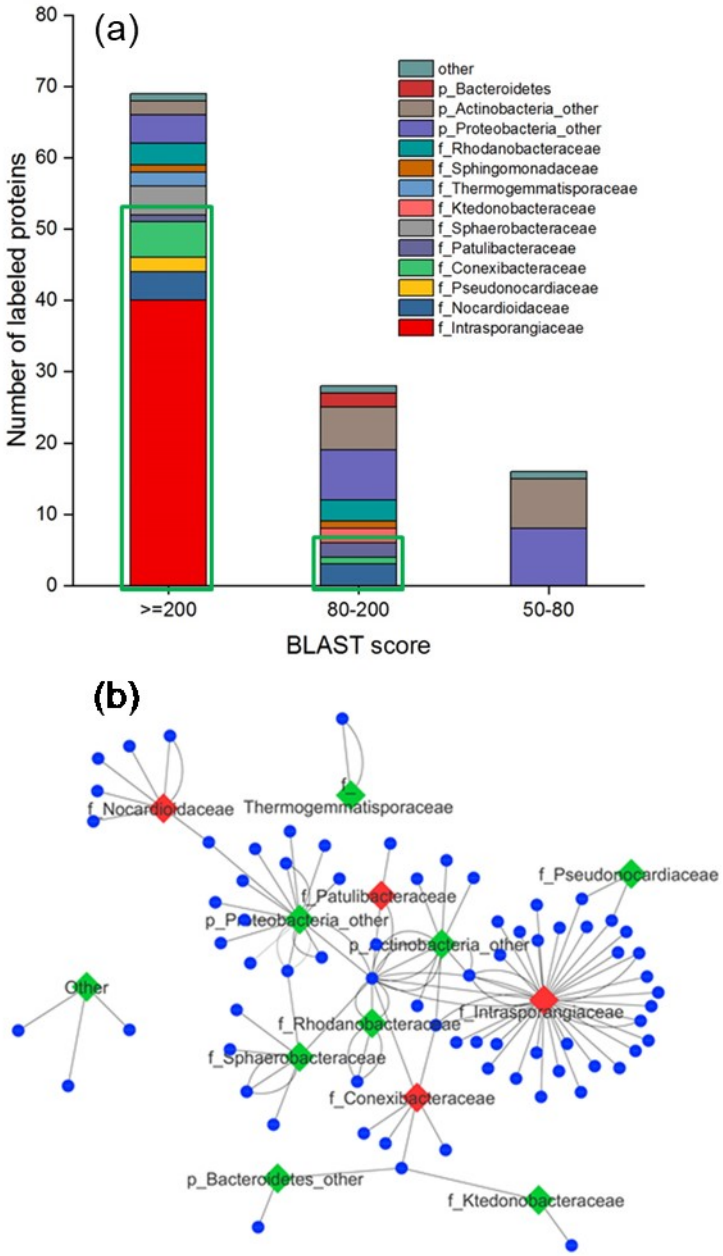

Figure 15. Taxonomic affiliation of ^{13}C-labeled proteins after incubation with ^{13}C-SMX for 14 days. **a)** Taxonomic affiliation of labeled proteins categorized by BLASTn scores (≥ 200 as high score, 80-200 as medium score, 50-80 as low score, in line with standard NCBI settings). The green boxes highlight taxonomic families that were also labeled in the DNA-SIP experiment. **b)** Bipartite network showing the relationship between labeled proteins with distinct annotated functions (blue circles) and their host organism group (diamonds) demonstrates that the results of DNA-SIP and protein SIP support each other. Red diamonds indicate organism groups which were labeled in protein-SIP and DNA-SIP, green diamonds were found by protein-SIP but not by DNA-SIP. The number of connection lines from a diamond represents the number of detected labeled proteins belonging to this taxonomic group. In both panels, the taxonomic groups are given with their name and a letter indicating the taxonomic level ("f_" = family; "p_" = phylum).

3.1.6 Indications for SMX metabolism within the community from labeled proteins

Evaluation of the ^{13}C incorporation pattern of all labeled proteins in regard to their $X(^{13}C)_{LP}$ and $X(LP)_{\Sigma P}$ values revealed different aspects (**Figure 16**). Whereas $X(LP)_{\Sigma P}$ values were almost homogeneously distributed over the whole analyzed range from 10 to 95%, the $X(^{13}C)_{LP}$ values (i.e. the incorporation degree of ^{13}C into proteins) were occurring in distinct steps. We observed a low ^{13}C incorporation group (<30% $X(^{13}C)_{LP}$), a medium ^{13}C incorporation group (30-50% $X(^{13}C)_{LP}$) and a high ^{13}C incorporation group (>50% $X(^{13}C)_{LP}$). The low ^{13}C incorporation group included most of the labeled proteins (147 out of 185 = 80%). Within the high ^{13}C incorporation group, 6 out of the 8 taxonomically classified proteins were affiliated within the families *Intrasporangiaceae*, *Nocardioidaceae* or *Conexibacteraceae*, all of which were identified by DNA-SIP (indicated in **Figure 16** with red circles). Four of the high ^{13}C incorporation proteins were from the *Intrasporangiaceae.* Functional annotation of the labeled proteins showed that the dominant labeled proteins were related to catalytic activity (34.4%), binding (26.8%) or transport (13.1%), accounting for 74% of total functional annotation (**Figure 17**). However, a prediction which enzymes were involved in SMX degradation was not possible with the obtained set of labeled proteins.

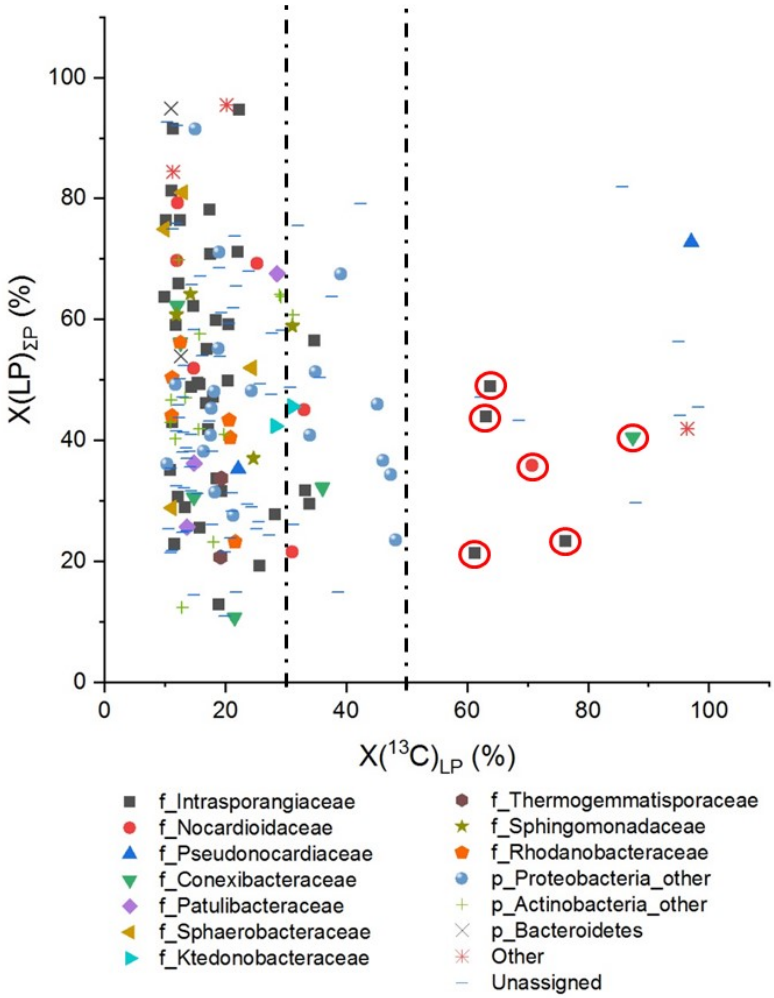

Figure 16. Incorporation of ^{13}C into proteins and taxonomic affiliation of the labeled proteins. Shown are 185 proteins for which incorporation of ^{13}C was found. Proteins are placed in the graph according to their $X(^{13}C)_{LP}$ and $X(LP)_{\Sigma Pep}$ values. For 113 of these proteins taxonomic affiliation was possible and is indicated by the color code. The taxonomic level is indicated in the name ("f_" indicates family; "p_" indicates phylum).

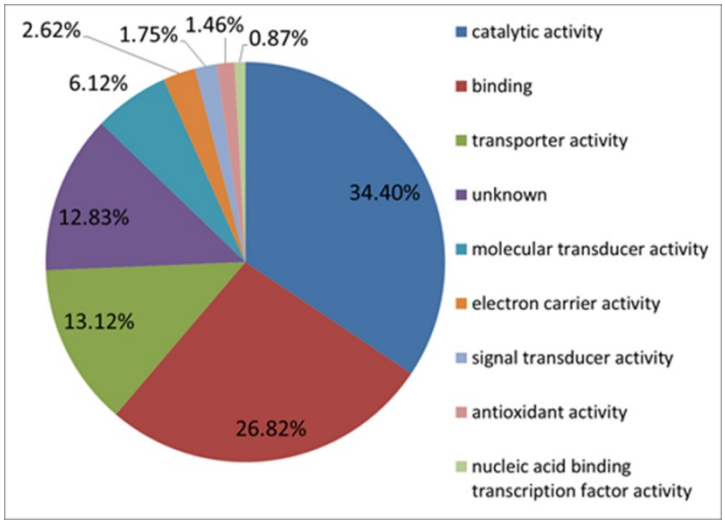

Figure 17. Predicted functional categories of labeled proteins.

3.2 Anaerobic transformation and detoxification of SMX by sulfate-reducing enrichments

SMX is widely detected in the environment because routine activated sludge treatment cannot efficiently eliminate it from wastewater. Here we investigated how microbial anaerobic transformation contributes to removal of SMX in constructed systems. We enriched SMX-transforming cultures from sediment of a constructed wetland and digester sludge from a wastewater treatment plant. To further characterize the SMX-transforming cultures under sulfate-reducing conditions, we tested the inhibitory effect of SMX on the sulfate-reducing enrichments, detected and identified transformation products, evaluated the toxicity of transformation products, determined whether the transformation was catalyzed by microbial cells and identified key players in the sulfate-reducing enrichments. This work evaluated the feasibility of including an anaerobic step in constructed systems to reduce antibiotic residues in effluents and recipient environments.

3.2.1 Establishment of particle-free SMX-transforming cultures with different electron acceptors

SMX-transforming cultures were established from two inocula (sediment and digester sludge) and with three electron acceptors. In the initial particle-containing cultures ('Passage 1' (P1)) that were amended with low concentrations of SMX of about ~0.7 μM, we observed SMX removal with both inocula, digester sludge and constructed wetland sediment under sulfate-reducing and methanogenic conditions (**Figure 18**a). Under nitrate reducing conditions no SMX transformation was detected. No transformation of SMX in the no-cell controls confirmed SMX was chemically stable in the anaerobic medium. Also, no transforming activity was observed in the autoclaved controls, demonstrating that adsorption of SMX to sludge or sediment did not contribute to removal of SMX, and that the transformation process was directly or indirectly mediated by microorganisms. SMX transforming activity was conserved after transferring 10% (v/v) of particle-free inocula from P1 to fresh medium (P2, **Figure 18**b), again with low concentrations of SMX (~1.5 μM). Among these particle-free cultures, cultures originating from digester sludge and cultivated under sulfate-reducing conditions showed the highest SMX removal activity. Further subculturing of particle-free cultures with higher SMX concentrations (2, 5, 25 and 140 μM) validated the stable transforming activity of cultures with digester sludge inoculum under sulfate-reducing conditions, in comparison, SMX transformation in cultures originating from constructed wetland sediment and cultivated under

methanogenic conditions was inhibited with the same SMX concentrations (2, 5, 25 and 140 µM) (**Figure 19**).

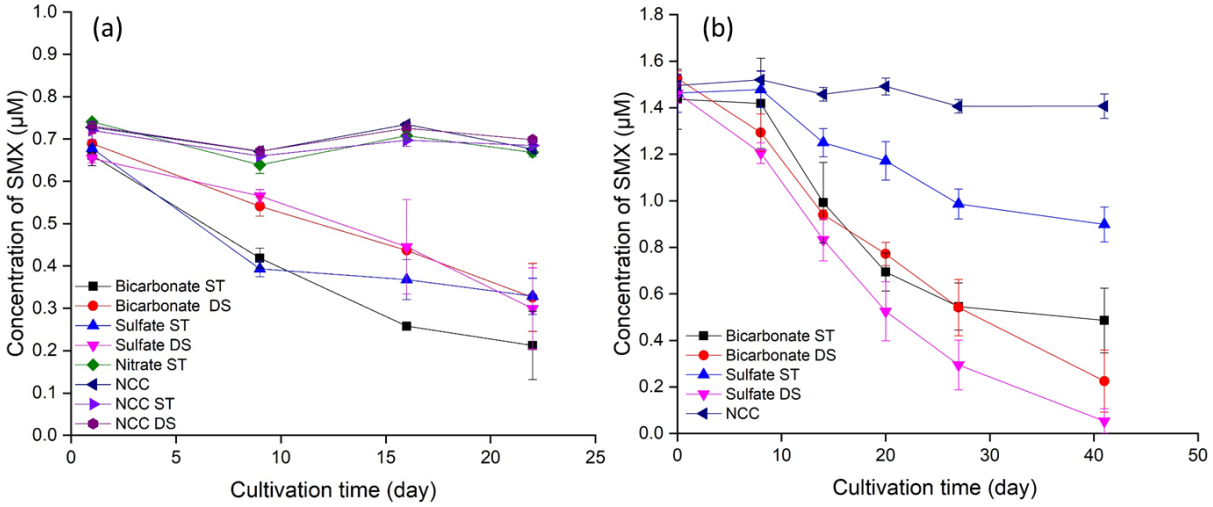

Figure 18. Anaerobic removal of SMX in cultures established from digester sludge (DS) and constructed wetland sediment (ST) in the presence of bicarbonate, sulfate or nitrate as electron acceptors. Controls were established as no-cell control (NCC) containing bicarbonate and sulfate and autoclaved cell controls (NCC ST/DS). **a)** Passage one (P1): one milliliter of digester sludge or one gram of constructed wetland sediment was used as inoculum; **b)** Passage two (P2): 10% supernatants from P1 without particles was used as inoculum. All data is shown as mean of triplicate cultures ± standard deviation (SD).

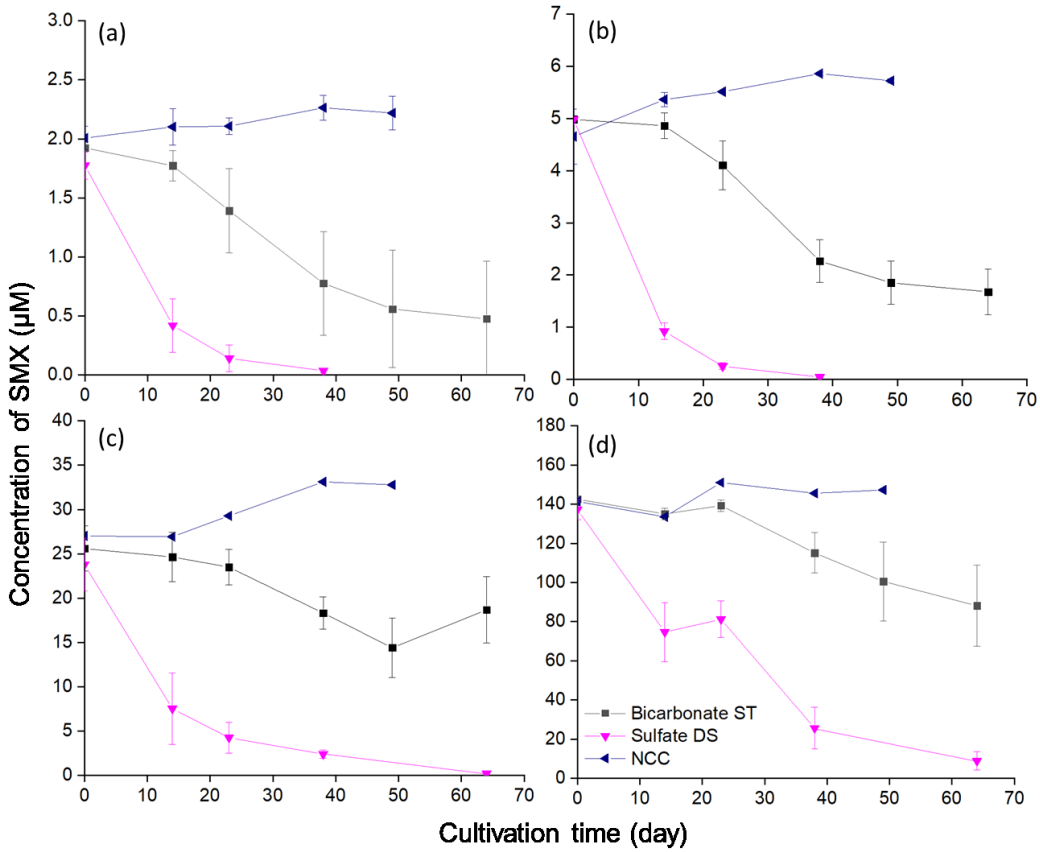

Figure 19. Anaerobic transformation of SMX in particle-free cultures (P3) with bicarbonate or sulfate as electron acceptors. Panels (a)-(d) show cultures with different initial SMX concentrations (2, 5, 25 and 140 µM, respectively). Shown are means of triplicate cultures ± SD, but single no cell controls in panels (b)-(d). Colors: blue, no-cell control, NCC; black, cultures originating from sediment inoculum under methanogenic conditions; pink, cultures originating from digester sludge inoculum under sulfate-reducing conditions.

3.2.2 Inhibition of SMX on transforming activity of sulfate-reducing cultures

We focused on SMX-transforming cultures with 1 mM sulfate as electron acceptors to evaluate the inhibitory effect of SMX on transforming activity and for the following characterization, as these cultures showed the highest transforming activity after two passages. In the anaerobic medium, 4 mM cysteine was added as reducing agent. No significant inhibition of SMX transformation was observed at initial SMX concentrations of 2-140 µM (**Figure 19**). Therefore, SMX concentrations of 100-750 µM which were above the reported minimal inhibitory concentration (2-126 µM) tested for *Haemophilus* spp were utilized here.[198] We monitored SMX concentrations over time and calculated the transformation rates as the average of removed SMX concentration between sampling points (**Figure 20**). For 100 and 150 µM initial SMX concentrations, the transformation started without any lag phase and removal was detected already at the first sampling point after 9 days. In cultures with initial SMX

concentrations of 250 µM or above, a lag phase was observed ranging from 15 to 29 days until SMX removal started.

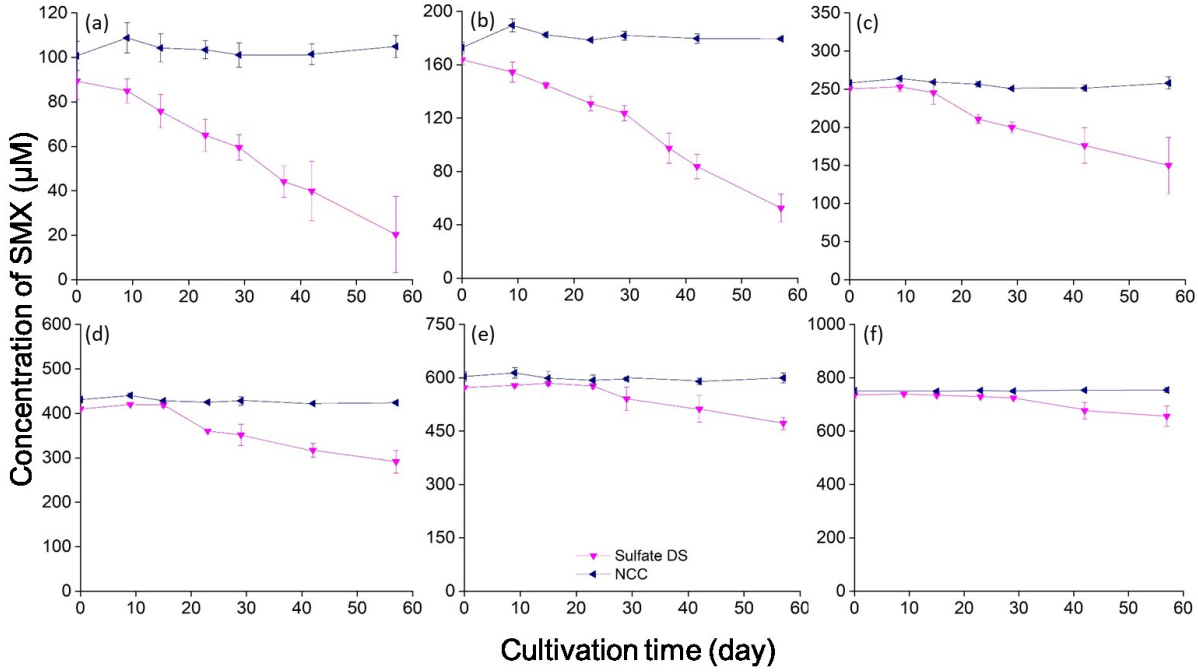

Figure 20. Removal of SMX over time with different initial SMX concentrations in particle-free cultures originating from digester sludge inoculum in the 4th passage (P4) with 1 mM sulfate as electron acceptor. Panels (a)-(f) show cultures with initial SMX concentrations of 100, 150, 250, 400, 600 and 750 µM, respectively. Shown are means of triplicate cultures ± SD. NCC – no-cell control.

3.2.3 Kinetics of SMX transformation by sulfate-reducing cultures

To evaluate the kinetics of SMX transformation in passage four (P4), the maximal transformation rates in the treatments with different initial SMX concentrations were calculated. We observed that the maximal transformation rates increased along initial SMX concentrations from 1.52 to 6.54 µM d^{-1} in a way resembling Michaelis-Menten-Kinetics of enzymes, indicating that the process was enzymatically mediated (**Figure 21**).

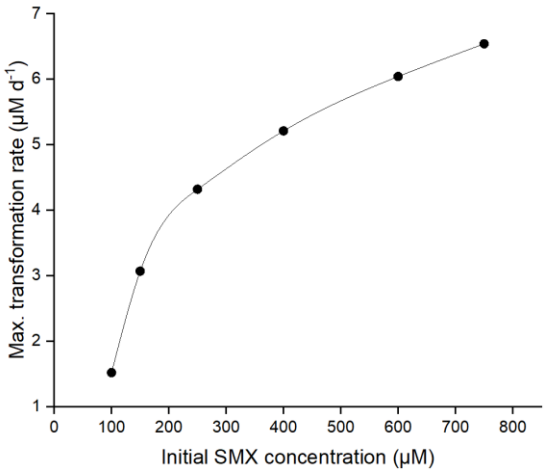

Figure 21. Maximum transformation rate in sulfate-reducing cultures (Passage four) spiked with different initial concentrations of SMX (100, 150, 250, 400, 600 and 750 μM, respectively).

3.2.4 Detection and identification of transformation products

The P4 sulfate-reducing cultures from digester sludge were further cultivated for 6 months to search for SMX transformation products (TPs). We detected residual SMX and two TPs with earlier elution time than SMX: TP1 eluted at 6.16 min while TP2 eluted at 6.95 min (**Figure 22**), indicating the two TPs were more polar than SMX. The cultures were further incubated to a total of 14 months to investigate the maximum SMX transformation degree (defined as the removed SMX over the initial SMX) (**Figure 22**). The transformation degree varied in cultures with different initial concentrations of SMX. In cultures with initial SMX concentrations of 100-250 μM, ~90% of the initial SMX was removed (**Figure 22**, left panels). In contrast, in cultures with SMX concentrations of 400-750 μM, the transformation degree decreased from 78% to 9%, and no more decrease of SMX was observed in the subsequent cultivation (**Table S2**). This showed that SMX suppressed the transforming activity on the long term.

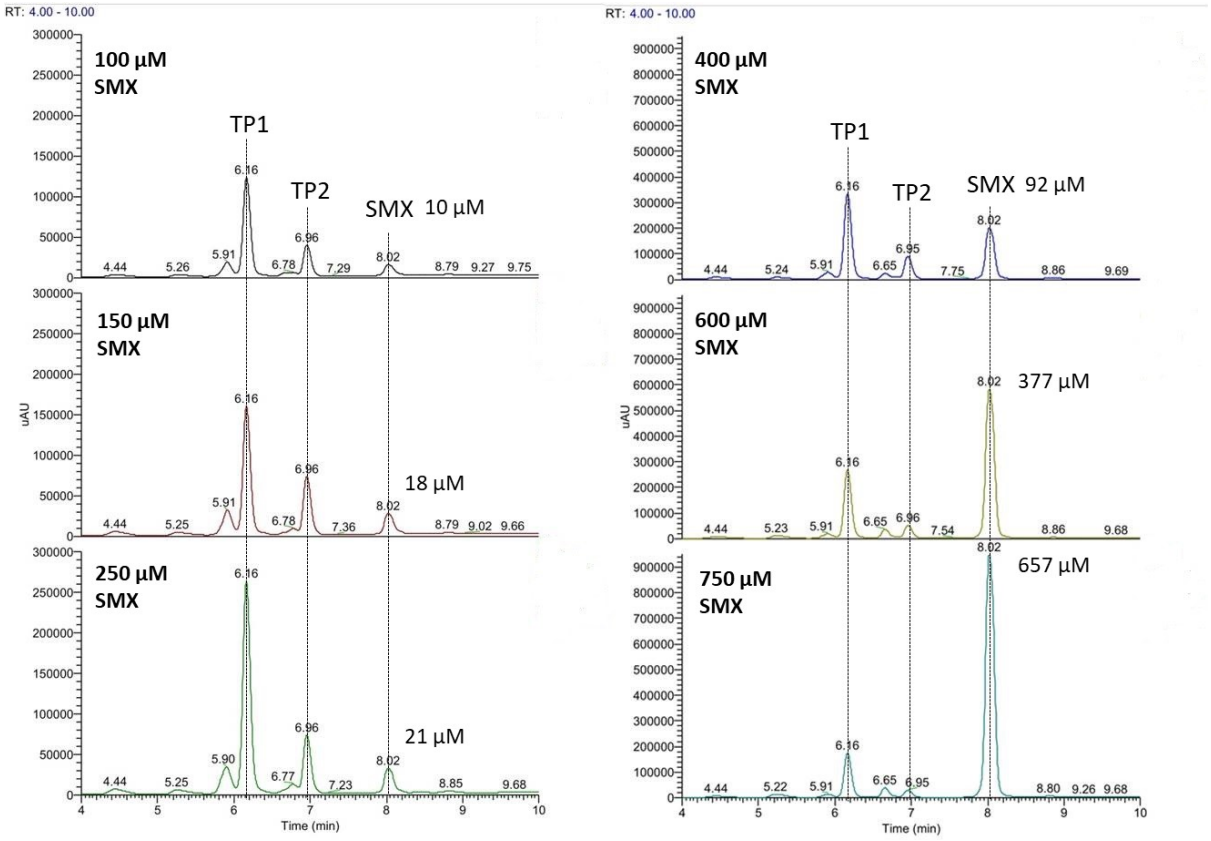

Figure 22. Absolute quantification of SMX (using an external standard; numbers near the SMX peaks) and relative quantification of transformation products (for which no external standard was available) in the cultures shown in (**Figure 20**) after 14 months of incubation. Data represents the absorption at 270 nm. Numbers in bold represent initial concentrations of SMX. Note that the scale of the Y-axis of the three graphs on the left side is different from the scale of the three graphs on the right side. No transformation products were detected in negative controls with no cells or with autoclaved cells (data not shown). TP – transformation product.

Dominant $[M+H]^+$ ions of SMX and the two transformation products were detected in MS1 scans with a series of expected isotope peaks (**Figure 23**, panels (a), (c), and (e), and **Table S3**). Fragment mass spectra supported the prediction of the chemical structure (**Figure 24**). The *m/z* values of the dominant fragment ions of SMX were 92, 99, 108, 110 and 156. The *m/z* 92 ion was affiliated to the aniline moiety ($C_6H_4NH_2$) which was generated by cleaving the S-C bond, the *m/z* 99 ion was affiliated to the protonated isoxazole moiety ($C_4N_2OH_7$) by cleaving the sulfonamide bond, the *m/z* 108 ion was affiliated to the oxidized *m/z* 92 ion, the *m/z* 110 ion was generated by replacing a hydrogen by a hydroxyl group on the m/z 92 ion, the *m/z* 156 ion was affiliated to the aniline moiety with a sulfo group by cleaving the sulfonamide bond (**Figure 23**b, **Figure 24**, and **Table S3**). The protonated TP1 ion (*m/z*=256) contained 2 Da more than the protonated SMX ion (*m/z*=254), indicating TP1 was generated by reduction and addition of 2 hydrogen atoms (hydrogenation). TP1 had all the fragment ions as described for

SMX except the *m/z* 99 ion. Instead an *m/z* 101 ion was detected for TP1, indicating the isoxazole moiety was hydrogenated (**Figure 23**c and d). The protonated TP2 ion (*m/z*=254) showed the same mass fragments as the protonated SMX ion (*m/z*=254) but eluted at a different retention time, indicating rearrangement occurred on the isoxazole ring (**Figure 23**e and f).[199,200] To analyze the oxygen stability of the transformation products, 15 mL samples were transferred from anaerobic bottles containing TP1 and TP2 to 50 mL Falcon tubes. These falcon tubes were not closed and the transformation products were exposed to oxygen for seven days. After this exposure no reverse transformation of TP1 or TP2 to SMX was detected (data not shown). As a chemical reaction we tested the reaction of SMX with 1 mM Ti(III) citrate[84] and found the formation of the transformation products TP1 and TP2 after 28 days of incubation.

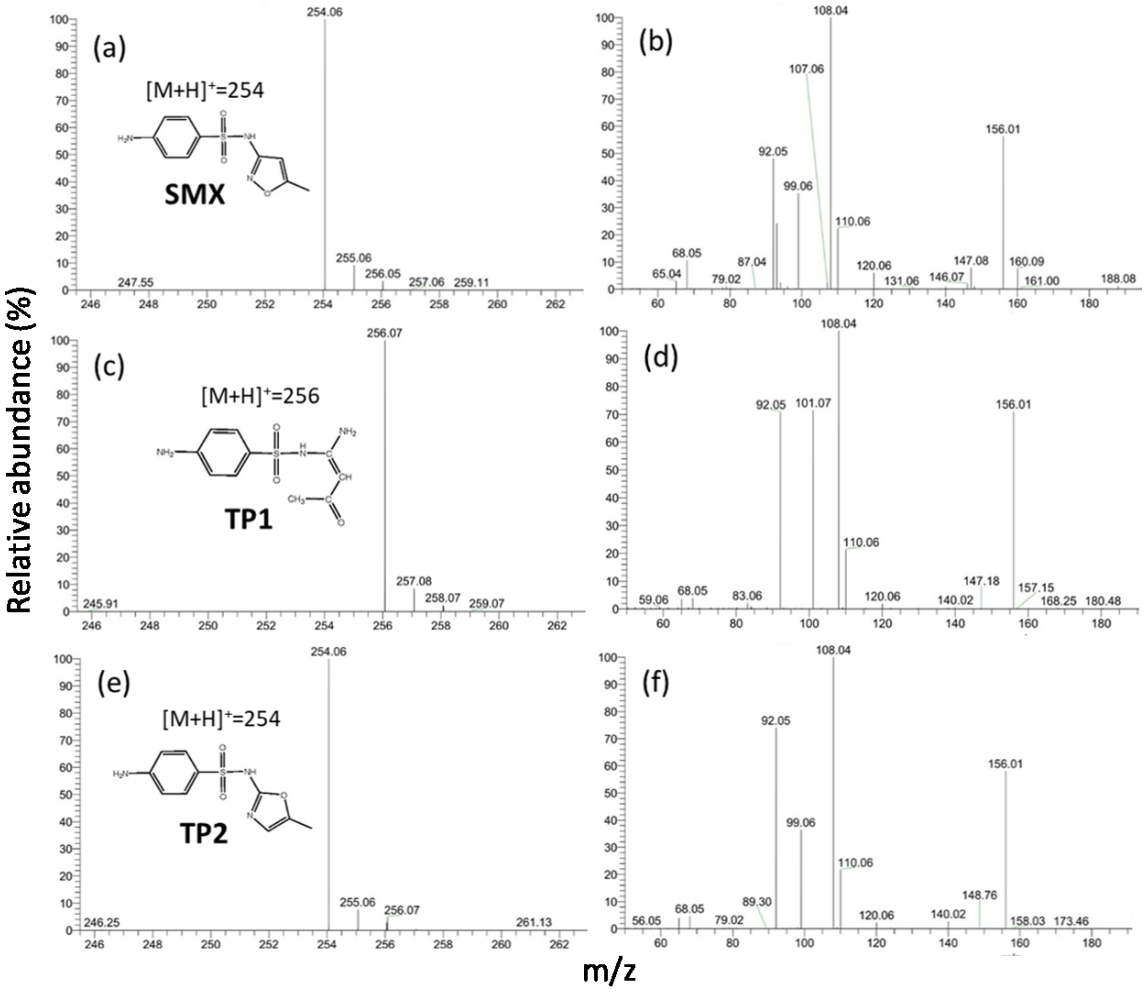

Figure 23. Precursor mass spectra (panels a, c, e) and fragment mass spectra (panels b, d, f) of SMX and the two identified transformation products TP1 and TP2 detected in positive ionization mode after electron spray ionization. Inferred chemical structure and the nominal mass of the $[M+H]^+$ ion are shown on MS1 spectra. The fragment with an *m/z* value of 101.01 represents the opened and reduced heterocycle of SMX (see text for this and further mass affiliations).

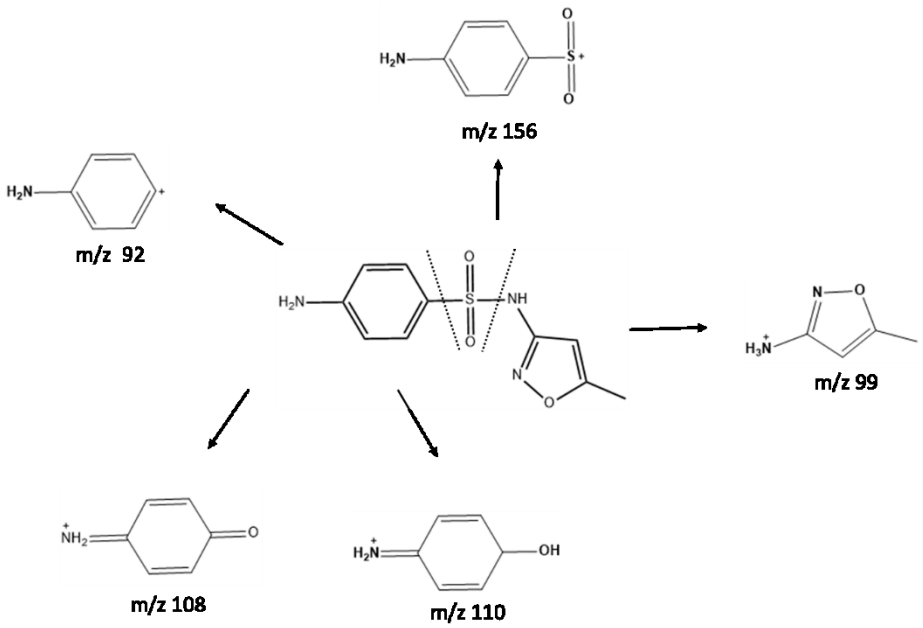

Figure 24. Structures proposed for the fragment ions of SMX according to our data and literature references.[201]

We tried to also quantify the two transformation products to evaluate if SMX was stoichiometrically converted or if further products were formed in significant amounts. Because standards of the transformation products were not available and as the structures of the detected transformation products, with the aromatic ring responsible for absorbance were similar to SMX (**Figure 23**), we assumed for quantification the transformation products have the same molar absorption coefficient at 270 nm as SMX. During cultivation, the peak area of SMX decreased steadily, while the peak areas of TP1 and TP2 steadily increased correspondingly. The calculated sum of SMX, TP1 and TP2 kept almost constant over the whole incubation period, suggesting that TP1 and TP2 were the only transformation products (**Figure 25**).

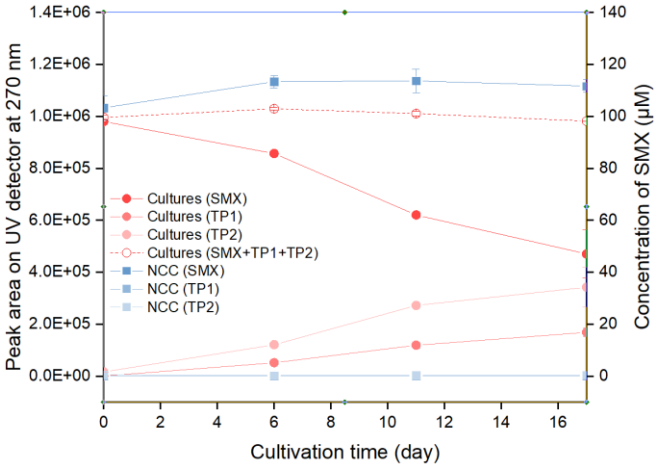

Figure 25. Transformation of SMX and formation of SMX transformation products over time in sulfate-reducing cultures amended with 100 µM SMX. All data is plotted against the peak area at 270 nm (left Y-axis). SMX absorption at 270 nm was calibrated with external SMX standards and the corresponding µM concentration is shown on the right Y-axis. The sum of the 270 nm peak areas of SMX, TP1 and TP2 was constant over time (dashed line). The blue curves show data of no-cell controls in which no formation of transformation products was detected.

3.2.5 Anaerobic transformation of SMX is a detoxification process

In the next step we evaluated the effect of the anaerobic transformation on toxicity (the toxicity test was described in 2.5.4). Added as a neat compound, 3 µM SMX impacted growth of *E. coli* in overnight cultures (OD600 of 0.2 with 3 µM SMX vs. OD600 of 0.3 without SMX, **Figure 26**a). At an SMX concentration of 10 µM or above, inhibition of *E. coli* growth reached a maximum degree (OD600 of only 0.05) after overnight incubation (**Figure 26**a). To test the toxicity of the transformation products, we exposed *E. coli* to filtrates with untransformed SMX (obtained from negative controls without cells) and to culture filtrates in which SMX was transformed to the two transformation products. Both were obtained by filtering the media/culture liquid described in **Figure 22** through 0.2 µm filters. An estimation of the concentrations of SMX and TPs in the filtrates is described in **Table S2**. Growth of *E. coli* in filtrates with untransformed SMX represented the inhibitory effect of SMX alone. In TPs-containing filtrates where initial SMX concentrations were 100-250 µM and residual SMX concentrations were 10-21 µM (**Table S2**) the growth of *E. coli* almost doubled compared to the corresponding filtrates with untransformed SMX (**Figure 27**). We observed less but still significant increase of *E. coli* growth with TPs-containing filtrates from higher initial SMX concentrations (600 µM) and higher residual SMX concentrations (377 µM) (**Figure 27**). In all treatments the concentrations of residual SMX surpassed 10 µM, and it should have already

inhibited *E. coli* growth to the highest extend after overnight growth according to our experiments shown in **Figure 26**. However, we observed the two transformation products counteracted the inhibitory effect of residual SMX. This indicates that the transformation products were not only less toxic but also reversed the inhibitory effect of SMX. In the treatments with 750 µM SMX filtrates, no significant difference on growth of *E. coli* was observed between TPs-containing filtrates in which only 9% of the SMX had been transformed and filtrates with untransformed SMX.

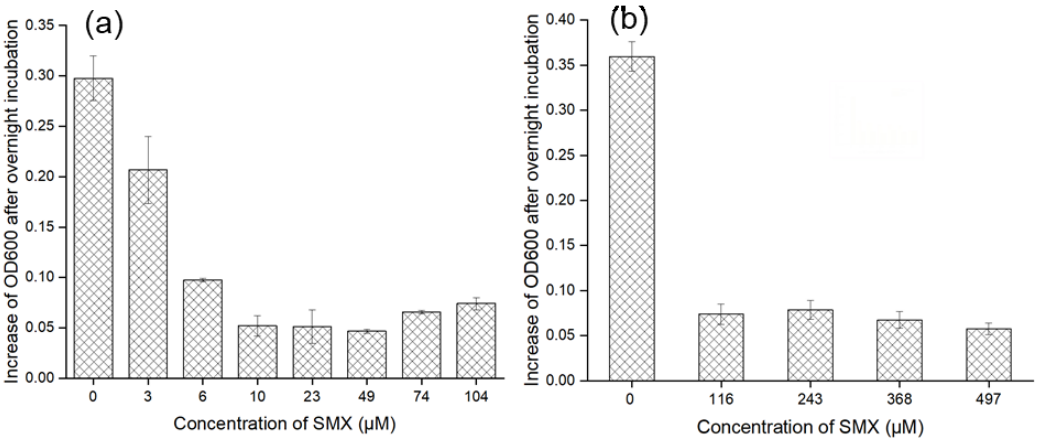

Figure 26. Test for growth inhibition of *E. coli* strain K-12 by different initial SMX concentrations. *E. coli* cultures were set up in medium as used for sulfate-reducing cultures and amended with different initial concentrations of SMX. **a)** The initial concentrations of SMX ranged from 0 to 104 µM; **b)** The initial concentrations of SMX ranged from 0 to 497 µM. Shown are means of duplicate cultures ± SD.

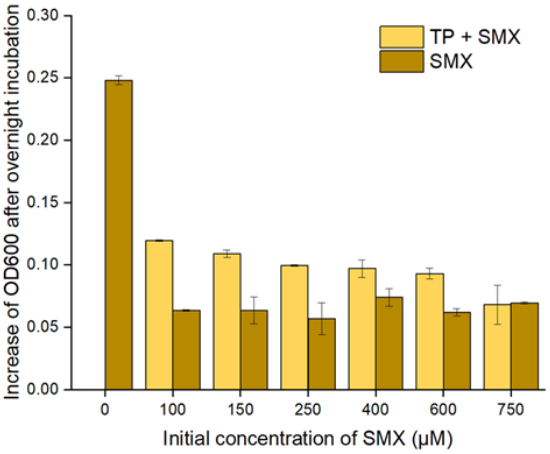

Figure 27. Effects of SMX transformation products on overnight growth of *E. coli* K-12. *E. coli* K-12 was incubated overnight either in SMX containing medium (SMX) or in culture filtrates containing transformation products and residual SMX (TP + SMX). Growth of *E. coli* K-12 was calculated by subtracting initial OD600 values from final OD600 values for each bottle. NCC - no-cell control, TP - transformation products. Shown are means ± SD (n=2).

3.2.6 Transformation of SMX is catalyzed by microbial cells

After characterizing the structure and toxicity of transformation products we investigated the role of bacterial cells in the transformation process. Previous studies under iron-reducing and denitrifying conditions showed SMX transformation by abiotic reaction of SMX with the reduced respiration products Fe(II) and nitrite, respectively,[109-111] and therefore we hypothesized that sulfide as the respiration product of sulfate-reducing bacteria could abiotically react with SMX over time. However, we found no abiotic reduction of SMX by sulfide at a concentration of 8 mM sulfide after 28 days of incubation (data not shown). Therefore, we set up two sulfate-reducing cultures (A and B) to compare the transforming activity of active cultures with that of culture filtrates that contained all respiration products but no bacterial cells. Culture A transformed 95% of the initial SMX within 24 days, with a transformation rate of 6 µM d^{-1} during the first 8 days, but no transformation of SMX was observed in culture A filtrates without cells. Culture B transformed 35% of the initial SMX over 24 days, with a transformation rate of 3 µM d^{-1} during the first 8 days, but again, culture B filtrates without cells did not show any transforming activity (**Figure 28**). Hence, we concluded SMX transformation was directly catalyzed by microbial cells.

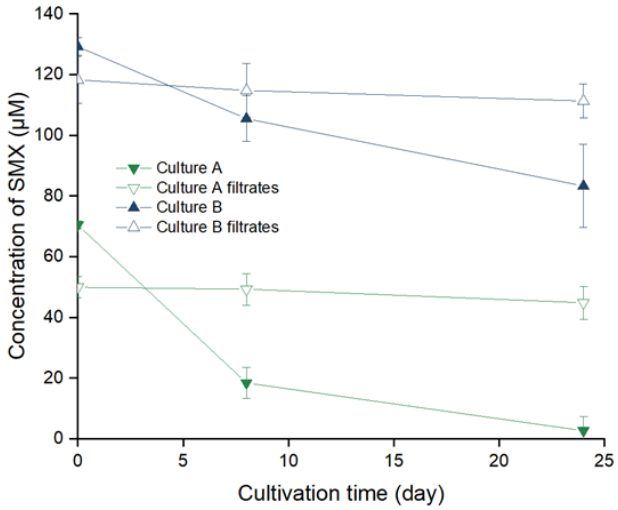

Figure 28. Transformation of SMX by active sulfate-reducing cultures and corresponding culture filtrates (using a 0.2 µm filter) over time. Culture A and culture B were initially incubated with 100 µM SMX. When 30 µM SMX was transformed in culture A, half of the culture volume was taken out and filtered to obtain culture A filtrate without cells; when 70 µM SMX was transformed in culture B, additional 100 µM SMX was re-spiked and half of the culture volume was taken out and filtered to obtain culture B filtrates without cells. Then, cultures and culture filtrates were incubated at 30°C in the dark for 24 days. Data show means of triplicates ± SD.

3.2.7 Population analysis to identify potential key players in the sulfate-reducing cultures

Samples from two passages were taken for 16S rRNA gene sequencing when SMX transformation activity in the cultures was high. Within the determined communities, sequences belonging to the genus *Desulfovibrio* strongly increased in relative abundance from passage 3 to passage 5. (**Figure 29**, **Figure 31**) In the cultures of passage 3, the relative abundance of *Desulfovibrio* increased from 3.5 to 38.6% with increasing SMX concentrations from 0.25 to 140 µM (**Figure 29**). Three other sulfate-reducing bacteria were found in the cultures of passage 3 belonging to the genus *Desulfomicrobium*, genus *Desulfobulbus* and family *Dethiosulfovibrionacea.* (**Figure 29**, **Figure 31**) Sequences of the genus *Desulfomicrobium* accounted for more than 10% in the cultures of passage 3 with 25 µM SMX and the cultures of passage 5 with 200 µM SMX. (**Figure 29**, **Figure 31**) Sequences of the family *Dethiosulfovibrionacea* were abundant (above 10%) in the passage 3 but their abundance decreased to less than 1% in passage 5. (**Figure 29**, **Figure 31**) In the cultures of passage 5 *Desulfovibrio* dominated the sulfate-reducing cultures with a relative abundance of 60% and up to nearly 80% in the presence of the methanogen inhibitor BES (**Figure 31**). This indicates *Desulfovibrio* played a key role in SMX transformation.

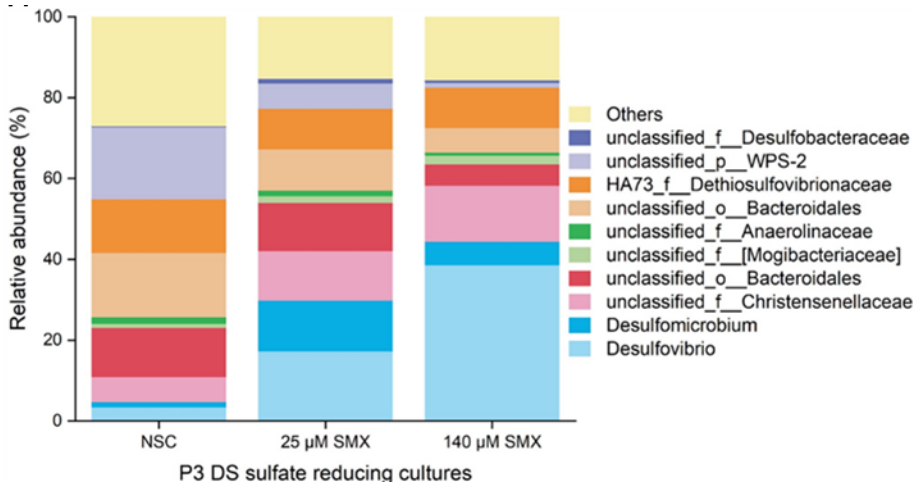

Figure 29. Population analysis of SMX-transforming cultures with sulfate as electron acceptor from different passages at genus level analyzed by 16S rRNA gene amplicon sequencing. Cultures from passage 3 (P3) cultivated with different concentration of SMX. No-substrate control (NSC) represents cultures cultivated without SMX.

3.2.8 Methanogens did not contribute to SMX transformation in the sulfate-reducing cultures

Population analysis showed that *Desulfovibrio* were the dominant population in the sulfate-reducing mixed cultures (4 mM cysteine as reducing agent, 1 mM sulfate as electron acceptors and 100 µM SMX), however, the methanogenic mixed cultures (4 mM cysteine as reducing agent, 10 mM bicarbonate as electron acceptors and 100 µM SMX) also showed transformation activities. In order to investigate whether methanogens could grow in the sulfate-reducing mixed cultures and the potential effects of methanogens in the sulfate-reducing cultures on SMX transformation, a new passage of sulfate-reducing mixed cultures were established with 4 mM bromoethanesulfonate (BES) to inhibit the potential growth of methanogens, meanwhile cultures without BES were also set up as controls. After 140 days cultivation, the spiked 200 µM SMX was almost consumed in both treatments, and no significant difference of transformation activity was observed between BES treatments and treatments without BES at any sampling point (**Figure 30**). Population analysis was conducted for samples on the 21st day with high transformation activity, but no significant proportion of methanogens were detected in both treatments, at the meantime, we observed that the presence of BES significantly promoted the percentage of genus *Desulfovibrio* and decreased the proportion of genus *Desulfomicrobium* (**Figure 31**). Both transformation experiments and population analysis showed methanogens did not contribute to SMX transformation in the sulfate-reducing cultures even though methanogenic mixed cultures themselves showed transformation activity.

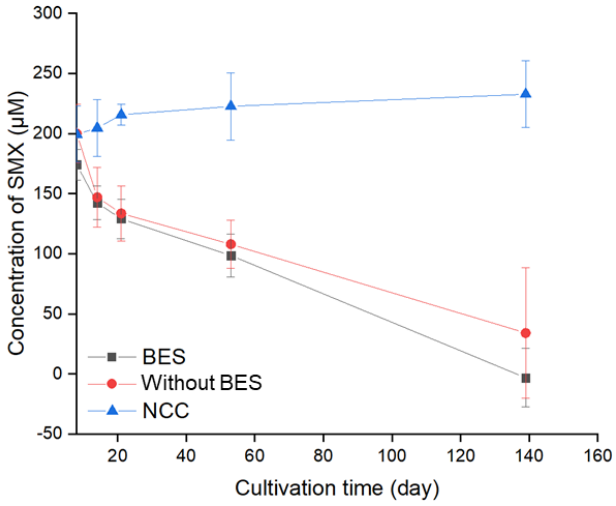

Figure 30. Transformation of SMX by sulfate-reducing cultures with or without BES. Controls were established as no-cell control (NCC). All data is shown as mean of triplicate cultures ± standard deviation (SD).

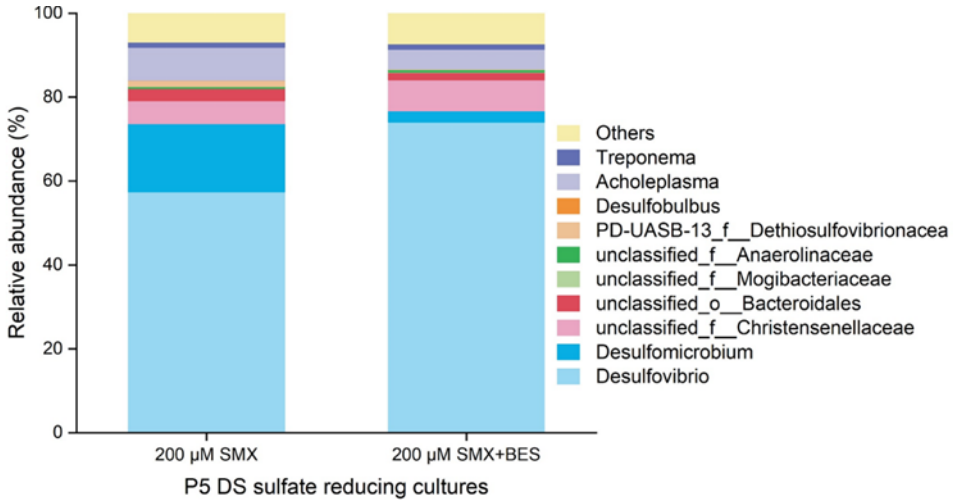

Figure 31. Population analysis of SMX-transforming cultures with sulfate as electron acceptors at genus level analyzed by 16S rRNA gene amplicon sequencing. Passage 5 (P5) were cultivated with either 200 µM SMX or 200 µM SMX plus 4 mM bromoethanesulfonate (BES) to suppress the growth of methanogens. Sequencing was conducted on the 21st cultivation day. Only the 10 most abundant taxa are shown individually, all others are summarized as "Others". For unclassified genera the family or order is also indicated in the legend. DS – digester sludge.

3.3 Physiology of SMX-transforming sulfate-reducing mixed cultures

In our previous study, stable SMX-transforming cultures were established under sulfate reducing conditions, two transformation products with less toxicity compared to SMX are generated stoichiometrically, and the process is directly catalyzed by cells. In order to optimize the growth conditions and reveal the transformation mechanism, we further investigated the physiology of the SMX-transforming mixed cultures. Grown with sulfate as electron acceptor, we tried to identify the electron donor in the sulfate-reducing cultures for SMX transformation, and the effects of additional electron donor and carbon source on the transformation. Besides, we also investigated the abiotic transformation of SMX by reductants, and tried to enrich another group of cultures which could metabolically reduce sulfonamides as electron acceptors for energy conservation. Overall, characterizing the SMX-transforming sulfate-reducing cultures is essential for understanding the anaerobic transformation process and selecting remediation strategy.

3.3.1 Abiotic transformation of SMX by reducing agents

We investigated the abiotic transformation of SMX by different reducing agents to test whether similar transformation products could be generated as the ones by microbial transformation, as the structure of TP1 indicates a reductive transformation process. SMX is sensitive to redox

potentials, and it is reported that the transformation of SMX by iron reducing bacteria is a microbially mediated abiotic process triggered by iron(II).[111] We tested the abiotic transformation of SMX by Na_2S, cysteine, dithionite, Ti(III)NTA and Ti(III) citrate in two batches. No abiotic transformation of SMX by 4 mM cysteine, or 1 mM dithionite or 0.5 mM Na_2S was observed after 35 days incubation (**Figure 32**). We further tested two more reducing agents with low redox potentials: Ti(III) citrate and Ti(III) NTA. Precipitation was formed in Ti(III) NTA treatments and no SMX was detected even at the starting point, one explanation could be SMX was embedded in the precipitation instead of being released in the medium. In contrast, 1 mM Ti(III) citrate transformed SMX to the two typical transformation products as detected in the microbial transformation by sulfate-reducing mixed cultures (**Figure 22, Figure 33**). Besides, 8 mM sulfide in the medium containing 4 mM cysteine was also tested, no significant decrease of SMX was observed and also no transformation products were detected (**Figure 33**), and therefore, we could exclude the possibility of abiotic transformation in the sulfate-reducing mixed cultures in which high amounts of sulfide were generated by the activity of sulfate-reducing bacteria. In summary, among all the tested reducing agents, only 1 mM Ti(III) reductively transformed SMX to the two transformation products TP1 and TP2.

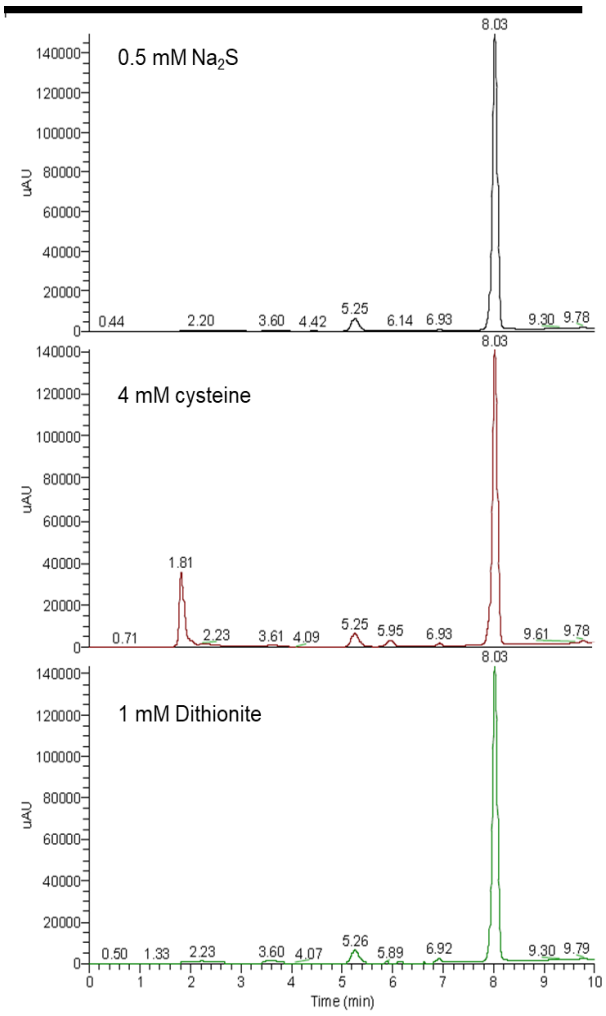

Figure 32. Abiotic transformation of SMX by three different reducing agents. Shown are chromatogram of SMX the transformation products after 35 days incubation with 0.5 mM Na_2S, or 4 mM cysteine, or 1 mM dithionite in Milli-Q water, the initial concentration of SMX was 100 µM.

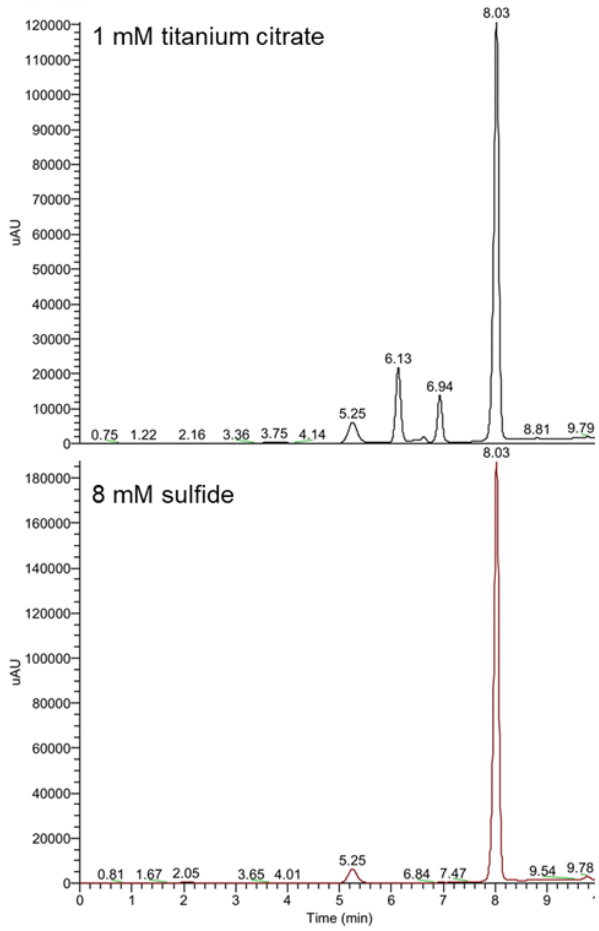

Figure 33. Abiotic transformation of SMX by two different reducing agents. Shown are chromatogram of SMX and the transformation products after 28 days incubation with 1 mM Ti(III) citrate in Milli-Q water or 8 mM Na_2S in anaerobic medium containing 4 mM cysteine, the initial concentration of SMX was 100 µM.

3.3.2 Identification of the electron donor in the sulfate-reducing cultures

Our initial hypothesis was that SMX could act as electron donor in the sulfate-reducing cultures with 1 mM sulfate as electron acceptor, but both structure analysis of transformation products (3.2.4) and abiotic transformation test (3.3.1) indicated that SMX was reductively transformed. Thus, we proposed that the reducing agent in the medium could act as electron donor in the sulfate-reducing cultures. We investigated whether cysteine which was consistently added as reducing agent in the previous experiments could act as electron donor in the sulfate-reducing cultures, besides, three different reducing agents were also tested in parallel on how they influenced transformation of SMX in the sulfate-reducing cultures.

Firstly, a batch of sulfate-reducing cultures were established with sulfate as electron acceptor and cysteine as electron donor, different concentrations of cysteine and sulfate were combined in four treatments, and the initial concentration of SMX for all treatments was 100 µM (**Figure**

34). Sulfide generation was measured in the cultures to evaluate the sulfate reducing activities. The concentrations of generated sulfide were positively correlated with cysteine added in the cultures (**Figure 34**). The ratio between sulfate and cysteine was also estimated based on sulfide generation. We observed that there was no difference on sulfide generation when sulfate concentrations increased from 1 mM to 10 mM combined with 4 mM cysteine, indicating within this range sulfate was excess compared to cysteine (**Figure 34**). According to this result, cysteine concentrations increased from 4 mM to 12 mM combined with 10 mM sulfate, sulfate was still excess and the cysteine: sulfate ratio was around 2:1. Besides, we observed the trend that higher cysteine induced higher SMX transformation (**Figure 35**).

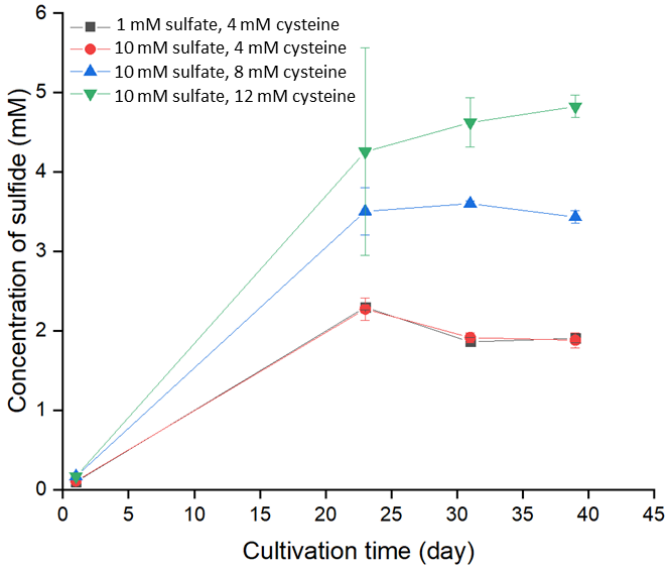

Figure 34. Production of sulfide in the sulfate-reducing cultures incubated with different concentrations of sulfate and cysteine. Four treatments were established as: 1) 1 mM sulfate + 4 mM cysteine; 2) 10 mM sulfate + 4 mM cysteine; 3) 10 mM sulfate + 8 mM cysteine; 4) 10 mM sulfate + 12 mM cysteine.

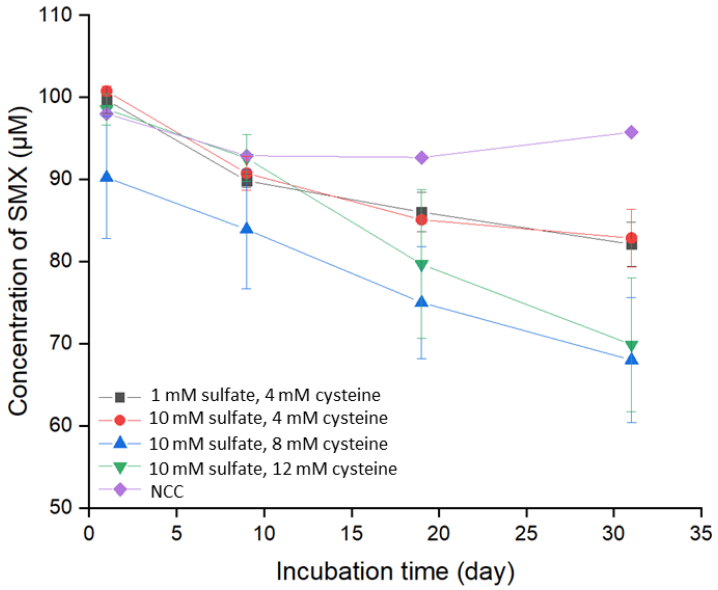

Figure 35. Transformation of SMX in the sulfate-reducing cultures incubated with different concentrations of sulfate and cysteine. NCC represents triplicate no cell controls. All data is shown as mean of triplicate cultures ± standard deviation (SD).

To further test the influence of different reducing agents on SMX transformation, we established another batch of sulfate-reducing cultures with 1 mM sulfate as electron acceptor and different reducing agents as electron donors. Apart from cysteine, two inorganic reducing agents dithionite and Na_2S were tested separately and the concentrations applied were conventional ones in anaerobic cultivation. Abiotic test showed cysteine, dithionite and Na_2S under tested concentrations did not transform SMX abiotically (**Figure 32**). After 35 days cultivation, the cultures with 1 mM dithionite as electron donor transformed more SMX compared with the cultures with 4 mM cysteine, besides, both the cultures with 0.5 mM Na_2S and the cultures with no reducing agents did not transform SMX (**Figure 36**). In summary, cysteine acted as electron donor in the sulfate-reducing SMX-transforming cultures, additionally, the sulfate-reducing cultures can also utilize dithionite as electron donor and transform SMX.

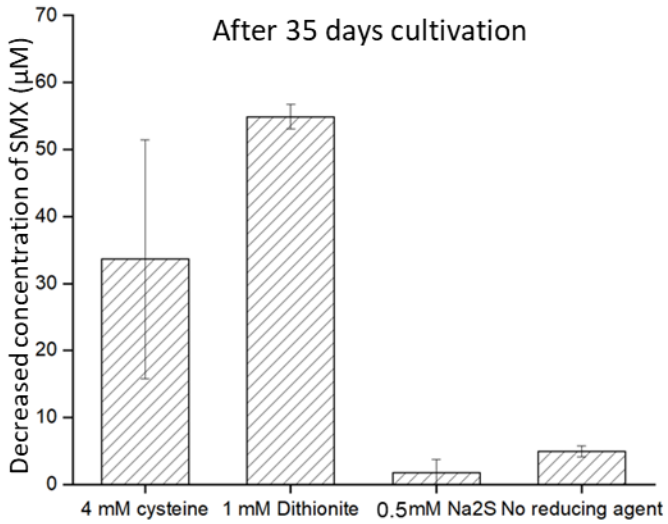

Figure 36. Transformation of SMX in the sulfate-reducing mixed cultures incubated with different reducing agents as electron donors. Different reducing agents were added in three treatments: 4 mM cysteine, 1 mM dithionite, 0.5 mM Na_2S, and the concentrations of reducing agents applied here refer to conventional concentrations used in anaerobic cultivation. The initial concentration of SMX was 100 µM. Note, Y axis shows the concentrations of SMX transformed by the cultures after 35 days cultivation. All data is shown as mean of triplicate cultures ± standard deviation (SD).

3.3.3 Effect of H_2 on SMX transformation

We observed that the sulfate-reducing cultures can utilize cysteine and dithionite as electron donors to transform SMX. To investigate whether more electron donors can promote SMX transformation, we established one batch of sulfate-reducing cultures (1 mM sulfate as electron acceptor and 4 mM cysteines as electron donor and reducing agent) incubated with different amounts of H_2 (0-6 mL) as additional electron donors. After 140 days cultivation, in all four treatments (0 mL, 1 mL, 3 mL, 6 mL H_2) more than 70% of spiked SMX was transformed, while no significant difference on SMX transformation at any time point was observed among treatments (**Figure 37**). The results showed no inhibition effect and no stimulating effect of H_2 on SMX transformation in the sulfate-reducing cultures.

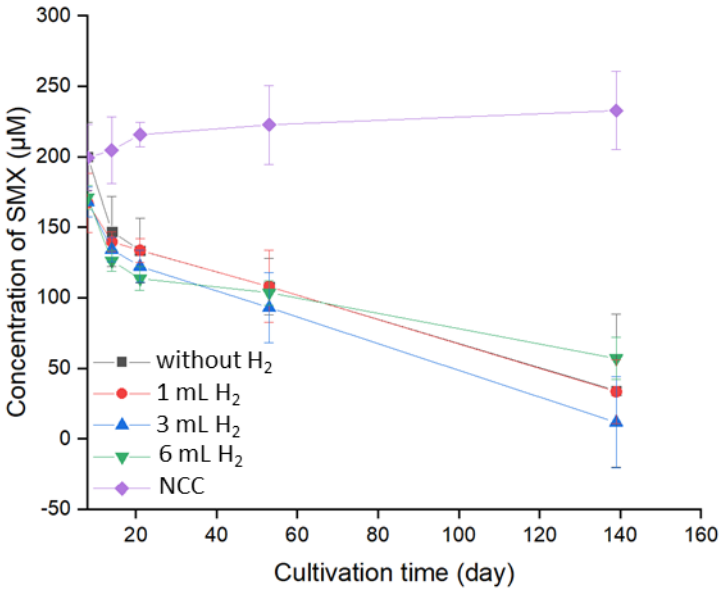

Figure 37. Transformation of SMX in the sulfate-reducing mixed cultures with different amounts of H_2 as electron donor. The initial concentration of SMX was 200 µM. 1 mM sulfate was added as electron acceptor and 4 mM cysteines was added as electron donor and reducing agent. NCC represents no-cell control. All data is shown as mean of triplicate cultures ± standard deviation (SD).

3.3.4 Effect of additional carbon source on SMX transformation

Previous results showed that electron donors had impact on SMX transformation in the sulfate-reducing cultures, apart from electron donors, carbon source is also a factor which could influence microbial degradation. Therefore, to investigate the effect of three different carbon sources (pyruvate, acetate and citrate) on SMX transformation we established one batch of sulfate-reducing cultures with 1 mM sulfate as electron acceptor and 4 mM cysteines as electron donor (**Figure 38**). After 77 days cultivation, in the cultures without additional carbon source (Cys in **Figure 38**) around 100 µM SMX was transformed, in the meantime, we observed the same SMX transformation degree occurred in the treatments with either acetate or citrate. In contrast, in the treatment cultivated with pyruvate almost all spiked 300 µM SMX was transformed, showing significantly higher transformation activity than other treatments (**Figure 38**).). No transformation of SMX was observed in all no-cell controls with the three tested carbon source (data not shown). The results revealed that pyruvate added as co-substrate can significantly promote SMX transformation, while the presence of acetate or citrate did not influence SMX transformation.

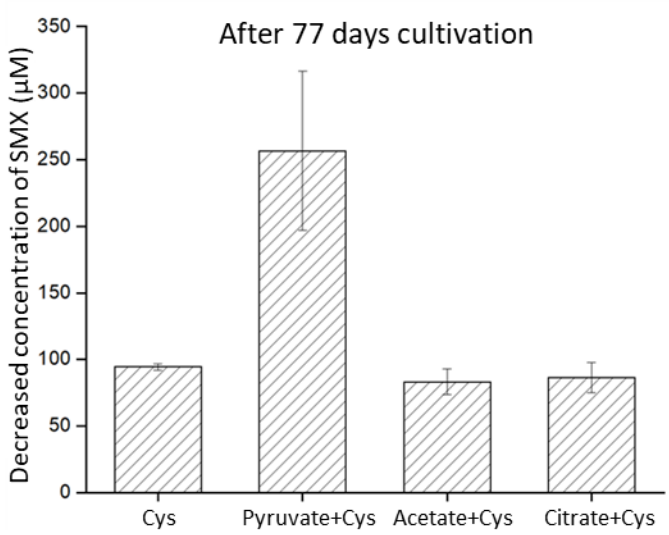

Figure 38. Transformation of SMX in the sulfate-reducing mixed cultures with different additional carbon source. In all cultures, 1 mM sulfate was added as electron acceptor and 4 mM cysteine was added as electron donor. Cys means "cysteine" which represents the treatment without additional carbon source but only with cysteine, three tested carbon source are: 5 mM pyruvate, 5 mM acetate and 5 mM citrate. Note, Y axis shows the concentrations of SMX transformed by the cultures after 77 days cultivation. The initial concentration of SMX was 300 µM. All data is shown as mean of triplicate cultures ± standard deviation (SD).

3.3.5 Establishment of sulfanilamide/sulfonic acid-transforming mixed cultures

We also tried to establish enrichment cultures transforming other sulfonamides. Our hypothesis was that sulfonamides could act as electron acceptors and energy can be conserved from it for bacteria to grow. In this case, the sulfonamide bond could accept electrons and be reduced, and the sulfonamide bond is the key structure for the antibacterial activity. In our previous study, reductive transformation of SMX occurred on the isoxazole moiety in the sulfate-reducing cultures. We selected two substrates for enrichment cultivation: one was sulfanilamide known as the least active sulfonamide antibiotic, and another one was sulfanilic acid having the similar structure of sulfanilamide (**Figure 39**). The medium used for enrichment cultivation was chemically defined, containing 0.5 mM sulfanilamide or 1 mM sulfonic acid as electron acceptor and 0.5 Bar H_2 as electron donor, 2 mM cysteine was added as reducing agent and no additional carbon source was added in the medium. Digester sludge from a biogas reactor and sediment from constructed wetland were used as inocula. However, no significant decrease of sulfanilic acid and sulfanilamide was observed after 9 months incubation (**Figure 40**), indicating no sulfanilic acid or no sulfanilamide was reduced with H_2 as electron acceptor.

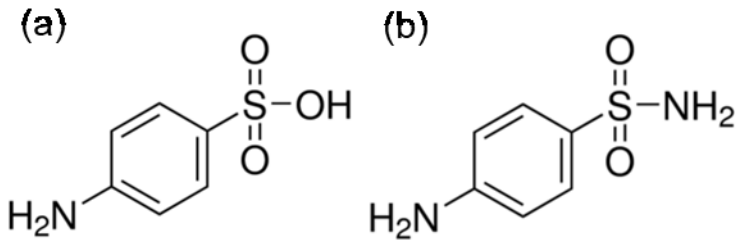

Figure 39. Chemical structures of sulfanilic acid and sulfanilamide. **a)** Sulfanilic acid; **b)** sulfanilamide

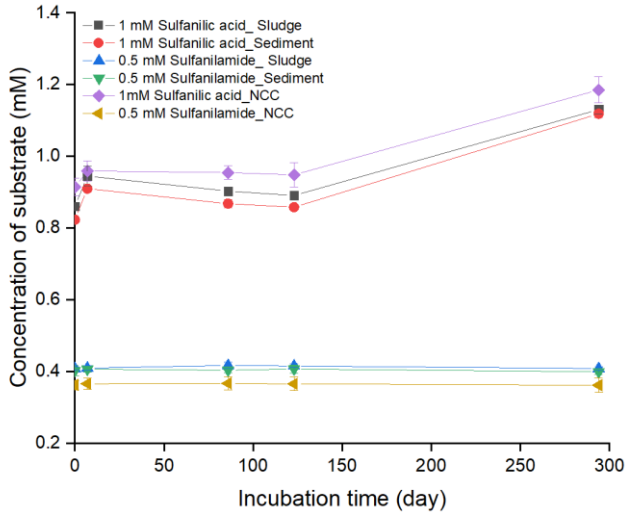

Figure 40. Quantification of sulfanilic acid and sulfanilamide in culture bottles during nine months incubation. All data is shown as mean of triplicate cultures ± standard deviation (SD).

3.4 Cometabolism of SMX by *D. vulgaris* Hildenborough

The type strain *D. vulgaris* Hildenborough was obtained from DSMZ for investigation of its SMX transformation activity, as *Desulfovibrio* was identified as dominant bacteria in the SMX-transforming sulfate-reducing cultures. In the *D. vulgaris* cultures, sulfate was added as electron acceptor and lactate was added as electron donor and carbon source. Different concentrations of SMX were spiked in the pure cultures to test the inhibitory effects of SMX on sulfate reducing activity, cell growth and SMX transformation activity. Close monitor of metabolism of *D. vulgaris* and transformation of SMX was conducted for one batch of *D. vulgaris* cultures to establish correlation in between. As SMX transformation is dependent on available electrons, here we also tested how lactate as electron donor affected the reductive transformation of SMX by *D. vulgaris*. In addition, intact-cell activity for SMX transformation was developed in our study, to examine factors influencing SMX transformation by *D. vulgaris*.

3.4.1 Anaerobic transformation of SMX by *D. vulgaris*

The genus *Desulfovibrio* was shown to be dominant in the mixed SMX-transforming sulfate-reducing cultures (**Figure 29**, **Figure 31**). Hence, we obtained the type strain *D. vulgaris* Hildenborough from the German Collection of Microorganisms and Cell Cultures (DSMZ) to test the SMX transformation activity. *D. vulgaris* was cultivated in the defined medium with 1 mM sulfate as electron acceptor and 4 mM cysteine as electron donor, and spiked with 100 µM SMX, the rest components were the same as the medium use for the mixed SMX-transforming sulfate-reducing cultures. Subculture was established with 3% inoculum. After cultivation for 14 days, 38% of SMX was transformed to the two transformation products TP1 and TP2 by *D. vulgaris* (**Figure 41**). Here we verified the transformation capacity of *Desulfovibrio* in a pure strain, and more correlation between the metabolisms of *D. vulgaris* and SMX transformation activity will be investigated in our subsequent study of the active pure strain.

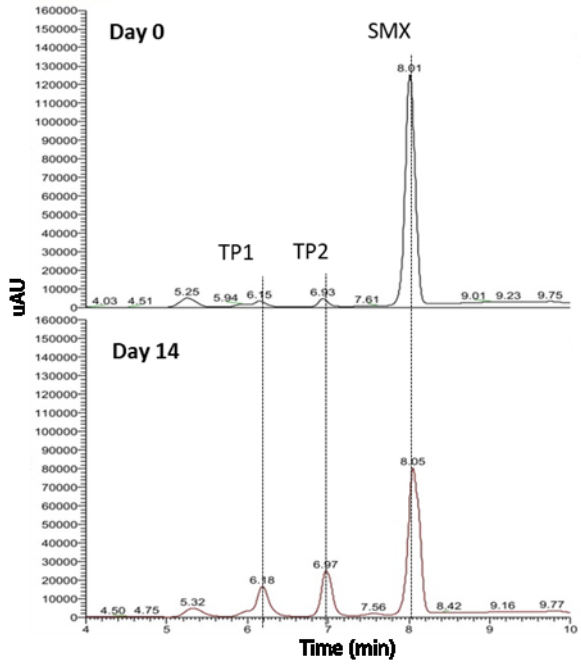

Figure 41. Transformation of SMX by *D. vulgaris* after 14 days cultivation. a) HPLC chromatogram of SMX, TP1 and TP2 in the *D. vulgaris* cultures on Day 1; b) HPLC chromatogram of SMX, TP1 and TP2 in the *D. vulgaris* cultures after 14 days cultivation. TP1 represents transformation product 1, and TP2 represents transformation product 2.

3.4.2 Inhibition and kinetics of SMX transformation by *D. vulgaris*

We investigated the transformation of SMX by *D. vulgaris* under different SMX concentrations (from 50 µM to 650 µM) to monitor the transformation kinetics, and evaluate the toxicity of

SMX on cell growth, sulfate reduction activity and transformation capacity. The cultivation medium contained 21 mM sulfate as electron acceptor and 17.8 mM lactate as electron donor and carbon source in each treatment. All cultures were established with 3% 10-days-old inocula. Inhibition of SMX on *D. vulgaris* growth was observed, but the cell still could grow even in the presence of SMX (**Figure 42**). A lag phase on *D. vulgaris* growth was detected for all SMX amended cultures, and after 11 days cultivation cells started growing in SMX treatments, while the cell density in the cultures with SMX was significantly lower than that in the cultures without SMX (**Figure 42**). Concentrations of sulfide and sulfate were measured in the medium, we found that the amounts of consumed sulfate were in line with generated sulfide, hence, we utilized generated sulfide to evaluate the extent of sulfate reduction. No inhibition of SMX on sulfate reduction was observed (**Figure 43**), indicating that there existed time gaps between energy conservation via sulfate reduction and cell growth in this batch of *D. vulgaris* cultures. In contrast, we observed no significant inhibition of SMX on transformation capacity of *D. vulgaris* under any SMX concentration (**Figure 44**), as cultures showed no lag phase during transformation. With initial SMX concentration of 50 μM SMX was completely transformed (**Figure 44**). When the concentration of SMX surpassed 200 μM, more SMX was consumed by *D. vulgaris* under higher SMX concentrations, but a trend that the transformation slowly ceased was also observed (**Figure 44**). Average transformation rate was calculated for each sampling interval in all SMX amended cultures, and the maximum transformation rate was found for the first 8 days (**Figure 44**), indicating that transformation activity decreased along the cultivation. We plotted the maximum transformation rate with SMX concentrations and found that the kinetics of transformation obeyed the first order kinetics, fitting the beginning period of Michaelis-Menten kinetics (**Figure 45**).

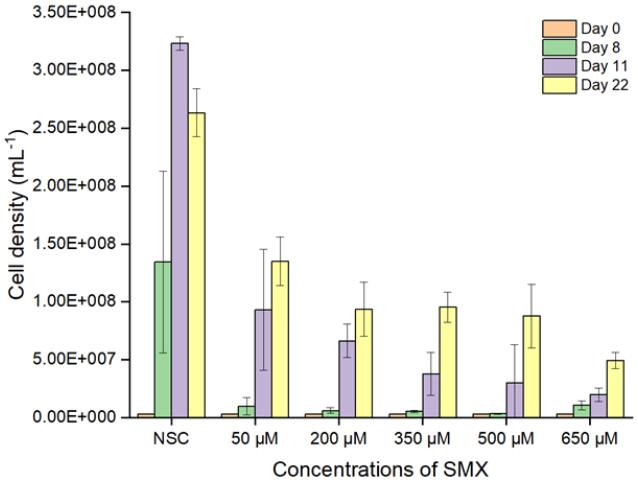

Figure 42. Cell density of *D. vulgaris* cultivated with different initial concentrations of SMX. Cultures were established with 21 mM sulfate as electron acceptor and 17.8 mM lactate as electron donor and carbon source, and with 3% inoculum. The reducing agent in the medium was 2 mM cysteine. Controls without SMX were set up as NSC (no substrate control). Shown are means of triplicate cultures ± SD.

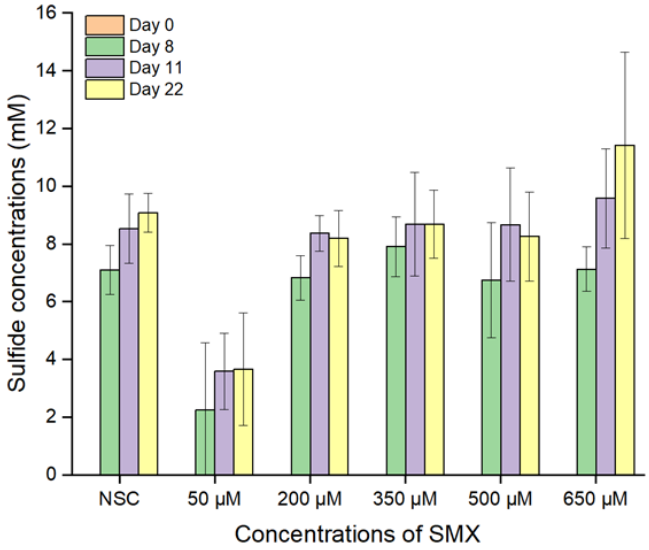

Figure 43. Sulfide generation by *D. vulgaris* cultivated with different initial concentrations of SMX. Shown are means of triplicate cultures ± SD. Note that the sulfide concentration in the "50 µM" treatment is lower than that in other treatments, via measuring the initial concentration of sulfate we found that less sulfate was added in this treatment by mistake.

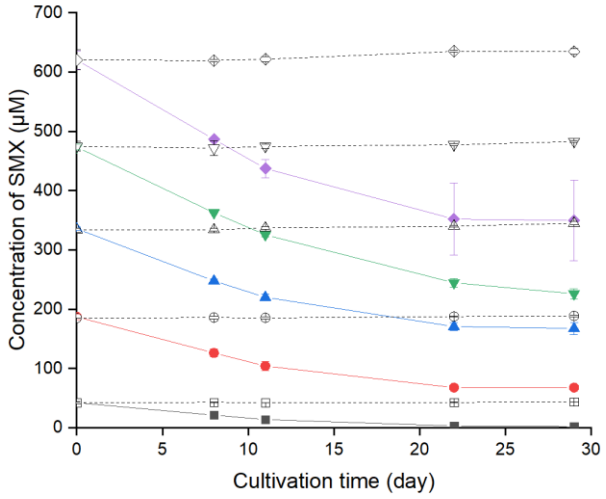

Figure 44. Transformation of SMX by *D. vulgaris* with different initial concentrations of SMX. Active cultures and no-cell control (NCC) were established for all five concentrations (50, 200, 350, 500 and 650 µM). Active cultures and NCC for one concentration share the same shape of symbols and the NCC are shown by dashed curves and empty symbols. All the treatments were cultivated for 29 days. Shown are means of triplicate cultures ± SD.

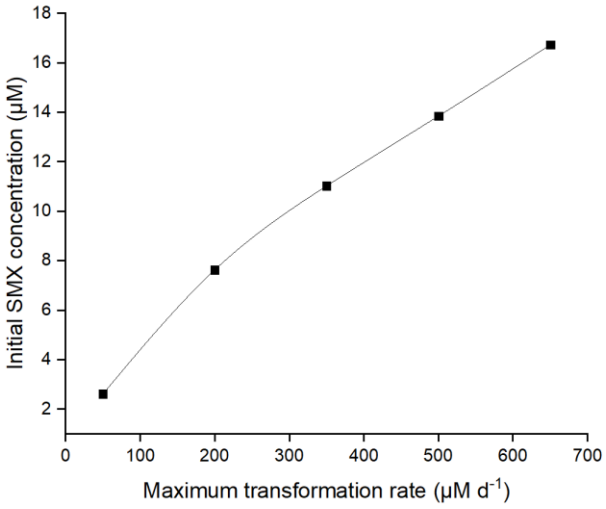

Figure 45. Maximum SMX transformation rate by *D, vulgaris* spiked with different initial concentrations of SMX (50, 200, 350, 500 and 650 µM)).

3.4.3 Correlation between metabolism of *D. vulgaris* and SMX transformation capacity

In order to investigate whether SMX transformation is coupled to the growth of *D. vulgaris*, we established a batch culture of *D. vulgaris*, with 21 mM sulfate as electron acceptor and 17.8 mM lactate as electron donor and carbon source, spiked with 100 µM SMX. Cultures were established with 3% 3-day-old inocula and the initial cell density was 1.8×10^6 cells mL^{-1}.

Meanwhile, abiotic controls containing 7 mM sulfide were also set up to monitor the potential interference of sulfide on SMX transformation. Samples were taken from each culture bottle every 12-24 hours for measurement of sulfide, SMX and cell density in the cultures.

Sulfate reduction started from time zero and finished at 72 h in both SMX spiked cultures and NSC, after 72 hours cultivation the concentrations of sulfide almost kept constant in all cultures. No effect of SMX on sulfate reduction process was detected (**Figure 46**a), which was in line with what we observed in the batch cultures with different initial concentrations of SMX (**Figure 44**). Cell number increased from time zero to 120 h reaching 1.5-1.87×10^8 cells mL^{-1}, but cell growth was slower in the first 72 hours compared to the later phase. Almost no inhibition of SMX on cell growth was observed in the whole cultivation period (**Figure 47**).

Transformation of SMX was initiated gradually and steadily with the generation of two transformation products TP1 and TP2, only small amounts of SMX were transformed, and no significant increase of SMX transformation was observed after 72 hours when cell growth accelerated, indicating that SMX transformation was not coupled to growth of *D. vulgaris* (**Figure 46**b). During the 14 days cultivation, transformation of SMX was not observed in abiotic controls with 7 mM sulfide, which excluded the interference of sulfide on transformation of SMX (**Figure 46**b).

In summary, SMX did not impact sulfate reduction activity and SMX transformation was not coupled to cell growth. The toxicity of SMX on cell growth was highly dependent on the age of the inoculum, young cells were more resistant to SMX than old cells (**Figure 42**, **Figure 47**).

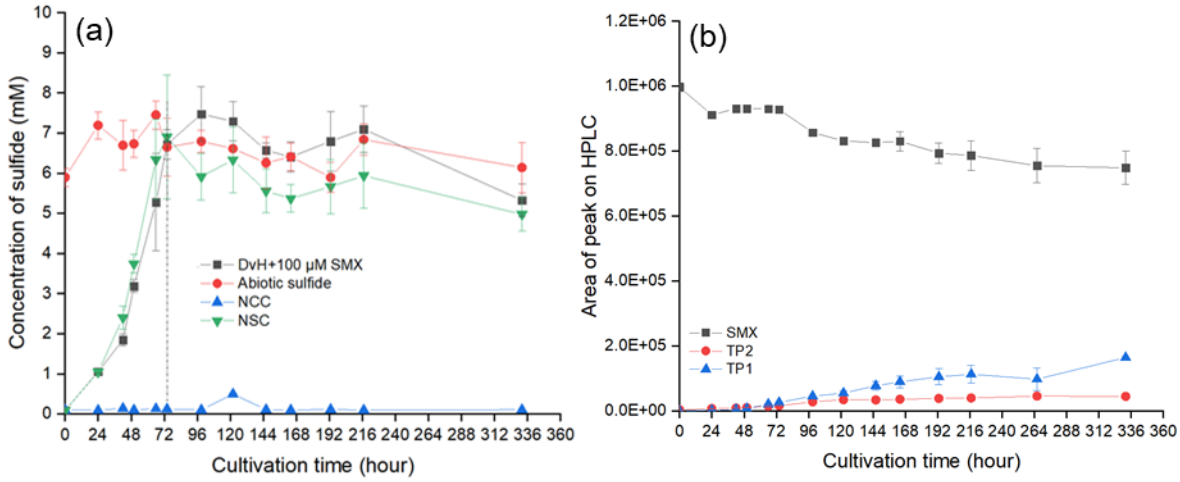

Figure 46. Sulfate reduction and SMX transformation by *D. vulgaris* during incubation with 100 µM SMX. Cultures were established with 21 mM sulfate as electron acceptor and 17.8 mM lactate as electron donor and carbon source, and with 3% inoculum. The reducing agent in the medium was 2 mM cysteine. **a)** Production of sulfide; **b)** decrease of SMX and generation of TP1 and TP2 during transformation process, Y-axis shows the peak area of SMX, TP1 and TP2 on HPLC. NCC: no cell control, NSC: no substrate control, abiotic controls contain 7 mM sulfide in the cultivation medium.

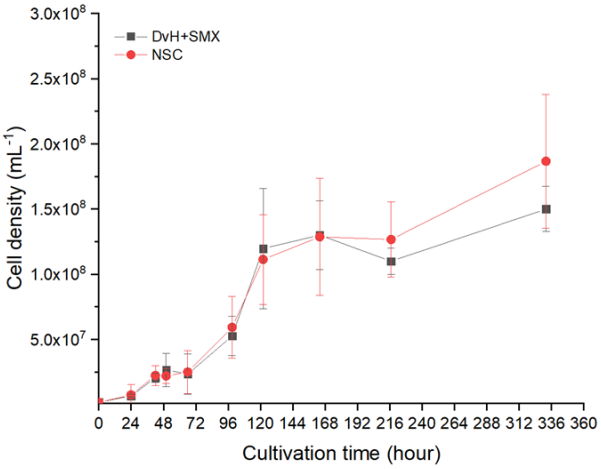

Figure 47. Cell density of *D. vulgaris* cultivated with 100 µM SMX. NSC: no substrate control.

3.4.4 Addition of lactate can promote transformation of SMX by *D. vulgaris*

As SMX transformation is a cometabolic reducing process by *D. vulgaris*, we tried to investigate the mechanism of SMX transformation and search for approaches of improving transformation capacity of *D. vulgaris*. We hypothesized that addition of electron donor can promote reductive SMX transformation. Hence, we established batch cultures with 100 µM SMX and different concentrations of lactate (12.7 and 18.5 mM) as electron donor and carbon source, in order to monitor the quantitative relationship between transformed SMX and

consumed lactate. Lactate was selected as tested electron donor as it can support fast growth of *D. vulgaris*, 8 mM sulfate was added in all treatments as electron acceptor and 2 mM cysteine was added as reducing agent.

Firstly, oxidation of lactate was evaluated in the batch cultures, by detecting the consumption of lactate and production of acetate. In the cultures amended with 12.7 mM lactate, lactate was used up after 3 days and same amounts of acetate was produced. In the treatment with 18.5 mM lactate it took 4 days until all added lactate was consumed and same amounts of acetate was generated (**Figure 48**).

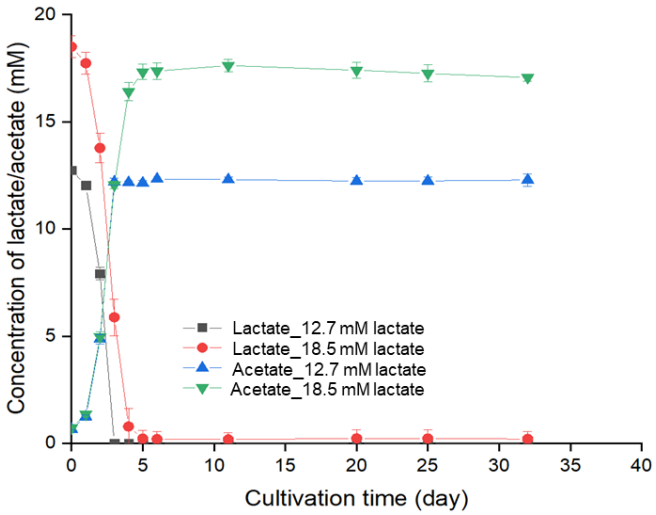

Figure 48. Quantification of lactate and acetate in *D. vulgaris* cultivated with different concentrations of lactate. Sulfate concentration was 8 mM in all treatments, concentrations of lactate were set as 12.7 mM and 18.5 mM in different treatments. Controls were set up in cultivation medium with 12.7 mM lactate or 18.5 mM lactate together with or without 7 mM sulfide (four controls as NCC1-4).

Meanwhile, we also monitored the sulfate reduction activity of *D. vulgaris*. Sulfide generation stopped on day 3 when 7.0 mM was produced in the 12.7 mM lactate treatment, and on day 5 8.6 mM sulfide was produced in the 18.5 mM lactate treatment (**Figure 49**). Sulfide generation was concurrent with lactate consumption and acetate generation. The generated sulfide represented consumed sulfate, here we observed that the stoichiometric ratio between consumed lactate and sulfate was approaching 2:1.

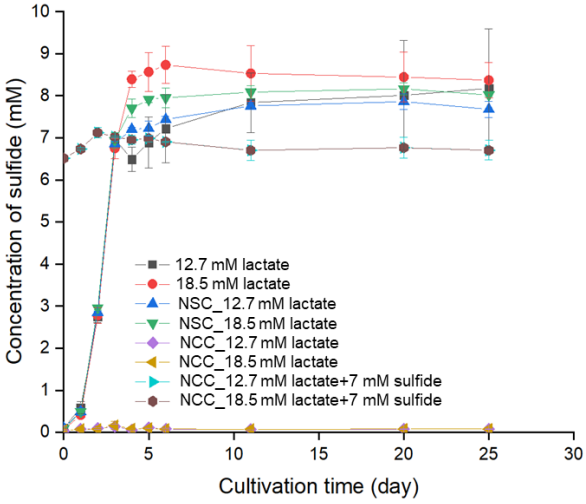

Figure 49. Quantification of sulfide in *D. vulgaris* cultivated with different amounts of lactate as electron donor and carbon source and 8 mM of sulfate as electron acceptor. The cultures are the same batch as described in **Figure 48**.

However, SMX transformation was not concurrent with lactate oxidation and sulfate reduction. We observed that transformation of SMX started after 4 and 6 days cultivation in two treatments with different concentrations of lactate (**Figure 50**). From day 0 to day 12 a similar trend on SMX transformation was observed in the two treatments, afterwards more SMX was transformed in the treatment with 18.5 mM lactate than that in the treatment with 12.7 mM lactate (**Figure 50**). After 32 days cultivation, we found that the transformed amounts of SMX were proportional to the amounts of consumed lactate: 30 µM SMX was transformed with 12.7 mM lactate, and 45 µM SMX was transformed with 18.5 mM lactate

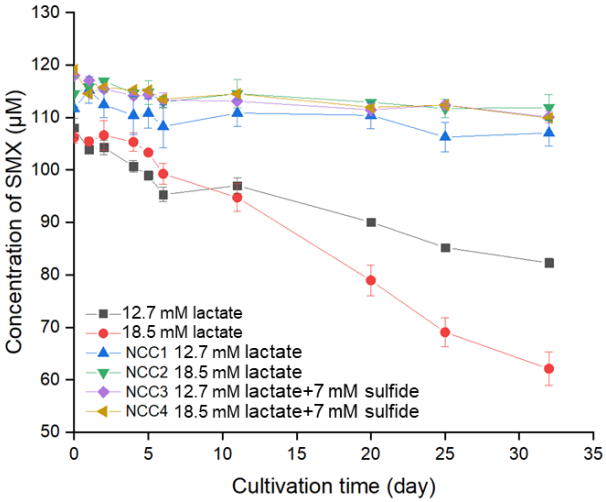

Figure 50. Transformation of SMX by *D. vulgaris* cultivated with different concentrations of lactate. The cultures are the same batch as described in **Figure 48**.

In order to further test the long term effects of electron donor on SMX transformation, we established another batch of *D. vulgaris* cultures with three different concentrations of lactate (8 mM, 16 mM and 24 mM) as electron donor and carbon source, and a fixed concentration of sulfate (8 mM) as electron acceptor. As we did not monitor lactate in this batch of cultures, consumed amounts of lactate were calculated. We calculated lactate oxidation based on our observation above that the stoichiometric ratio between lactate and sulfate was 2:1, hence, 8 mM and 16 mM lactate can be completed oxidized with 8 mM sulfate as electron acceptor, while in the treatment cultivated with 24 mM lactate only 16 mM lactate can be oxidized and 8 mM lactate will be left in the medium after sulfate reducing process. Sulfate reduction stopped on day 5 (data not shown). On day 7, decreased concentrations of SMX were proportional to calculated consumed concentrations of lactate, same concentrations of SMX were transformed in the treatments with 16 mM lactate and 24 mM lactate (**Figure 51**a), as theoretically 16 mM lactate was consumed in both treatments. After 16 days cultivation, decreased concentrations of SMX were proportional to added concentrations of lactate (**Figure 51**a), which indicated that probably excess lactate in the treatment amended with 24 mM lactate can continue to be slowly oxidized after sulfate reducing process and provide electrons for SMX transformation. From day 16 to day 132, less than 5 µM SMX was further transformed in the treatments amended with 8 mM and 16 mM lactate, while in the treatment amended with 24 mM lactate, more than 40 µM SMX was transformed (**Figure 51**b), which further indicated that electrons could directly flow from lactate oxidation to SMX transformation.

Overall, we observed that more lactate can induce more SMX transformation, and continuous transformation of SMX after sulfate reduction indicated that lactate could be slowly oxidized without being coupled with sulfate reduction and provide electrons for SMX transformation.

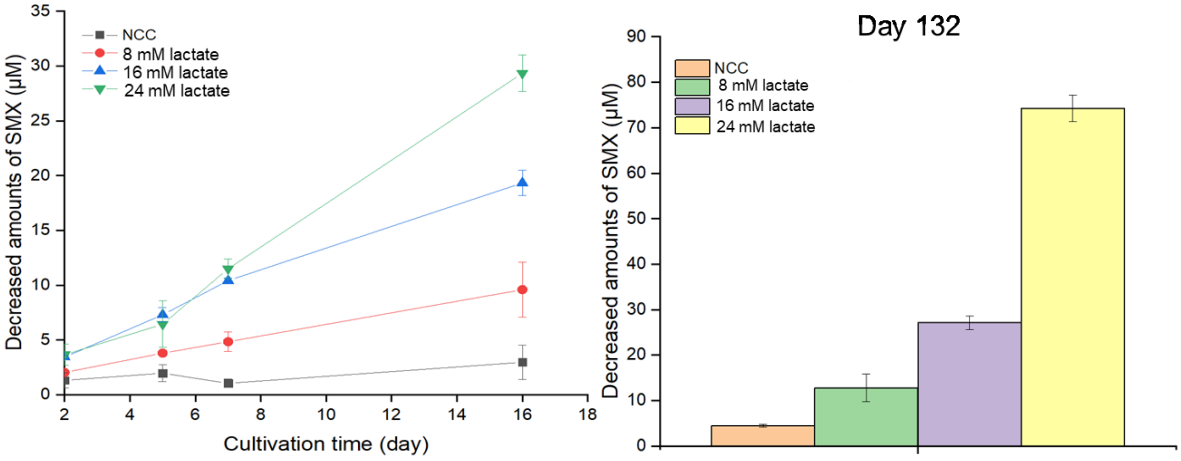

Figure 51. Transformation of SMX in *D. vulgaris* cultivated with different amounts of lactate. Here, lactate concentrations were set as 8 mM, 16 mM and 24 mM respectively. a) Decrease of SMX within 16 days cultivation; b) Decrease of SMX on day 132.

3.4.5 Intact-cell activity test revealed anaerobic transformation of SMX as an enzymatic reduction process

In our work with sulfate-reducing mixed cultures, we found that transformation of SMX was a reduction process mediated by bacterial cells. Here we aimed to investigate the transformation process on the molecular basis by using both mixed cultures and pure strain *D. vulgaris*. Therefore, we developed an in-vivo intact-cell activity test for SMX transformation. The biochemical basis of this test is that the transfer of electrons from the artificial electron donor methyl viologen radicals to SMX can be catalyzed by *D. vulgaris* cells, meanwhile Ti(III) citrate is added stoichiometrically to reduce oxidized methyl viologen to reactive methyl viologen radicals.

In the primary test, we found that SMX was not reduced by methyl viologen radicals directly without cells, even though TP2 was detected after overnight incubation, but TP2 (the rearranged product) disappeared after 4 days of incubation (**Table 11**). Moreover, cells alone without methyl viologen radicals also cannot transform SMX. However, in the presence of cells and methyl viologen radicals SMX was transformed, and the corresponding transformation product TP1 (the reduced product) was detected and accumulated with time (**Table 11**), indicating that cells catalyzed electron transfer from reduced methyl viologen radicals to SMX and triggered transformation of SMX.

Table 11. Establishment of intact-cell activity test for SMX transformation by using cells from sulfate-reducing mixed cultures. Transformation of SMX was evaluated after overnight and after 4 days incubation. The initial concentration of SMX was 50 μM in all treatments, cells were harvested from sulfate-reducing mixed cultures by centrifugation and the final cell density was 9×10^7 mL^{-1} in the activity test.

	Overnight			**Day4**		
	SMX peak area	TP1 peak area	TP2 peak area	SMX peak area	TP1 peak area	TP2 peak area
MV+SMX_1	517641	N	1783	532116	N	N
MV+SMX_2	528047	N	1974	525742	N	N
MV+SMX_3	528615	N	1669	537278	N	N
MV+SMX+cell_1	542274	5270	N	517120	12698	N
MV+SMX+cell_2	538066	5900	N	511251	15329	N
MV+SMX+cell_3	543447	6489	N	515027	15505	N
SMX+cell_1	575922	N	N	569990	N	N
SMX+cell_2	557053	N	N	562078	N	N
SMX+cell_3	557553	N	N	563667	N	N

Based on the established intact-cell activity test, we further investigated the transformation activity of crude extracts. After 6 days incubation, transformation of SMX was observed for both intact cells and crude extracts with detection of TP1, while significantly less TP1 was generated with crude extracts than that with intact cells (**Table 12**), indicating that disruption of cells could induce loss of transformation activity of cells.

Table 12. Activity test for SMX transformation of intact cells and crude extracts from sulfate-reducing mixed cultures. Transformation of SMX was evaluated after 6 days incubation. The initial concentration of SMX was 50 μM in all treatments, cells were harvested from sulfate reducing mixed cultures by centrifugation and the final cell density was 9×10^7 mL^{-1}.

	Day6		
	SMX peak area	TP1 peak area	TP2 peak area
MV+SMX_1	535476	0	0
MV+SMX_2	531628	0	0
MV+SMX_3	537036	0	0
MV+SMX+cell_1	518668	15608	0
MV+SMX+cell_2	503956	18866	0
MV+SMX+cell_3	501170	21073	0
MV+SMX+extract_1	527717	5035	0
MV+SMX+extract_2	527310	6283	0
MV+SMX+extract_3	533323	4954	0

In order to test the impact of the growth phase on SMX transformation, intact-cell activity test was done with exponential phase cells (3-day-cells) and stationary phase cells (11-day-cells) from pure strain *D. vulgaris*, and the 3-day-cells just finished sulfate-reducing process. Transformation of SMX in the activity test was evaluated at two time points during incubation: 30 minutes and day 4. After 30 min incubation, decrease of SMX was detected for both exponential phase cells and stationary phase cells together with generation of TP1, but the transformation activity was higher in exponential phase cells than that in stationary phase cells (**Figure 52**). After 4 days incubation, the exponential phase cells continued to show significantly higher transformation activity compared with stationary phase cells, and generation of both transformation products (TP1 and TP2) were detected for both cells concurrent with consumption of SMX (**Figure 52**).

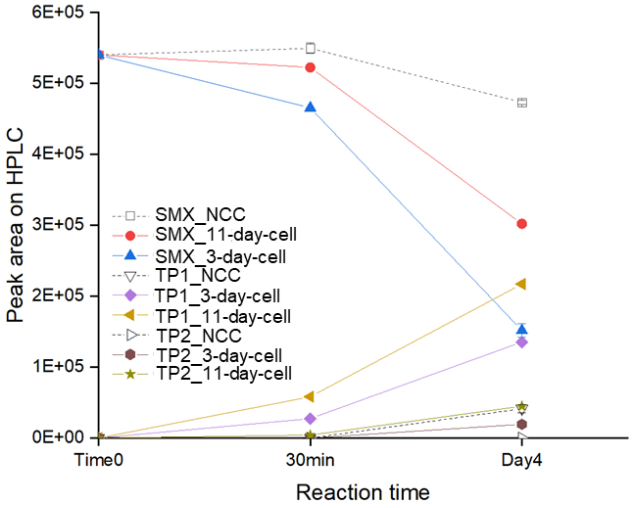

Figure 52. Intact-cell activity test on SMX transformation of cells from different growth phase. Cells were harvested from *D. vulgaris* cultures after 3 days cultivation (3-day-cells) and 11 days cultivation (11-day-cells). The final cell density of the harvested cells was 1.5×10^{9} mL^{-1}. The initial concentration of SMX was 50 µM, y-axis represents peak areas of SMX, TP1 and TP2 on HPLC. NCC: No cell controls are the same as "MV+SMX" in **Table 11**and **Table 12**. Note that the x-axis is not linear.

In order to investigate whether SMX can induce or promote the expression of specific transformation related proteins, intact-cell activity tests were done for cells cultivated with SMX (acclimated cells) and cells cultivated without SMX (unacclimated cells). Transformation of SMX was investigated in the activity test after 30 minutes and 4 days incubation. Decrease of SMX was observed in both acclimated cells and unacclimated cells at two time points, and no significant difference was observed between two types of cells (**Figure 53**). Similarly, the amounts of generated TP1 in acclimated cells were almost the same as that

in unacclimated cells (**Figure 53**). The results showed that cells acclimated by SMX did not significantly increase SMX transformation activity.

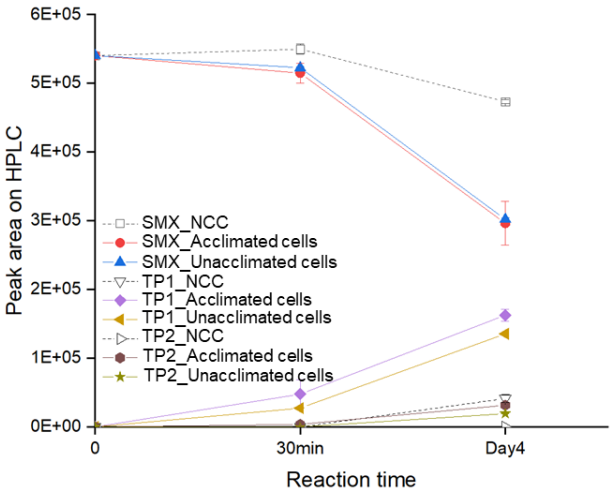

Figure 53. Intact-cell activity test on SMX transformation of acclimated cells and unacclimated cells. Acclimated cells were harvested from *D. vulgaris* cultures spiked with 100 µM SMX after 11 days cultivation, and unacclimated cells were harvested from *D. vulgaris* cultures after 11 days cultivation. The final cell density of harvested cells was 1.5×10^{9} mL^{-1}. The initial concentration of SMX was 50 µM. NCC: No cell controls are the same as "MV+SMX" in **Table 11** and **Table 12**. Note that the x-axis is not linear.

In order to identify the role that proteins play in SMX transformation, intact-cell activity tests were done for high-temperature-denatured cells and active cells of *D. vulgaris*. The denatured cells were achieved by treating *D. vulgaris* harvested cells at 80°C for two hours to inactivate proteins, the whole inactivated process was conducted in closed bottles to ensure anaerobic conditions. Transformation of SMX was evaluated after 5 days incubation by detecting SMX, TP1 and TP2 in the test system. In the denatured cell treatment significantly less transformation of SMX was observed compared to that in active cells (**Figure 54**). Even though small amounts of TP1 were detected in the denatured cell treatment, the amounts of TP1 were similar to that in NCC treatments (**Figure 54**). Our results showed that cells containing denatured proteins almost harbored no transformation activity, indicating that proteins in *D. vulgaris* cells could play an essential role in transformation of SMX.

In sum, an intact-cell activity test on SMX transformation was successfully developed and disruption of cells caused significant decrease of transformation activity. We found that exponential stage cells were more active on transformation of SMX than stationary phase cells. Besides, thermo instability of the transformation activity implied that transformation of SMX

may rely on the functions of proteins, and acclimation did not promote the transformation activity of cells.

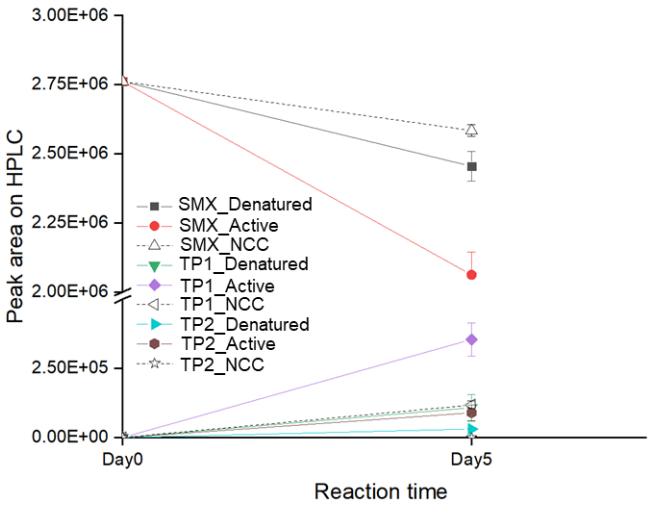

Figure 54. Activity test on SMX transformation of denatured cells and active cells. Cells were harvested from *D. vulgaris* cultures after 3 days cultivation. The final cell density of harvested cells was 1.5×10^{8} mL^{-1}. The initial concentration of SMX was 200 µM. NCC: No cell controls are the same as "MV+SMX" in **Table 11** and **Table 12**. Note that the x-axis is not linear.

3.5 Carbon and hydrogen isotopic fractionation of SMX during anaerobic transformation by *D. vulgaris* Hildenborough

3.5.1 Method development on GC-MS and GC-IRMS

In contrast to many other compounds readily accessible by gas chromatography (GC) measurement, SMX is a polar compound with high boiling point (482°C) and a low Henry's law volatility constant (6.4×10^{-13} atm·m^3/mol). HPLC is the routine method for detection of SMX. However, detection of SMX by GC has also been reported previously.[202] HPLC as a chromatographic separation sector connected with IRMS introduces aqueous mobile phase to IRMS, and the hydrogen from water can interfere with the detection of hydrogen isotopes of SMX.

In the first step, we established a separation method for SMX on GC without derivatization steps to overcome the drawbacks of HPLC, as derivatization could cause bias in isotope ratios. The eluting temperature of SMX on a ZB1 column (100% dimethylpolysiloxane) was found to be 320°C. The injector temperature was tested on GC-MS with 25 mM SMX from 180°C to 260°C to monitor the vaporization and decomposition of SMX (**Figure 55**a). SMX peak and

the corresponding by-products peaks were identified by NIST (National Institute of Standards and Technology) library with over 90% confidence. There were no significant differences of SMX's peak areas among different injector temperatures (**Figure 55**b). At the lowest tested temperature (180ºC), a tailing effect was observed on the SMX peak, resulting in unreproducible ion signals with the highest standard deviation (**Figure 55**a). The shape of SMX peak was improved at the temperatures above 200°C but by-products started to form. The three by-products from the thermal decomposition of SMX were tentatively identified by GC-MS. The most abundant by-product was proposed as sulfanilamide with N-C bond cleavage to split the sulfonamide group and isoxazole moiety. Aniline and 4-aminothiophenol were detected as less abundant compared to sulfanilamide (**Figure 56**, **Table S4**). The proportion of by-products ranged up to 5.5% of the total peak areas at different injector temperatures. The proportion of by-products increased along the injector temperatures from 180°C to 220°C. Higher injector temperatures significantly enhanced the tendency for SMX decomposition. At the temperatures higher than 240°C, the by-products proportion decreased without reproducibility which may imply that the primary by-products undergo further decomposition to unstable compounds or high molecular residues (**Figure 55**b). Within the tested temperatures the lowest decomposition of SMX was observed at 200°C (2.5%) (**Figure 55**b). Therefore, 200°C was selected as the optimal injector temperature for detection of SMX on GC.

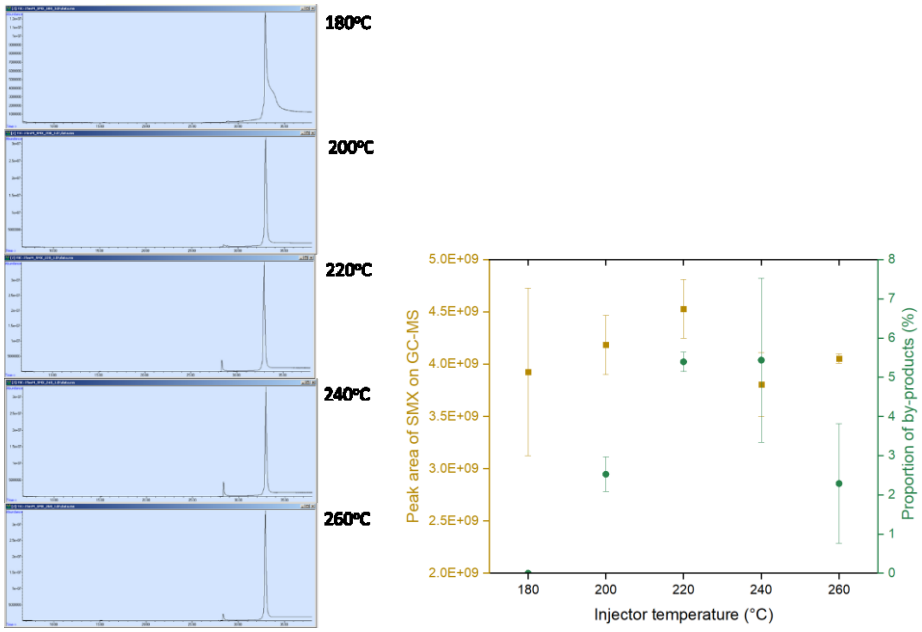

Figure 55. Vaporization and decomposition of SMX at different injector temperatures on GC-MS with 25 mM SMX injected. **a)** GC chromatogram for SMX standards with different injector temperatures; **b)** Peak areas of SMX with different injector temperatures (left Y-axis with yellow blocks) and proportion of the corresponding by-products (right Y-axis with green dots).

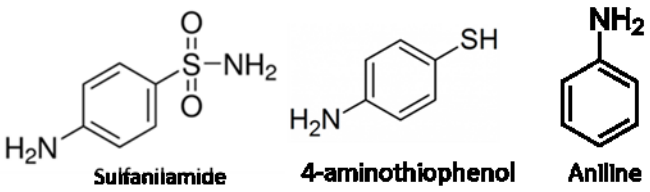

Figure 56. Proposed structures of by-products of SMX on GC-MS. Sulfanilamide is the most abundant by-product, and aniline is the least.

With the optimal injector temperature and the developed temperature program, we tested SMX standards with different concentrations from 1 mM to 125 mM on GC-MS, with the injected volume of 1 μL, for calibration. No signal was detected at 1 mM, and linear response was observed from 5 mM to 50 mM. When SMX concentrations were higher than 50 mM, signal intensities slightly increased along concentrations without a linear correlation (**Figure 57**a), implying that the evaporation of SMX were incomplete or by-products were formed. Additionally, we also observed that the proportions of by-products up to 11% were linearly relative to SMX concentrations (**Figure 57**b), suggesting that less injection can significantly reduce the decomposition of SMX.

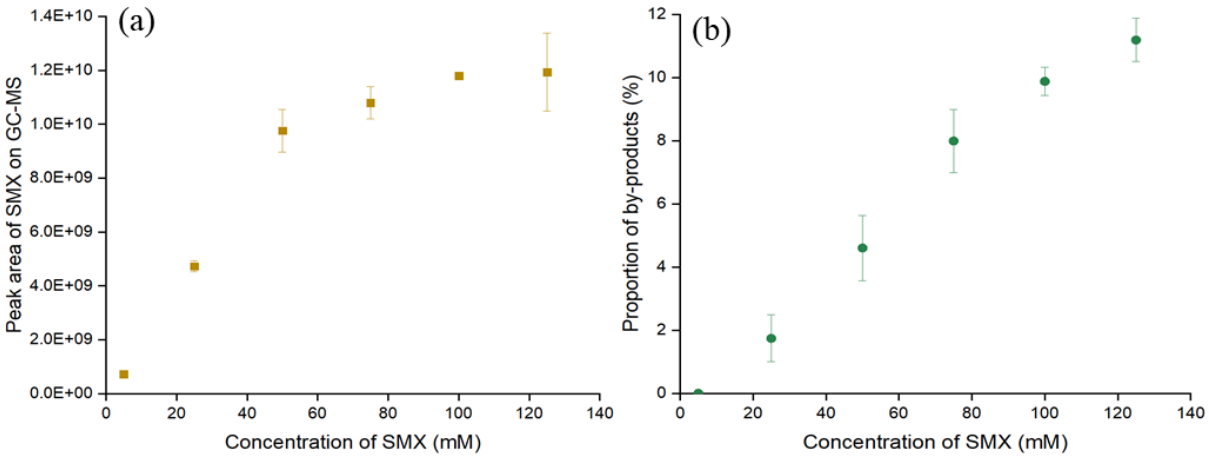

Figure 57. Signal response of SMX and proportions of by-products at different concentrations of SMX on GC-MS. **a)** Peak areas of SMX ions (yellow blocks) on GC-MS with different concentrations of SMX; **b)** proportions of by-products (green dots) in total signals with different concentrations of SMX.

3.5.2 Linear range of carbon and hydrogen isotopes

The dependency of isotope composition on the concentrations of SMX was determined to select the dynamic range of concentrations where the isotope composition can be reproducibly

determined. Therefore the peak areas of SMX were plotted against the isotope composition. Carbon and hydrogen isotope signatures ($\delta^{13}C$ and $\delta^{2}H$) of SMX were measured by GC-IRMS with the optimum GC operation parameters described above. A series of SMX standards (1 mM to 125 mM) were injected with different volumes (1 µL, 3 µL and 5 µL) to test the stable ranges of carbon and hydrogen isotope signatures, and the hydrogen data was adjusted based on H_3^+ factor. The results showed that when the injected SMX surpassed certain amounts, both carbon and hydrogen isotope ratios remained consistent with reproducible results. The fact indicates that within the stable ranges isotope ratios are independent of bulk concentrations of SMX. When peak area of SMX was over 5 Vs, carbon isotope ratio $\delta^{13}C$ was consistent as -26.5 ± 0.5‰ (**Figure 58**a). Higher peak areas of SMX (>13 Vs) were needed to reach the stable range of hydrogen isotope ratios $\delta^{2}H$ (-127.4 ± 6‰) (**Figure 58**b), as natural proportion of heavy hydrogen is less compared with that of carbon. Based on elemental analysis, the bulk carbon isotope ratio of SMX was -26.3 ± 0.1‰ (the horizontal dashed line indicates the mean value and the horizontal solid lines indicate the uncertainties in **Figure 58**a), and the bulk hydrogen isotope ratio of SMX was -124.5 ± 2.7‰ (the horizontal dashed line indicates the mean value and the horizontal solid lines indicate the uncertainties in **Figure 58**b). Both the carbon and hydrogen isotope ratios achieved from our developed GC-IRMS methods were in line with the bulk values directly obtained from elemental analyzer, which validates the feasibility of the developed GC-IRMS method for SMX analysis.

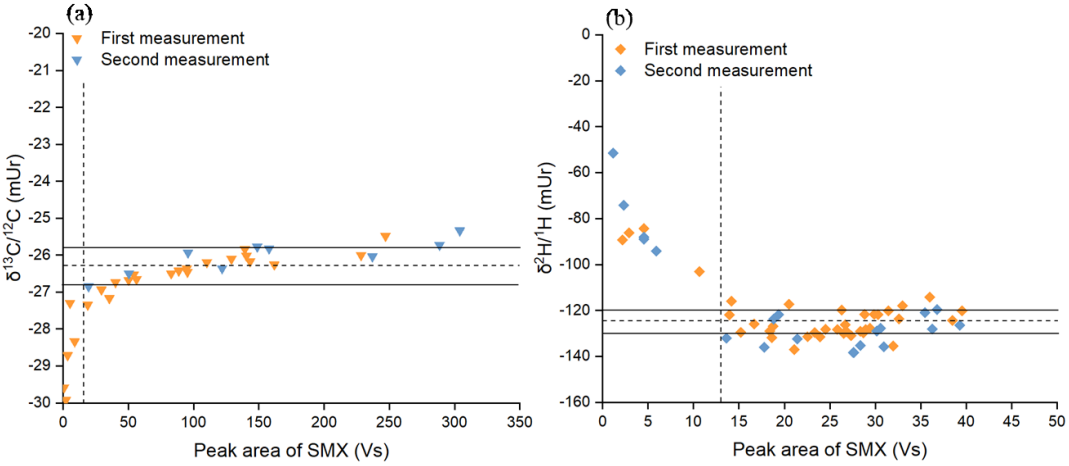

Figure 58. Carbon and hydrogen stable isotope ratios of SMX at different concentrations of SMX. **a)** Linearity of carbon isotope ratio (triangles) of SMX; **b)** Linearity of hydrogen isotope ratio (diamonds) of SMX. The vertical dash lines in panels a) and b) indicate the starting point of stable ranges for carbon and hydrogen. The horizontal dash line indicates the mean value and the horizontal solid lines indicate the uncertainties of the measurement. Two independent measurements were performed with the same SMX standards showing in different colors (orange and blue).

3.5.3 Carbon and hydrogen stable isotope fractionation during the anaerobic transformation of SMX by *D. vulgaris* Hildenborough

In order to analyze ^{2}H and ^{13}C isotope fractionation of SMX during anaerobic transformation, a batch of *D. vulgaris* cultures were established with 17.8 mM lactate as electron donor and carbon source and 21 mM sulfate as electron acceptor, 100 μM SMX was spiked in the cultures and 20 replicate bottles were set up in parallel. We already observed that *D. vulgaris* transformed SMX to two products (TP1 and TP2) stoichiometrically within a wide concentration range of SMX.[203] Transformation occurred on isoxazole moiety of SMX caused by reductive cleavage (TP1) and rearrangement (TP2) (**Figure 23**). In the established batch cultures, almost 75% of the spiked SMX (100 μM) was transformed by *D. vulgaris* after 9 days cultivation. As no transformation was observed for the first 4 days cultivation, 10 culture bottles were sacrificed from day 5 to day 9 for carbon and hydrogen isotopes analysis covering transformation degree from 0 to 75%.

Distinct carbon and hydrogen stable isotope fractionations of SMX were observed during anaerobic transformation of SMX by *D. vulgaris*. The carbon isotope composition of SMX changed from -26.5 to -18.6 for 65% transformation of SMX after 8 days cultivation (**Figure 59**). The isotope fractionation can be quantified by using the Rayleigh equation, yielding an enrichment factor (ε_C) for carbon as -5.8±0.7‰ during anaerobic transformation of SMX with a good correlation as indicated by the factor of determination (R^2=0.98) (**Figure 60**). Hydrogen isotope composition was also analyzed in culture samples, as more loading amounts were needed for hydrogen isotope analysis we only obtained valid data for 7 samples out of 10 samples which were used for carbon isotope analysis. The hydrogen isotope composition shifted from -148.2% to -123.7% for 52% transformation of SMX after 7 days cultivation, but the two points with the lowest SMX concentrations showing relatively large standard deviation may introduce uncertainties to hydrogen isotope analysis (**Figure 59**). We observed that the enrichment factor for hydrogen (ε_H) during anaerobic transformation of SMX by *D. vulgaris* was -33.8±9.2‰ with significant correlation between SMX concentration and hydrogen isotope signatures (R^2=0.82) (**Figure 60**).

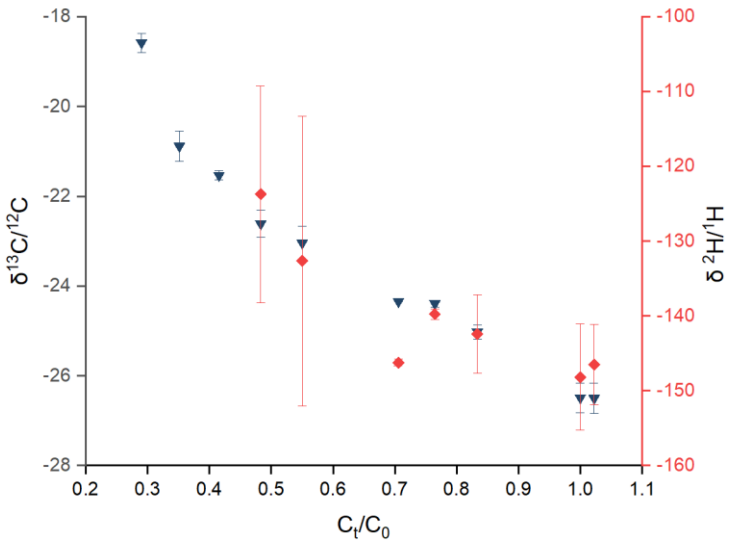

Figure 59. $\delta^{13}C/^{12}C$ and $\delta\ ^{2}H/^{1}H$ values of SMX during anaerobic transformation by *D. vulgaris* at different sampling points. The dark blue triangle symbols represent $\delta^{13}C/^{12}C$ values, and the red diamond symbols represent $^{2}H/^{1}H$ values.

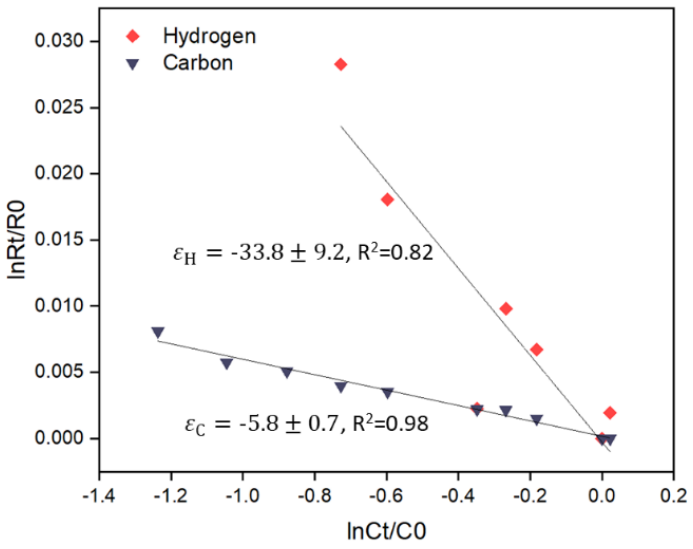

Figure 60. Carbon and hydrogen fractionations during the anaerobic degradation of SMX by *D. vulgaris* calculated by using the Rayleigh equation. The blue triangle symbols represent carbon and the red diamond symbols represent hydrogen. Enrichment factors (ε_C and ε_H) are shown along the data sets with correlation determinants.

3.5.4 Two dimensional isotope fractionation analysis

In order to investigate the relationship between carbon isotope fractionation and hydrogen isotope fractionation during anaerobic transformation of SMX, we plotted $\Delta\delta^{13}C$ with $\Delta\delta^{2}H$ for correlation analysis. We observed good correlation between change of carbon isotope ratios

and change of hydrogen isotope ratios during anaerobic transformation of SMX by *D. vulgaris*, and the $\Lambda^{H/C}_{bulk}$ value was 5.1±3.2 (R^2=0.77, **Figure 61**). This is the first dual-element isotope fractionation study for SMX, there is no reported lambda value available from literature to compare with that obtained one in our study. Nevertheless, the good correlation between carbon and hydrogen isotope compositions further confirmed the observed hydrogen isotope fractionation during anaerobic transformation.

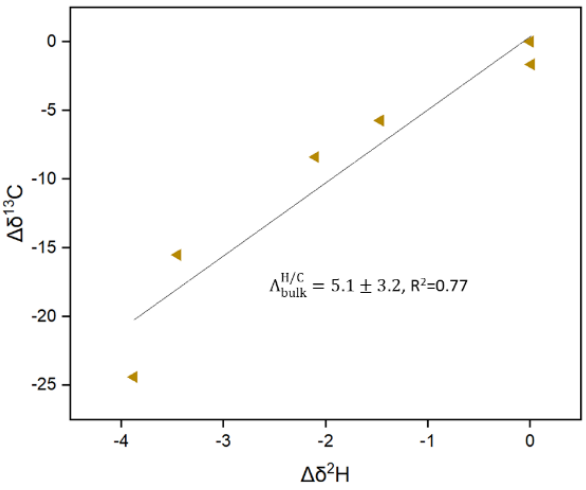

Figure 61. Two-dimensional compound specific stable isotope analysis of the anaerobic transformation of SMX by *D. vulgaris*.

4 Discussion

4.1 Microbial aerobic degradation of SMX in pig farm impacted soil

4.1.1 Microbial composition of in-situ SMX-degraders in pig-farm impacted soil

With the complementary results from DNA- and protein-SIP we here identified bacteria of the family *Intrasporangiaceae* as the major player of SMX assimilation in pig manure treated soil. Although other taxa within the phylum *Actinobacteria* have previously been associated with SMX degradation via cultivation approaches,[93,101] a crucial role of *Intrasporangiaceae* has yet never been observed. The closest isolate in this family, *Intrasporangium chromatireducens*, was isolated from manganese mining soil and was described to reduce chromate.[204] With the *Conexibacteraceae* and *Patulibacteraceae* we identified two further new groups within the phylum *Actinobacteria* as assimilating ^{13}C from $^{13}C_6$-SMX. Members of the *Nocardioidaceae* have previously been identified to degrade SMX[72,93] and also played a major role in our experiments.

The phylum *Actinobacteria* comprises many crucial microorganisms in soils with high metabolic versatility and potential for bioremediation of xenobiotics.[205] Also they naturally produce many different antibiotics[206-208] and harbor intrinsic multidrug resistance genes to synthetic antibiotics.[209,210] This broad metabolic versatility is reflected by large genomes and strong genomic plasticity as shown for *Rhodococcus* (*Nocardioidaceae*).[211]

4.1.2 Primary SMX-degraders in pig-farm impacted soil

The detection of $^{13}CO_2$ in the headspace of soil microcosms demonstrated that SMX was partially mineralized. In the microbial biomass we characterized the distribution of ^{13}C label within proteins. Between the different microbial populations strong differences in the ^{13}C incorporation degree $X(^{13}C)_{LP}$ were found (**Figure 16**). We hypothesize that these strong differences reflect that primary SMX degraders directly integrate ^{13}C from SMX and are thus higher labeled than secondary users growing on degradation products of SMX or on the necromass of primary degraders.[212] Within food chains the label will naturally dilute.[213] Such an interpretation of the results is supported by the detection of only a limited number of organism groups with high $X(^{13}C)_{LP}$ and a much higher number of organisms with low $X(^{13}C)_{LP}$. These two groups could represent primary and secondary SMX degraders, respectively. The high $X(^{13}C)_{LP}$ of 60-80% for *Intrasporangiaceae* is remarkable, given that the amount of $^{13}C_6$-

SMX that was added to the samples was relatively low, indicating a specific and preferential degradation of SMX as a carbon source. Such a specific and preferential degradation of SMX suggests that *Intrasporangiaceae* profit from SMX degradation, i.e. that they catalyze metabolic transformation of SMX. This has to be further investigated because it would allow the development of an efficient biotechnological process in which *Intrasporangiaceae* proliferate as long as the antibiotics are present.

4.1.3 Ecological risks of SMX-degraders

A major concern regarding antibiotic-degrading bacteria is that enrichment of these organisms may lead to the spread of resistance determinants in the environment.[214] For some antibiotics like beta-lactams, beta-lactamases responsible for inactivation are important contributors for antibiotic resistance, but in our case, few degradation related genes are reported as sulfonamide resistance genes. *Actinobacteria* do not have a dominant role as human or animal pathogen and most of the genes encoding the degradation pathway reside on the chromosome. This suggests that the resistance gene transfer potential from *Actinobacteria* to environmental bacteria or pathogens is lower than that from beta-lactam degraders.

4.1.4 Combination of DNA-SIP and protein-SIP

We used a combination of DNA- and protein-SIP together with a soil metagenomic database to link SMX degrading microorganisms in a soil microbiome with the anabolism of specific microbial populations. This approach was necessary because after addition of SMX no obvious population shifts at phylum level in the total community was observed; we did neither observe inhibition of SMX-susceptible populations nor enrichment of populations growing on SMX. Both effects would need higher SMX concentrations than could be used here due to the toxic effects of antibiotics. Also the low amount of applicable SMX prevented strong DNA labeling. Therefore, we analyzed the data for small OTU distribution shifts as done in quantitative DNA-SIP approaches previously.[215] The consistent results obtained with DNA- and protein-SIP confirm the reliability of the sensitive detection of the degrading bacteria under close-to-natural conditions and underpins the power of stable isotope probing as a critical method to link microbial identity to function.[216]

In fact, DNA-SIP and protein-SIP complement each other in their strengths: DNA-SIP is stronger on the precise phylogenetic identification due to the longer size of the amplified 16S rRNA gene sequences[217] and the larger database that can be used for BLASTn; on the other

side, protein-SIP is stronger in providing sensitive detection and even quantitative data of ^{13}C-incorporation.[158] Our metagenome database finally links the two data sets. Accordingly, in our study DNA-SIP identified four groups of potential SMX degraders with high ^{13}C incorporation of $X(^{13}C)_{LP}$ >50% and good taxonomic resolution, whereas protein-SIP identified more potential SMX degraders and also bacteria with lower incorporation degrees, that might have incorporated ^{13}C via indirect feeding within the microbial food web.

Whereas the results from the two SIP-methods mostly overlap, the family *Gaiellaceae* was identified by DNA-SIP but not by protein-SIP. We attribute this to the lower phylogenetic resolution of protein-SIP to affiliate labeled proteins, since the 16S rRNA gene of *Gaiellaceae* has high similarity with that of species of the genera *Thermoleophilum*, *Patulibacter*, *Conexibacter* and *Solirubrobacter*,[218] indicating even higher similarity in the proteins that are not differentiable. Similarly, a total of about 40% of the proteins identified as being labeled by protein-SIP could not be taxonomically affiliated, either due to the limited size of the metagenome database, or due to the limited size of the identified peptides. However, these limitations are outweighed by the power of protein-SIP to detect functional proteins allowing the development of hypotheses about carbon flux in the complex soil microbial community. Considering the limited size of the metagenome database and the high number of proteins present in the complex soil samples, we here focused on the phylogenetic origin of proteins identified by protein-SIP although principally, also degradation pathways can be analyzed if comprehensive protein data can be obtained.

4.1.5 Bias between cultivation-dependent and cultivation-independent methods

We conclude that different populations are degrading SMX in nature than previously identified by cultivation approaches in pure cultures. Future work focusing on the molecular monitoring of antibiotics-degrading populations should include such naturally active populations. In regard to our methodological approach we conclude that the concurrent application of DNA- and protein-SIP gives both, better taxonomic resolution and better incorporation sensitivity than application of one stable isotope approach alone. We hope this contribution supports the rational design of treatment approaches for sulfonamide-contaminated manure to avoid the further development and spread of ARGs. More detailed analyses of the genomic potential and enzymatic properties of *Intrasporangiaceae* are needed to explain the mechanism of SMX degradation and to develop a metabolic biotechnical process.

4.2 Anaerobic transformation of SMX by sulfate-reducing cultures

4.2.1 Transformation of SMX under different redox potentials

In our study, we obtained active and stable anaerobic SMX-transforming cultures under sulfate-reducing and methanogenic conditions, but sulfate-reducing cultures showed the highest transformation activity. A study in which behavior of SMX during bank filtration was investigated also suggested that the fate of SMX is redox-dependent and that SMX was eliminated more rapidly under anaerobic than under oxic conditions.[107] In fact, SMX was shown to be abiotically transformed by nitrite[109,110] to 4-nitro-SMX and reduced by Fe(II).[111] We obtained similar results with the strong reductant Ti(III) citrate. However, SMX does not readily react with sulfide. This indicates that the reduction of SMX in sulfate-reducing cultures is not abiotically-mediated by sulfide but that a reaction within the cells in sulfate-reducing cultures is responsible for SMX transformation. We obtained further evidence for this cell-mediated SMX reduction by comparing the activity of whole-cells and cell filtrates. Yet, we have no indication about the cellular processes underlying SMX reduction, but these processes do not seem to be coupled to energy conservation as we do not see growth based on SMX reduction. Such SMX-dependent growth would be expected if SMX were a terminal electron acceptor in an anaerobic respiration. Instead, SMX reduction could be a side reaction of a redox protein of sulfate-reducing bacteria. This might also explain the observation that SMX was not reduced under nitrate-reducing conditions, as nitrate would generally raise the redox potential in the cells.

4.2.2 Generation of transformation products in sulfate-reducing cultures

Our results suggest that SMX is stoichiometrically transformed to two alternative products TP1 and TP2 by the sulfate-reducing cultures. We observed that the ratio of TP1 to TP2 remained constant during the incubation of one batch of cultures (**Figure 25**), and none of the two products did react back to SMX after oxygen exposure. The stable ratio of TP1/TP2 indicates that TP1 and TP2 are not sequential transformation products but are formed in parallel. However, screening through the data of all cultures we also observed divergent TP1/TP2 ratios, and explain these by a different metabolic status of the cells.

We identified TP1 as a product with reductively cleaved isoxazole moiety and TP2 as one with rearranged isoxazole ring (**Figure 23**). The fact that these two products can also be detected during abiotic reduction of SMX by Ti(III) citrate suggests that the transformation is initiated

by a reductive mechanism. The heterocycle isoxazole possesses the typical properties of aromatic systems, but it contains a weak nitrogen-oxygen bond with a partially positively charged nitrogen atom which can be targeted by a nucleophilic attack.[219] Therefore, we propose anaerobic transformation of SMX is initiated by cleavage of the N-O bond via a nucleophilic attack by a reducing agent (R_{red}) on the nitrogen atom; the electron pair of the N-O bond is captured by the O-H bond in an opened ring that is the common intermediate of TP1 and TP2 (**Figure 62**). Then the electron pair of the O-H bond is either indirectly transferred along the molecule to the nitrogen atom to form a primary amino group under the addition of two protons and the removal of the reducing agent in its oxidized form (**Figure 62**, upper part); or the electrons are directly attacking the nitrogen atom leading to the release of the reducing agent in its reduced form and the formation of a three-membered cyclic structure which undergoes subsequent reorganization to an oxazole moiety (**Figure 62**, lower part). A reductive isoxazole ring cleavage was reported previously in other isoxazole containing pharmaceuticals.[220] Besides, it is reported that isoxazole can be thermally or photochemically converted to oxazole by a ring contraction-ring expansion mechanism, sharing the three-membered cyclic intermediate we propose.[200] The different ratios of TP1 to TP2 detected in different cultures could be due to different redox potentials of reductants in the cultures. The heterocycle isoxazole plays an important role in medicinal chemistry as it can have a variety of biological effects.[221,222] Nevertheless, under aerobic conditions the isoxazole moiety of SMX was recalcitrant and accumulated as dead-end products.[38] In our study, we revealed that anaerobic transformation by sulfate-reducing cultures did transform the pharmaceutically important isoxazole moiety of SMX and could therefore represent a promising process to avoid the formation of SMX dead-end products and also to deactivate isoxazole moieties of other pharmaceuticals.

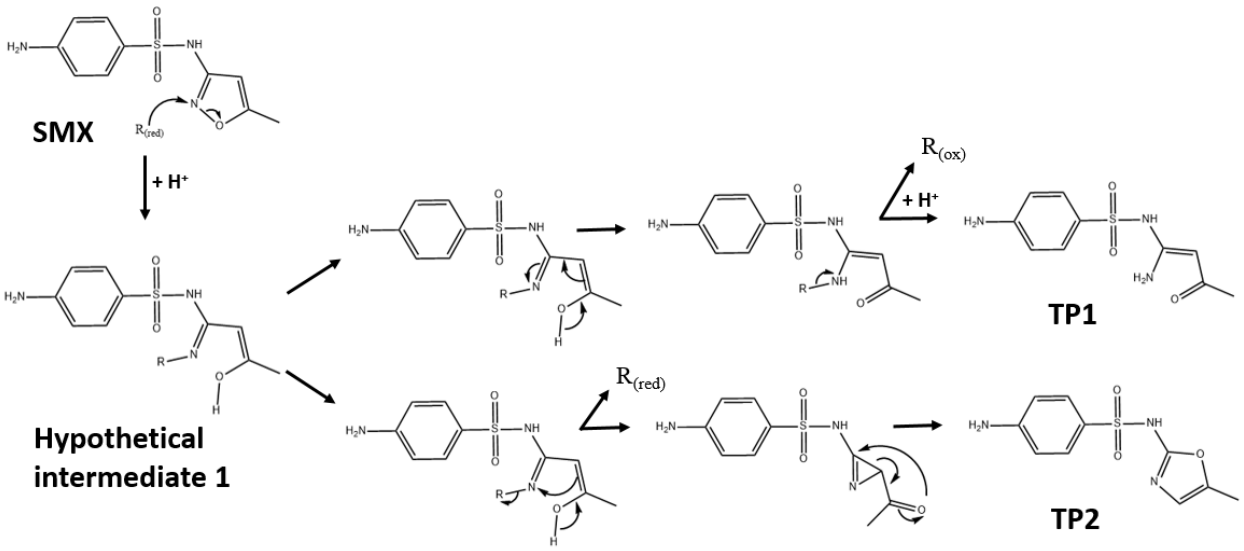

Figure 62. Proposed transformation mechanism of SMX to TP1 and TP2. Hypothetical intermediate 1 would be the common intermediate of TP1 and TP2. $R_{(red)}$ and $R_{(ox)}$ represent a reducing agent in its reduced and oxidized form, respectively.

4.2.3 Toxicity of transformation products from sulfate-reducing cultures

SMX is a bacteriostatic antibiotic inhibiting the synthesis of folic acid. In our study, transformation products of SMX with the modified isoxazole moiety showed less toxicity than SMX, and even counteracted the inhibitory effect of SMX. The antibacterial activity of SMX depends on the sulfanilamide moiety as an analog of *p*-aminobenzoic acid (PABA), and PABA is a substrate for the formation of dihydropteroate acid catalyzed by dihydropteroate synthase (DHPS). The crystal structure of DHPS revealed that the sulfanilamide binding site in the enzyme forms hydrogen bonds with the NH_2 group and one of the oxygen substituents of the sulfonamide bond.[223] Thus, SMX can compete with PABA for dihydropteroate synthase rendering folic acid deficiency in bacterial cells,[224] and the sulfonamide group in SMX is the bioactive part for its toxicity. Therefore, we assumed that SMX will lose its antibacterial activity if the sulfonamide group is destructed. However, in our study, already the modification of the isoxazole ring which is attached to the sulfonamide nitrogen atom significantly reduced toxicity of SMX. This can be explained by evaluating the electronic structure of the sulfonamide group. In SMX the sulfonamide group is electronically connected with the conjugated electron system of the isoxazole ring, however, in both TPs this electron system is disrupted. This confirms that indeed the side chain on the sulfonamide significantly influences the toxicity, a result that is known from the application praxis with the wide variety of different sulfonamides. The decrease of SMX toxicity by the presence of TP1 and TP2 in our

experiments is difficult to explain but possible reasons include the interference of the TPs with SMX transport into the cell or weakening the binding of SMX to dihydropteroate synthase. The consequence of this antagonistic effect is that even at partial SMX transformation, the toxicity of residual SMX is decreased, which has significance in both natural and engineered systems. In the future, we have to study the mechanism of this antagonistic effect in more detail.

4.2.4 Role of sulfate-reducing bacteria in bioremediation

We confirmed sulfide was not involved in the transformation of SMX, as was also not the case with any other extracellular substances from our SMX-transforming mixed cultures under sulfate-reducing conditions. Therefore, we hypothesize that other redox active compounds within the cells might trigger the reaction. *D. vulgaris* Hildenborough contains multiple redox proteins like ferredoxin, cytochrome c and proteins involved in sulfate reduction (e.g. *dsrC*). It has already been reported that substantial amounts of reduced cytochrome c can be stored in the periplasm as a reservoir of electrons and also as a linkage between different redox proteins.[127] Furthermore, the reduction of metal ions like Cr(VI) by *D. vulgaris* Hildenborough was reported to be connected with the cytochrome network.[149] Besides, other *Desulfovibrio* species can reduce and precipitate radioactive element like U(VI) to remove it from the water body.[133,147] For our future work to explain the molecular mediators within the cells we need to focus on the ability of redox proteins for transformation of xenobiotic compounds

4.3 Mechanism of anaerobic transformation of SMX by sulfate-reducing cultures

4.3.1 Effects of reducing agents/electron donors on transformation of SMX

We tried to calculate the sulfur mass balance in the sulfate-reducing cultures with cysteine as electron donor and carbon source and sulfate as electron acceptor (**Table 13**). We found that detected sulfide in the medium were significantly higher than theoretical values from sulfate reduction based on amounts of consumed sulfate. The ratio between cysteine and sulfate is approaching 4:1, as reduction of sulfate need 4 electron pairs, the ratio suggests that cysteine could provide 1 electron pair as electron donor. Depletion of cysteine was not observed in no-cell-controls. We assume that parts of detected sulfide is from the cysteine which acts as carbon source, and sulfur is cleaved from the carbon chain and released in the medium.[225]

Table 13. Sulfur mass balance in sulfate-reducing cultures incubated with cysteine as electron donor and carbon source.

	Total Sulfide (mM)	Consumed Sulfate (mM)	Sulfide (from Sulfate) (mM)	Sulfide from other sources (probably cysteine, mM)
1 mM SO4, 4 mM cysteine	2.33	0.60	0.60	1.73
10 mM SO4, 4 mM cysteine	2.40	0.90	0.90	1.50
10 mM SO4, 8 mM cysteine	3.76	1.90	1.90	1.86
10 mM SO4, 12 mM cysteine	4.87	2.70	2.70	2.17
NSC	2.26	0.40	0.40	1.86
NCC	0.00	0.00	0.00	0.00
Titanium Citrate	0.98	0.96	0.96	0.02

In sulfate-reducing mixed cultures, transformation of SMX was promoted with addition of reducing agents (cysteine and dithionite) and co-substrate (pyruvate). Besides, in *D. vulgaris* cultures, facilitation of SMX transformation was also observed with the presence of lactate. Therefore, we propose that addition of electron donors in sulfate-reducing cultures can significantly promote transformation of SMX. As SMX transformation was identified as an enzymatic reduction process, it is considered that the transformation degree is related with available reducing equivalence in cells. The high carbon isotope fractionation (**Figure 60**) observed in anaerobic transformation of SMX indicates that the transformation process may occur in the periplasm. The energy metabolism linking periplasmic dehydrogenase to the cytoplasmic terminal reductase in sulfate-reducing bacteria displays differences with other anaerobic respiration.[226] Several membrane-bound electron transfer complexes were identified in sulfate-reducing bacteria,[227] they can channel electrons from the periplasm and quinone pool to APS reductase and sulfite reductase. Besides, a pool of numerous periplasmic cytochromes *c* is distinct in *D. vulgaris*. With the presence of these periplasmic and membrane–bound electron transfer proteins, we hypothesize that the electrons from oxidation of electron donors could be directed to reductive transformation of SMX.

We also tried to quantify the relationship between electron donors and SMX transformation. In *D. vulgaris* cultures we observed positive correlation between lactate consumption and SMX transformation, and ratio is estimated to be 500:1, indicating that only small amounts of electrons generated from lactate oxidation are used for reductive transformation of SMX. We assume that SMX transformation may occur in parallel with sulfate reduction, while we also observed continuous transformation of SMX after sulfate reduction stopped. The explanation could be that the electrons are stored and slowly released, but we do not have direct evidence on how this process could occur.

4.3.2 SMX acts as cometabolic electron acceptor in sulfate-reducing cultures

The initial purpose of enrichment cultivation is to obtain active cultures utilizing metabolic process for SMX transformation, hence our medium with sulfate as electron acceptor did not contain additional carbon source and electron donor. However, based on the structures of the two identified transformation products, no loss of carbon atoms was detected during SMX transformation. SMX accepts two electrons during transformation. Therefore, SMX can neither act as carbon source nor electron donor during the transformation process, and we already revealed that reducing agent cysteine was electron donor and carbon source in the mixed sulfate-reducing cultures. No significant growth of cells was observed during transformation of SMX, it may indicate that even though SMX could be electron acceptor it cannot support cell growth. The reductive transformation of SMX may not be involved in energy conservation, but plays a role in recycling of redox cofactors, e.g. NADH. Based on the available results, SMX could act as a cometabolic electron acceptor in the ulfate-reducing cultures.

4.3.3 Toxicity of SMX on mixed sulfate-reducing cultures and *D. vulgaris*

SMX is a bacteriostatic antibiotic which can inhibit cell growth. Our results show that SMX can suppress the transformation activity of mixed sulfate-reducing cultures, as we observed that the cultures need longer lag phase with higher concentrations of SMX. However, the similar toxic effects of SMX were not observed in active *D. vulgaris* cultures even with the highest concentrations of SMX (**Figure 47**). In contrast, in another batch of *D. vulgaris* cultures with inocula from late stationary phase, longer lag phase and inhibition of cell growth were also observed (**Figure 42**). We propose that the effect of SMX on sulfate-reducing cultures are based on the status of cells, the more metabolically active of the cells the more resistance they display against SMX. Inhibition of cell growth is attributed to competitive inhibition of dihydropteroate synthase (DHPS) by SMX, as an analogue of precursor of folic acid: PABA. Metabolically active cells may contain enough amounts of DHPS, which could relieve the competitive pressure from the presence of SMX, resulting in less inhibition on cell growth. For sulfate-reducing mixed cultures, subculture was established only after at least half spiked SMX was transformed, to assure the presence of SMX-transforming bacteria in the mixed cultures, but the cells may already enter the stationary phase causing less resistance to SMX in the next passage. Hence, cell's metabolic status may trigger different response of cells to SMX. The fact may also explain the discrepancies of SMX's fate in natural environment and engineered systems reported in literatures.

4.3.4 Intact-cell activity test

Intact-cell activity test directly correlate transformation of SMX with cells' metabolic status. Heat-denatured cells lost transformation activity, indicating the important role of proteins play in SMX transformation. Besides, the transformation activity of disrupted cells decreased significantly compared with the intact cells, indicating that transformation of SMX may depend on functions of intact protein complexes or couple with energy consumption/generation. It is not clear whether disruption of cells completely destroys transformation activity or parts of activity is still maintained after disruption, as the activity we detected in crude extracts could come from small amounts of remained intact cells. Furthermore, exponential phase cells showed significantly higher SMX transformation than that of stationary phase cells, the explanation could be that during exponential phase more transformation related proteins are expressed.[228] However, no promotion of transformation activity was observed in SMX acclimated cells, indicating that the presence of SMX does not induce the expression of transformation related proteins, which is in line with the results from cultivation experiments that transformation of SMX is a cometabolic process.

4.4 CSIA to assess SMX attenuation

4.4.1 Distinctive carbon and hydrogen isotope features in anaerobic transformation of SMX

In anaerobic transformation of SMX, we observed distinct carbon and hydrogen isotope fractionations compared with microbial aerobic degradation, photolysis and oxidation (**Table 14**).[38,40,46] The ε_C value (-5.8±0.7‰) characterizing anaerobic transformation of SMX, was much higher than that of aerobic degradation by *Microbacterium* sp. strain BR1 (-0.6±0.1‰). The different mechanisms of aerobic and anaerobic transformation may result in diverse observed carbon fractionations. The activation step for anaerobic transformation by *D. vulgaris* is reductive cleavage of N-O bond while aerobic degradation by *Microbacterium* sp. is initiated by *ipso*-hydroxylation. Apart from mechanism differences, the much higher observed ε_C value for anaerobic transformation could also be attributed to less masking effect caused by mass transfer for periplasmic process compared with cytoplasmic process.[180] The anaerobic transformation was proposed as a periplasmic process referring to that periplasmic cytochrome c in *Desulfovibrio* can reduce heavy metals.[132,147,203] In contrast, for aerobic degradation Ricken et al. proposed that cytoplasmic NADH-dependent monooxygenase catalyzed

hydroxylation of SMX,[229] which could induce stronger masking effect and lower observed ε_C value. The reported ε_C value for direct photolysis was also lower than the one we observed for anaerobic transformation, and the ε_C value depended on wavelength and pH values. At pH 5 and 7.4 using artificial sunlight with a wavelength range of 300−800 nm the ε_C values were -3.0±0.1‰ and -2.0±0.1‰, respectively (**Table 14**). However, direct photolysis with short UV wavelength (254 nm) caused trivial (up to 0.8±0.1) to no observed carbon fractionations. The wavelength between 310-600 nm which may be relevant for sunlight at the surface at sea level gave ε_C values as -3.9±0.1‰ and -4.8±0.1‰ depending on the pH value. At pH 3 the most abundant photolysis product contains rearranged isoxazole ring which has the same structure as TP2 detected in anaerobic transformation by *D. vulgaris*, and the observed ε_C value was -4.8±0.1‰ approaching the carbon fractionation range in anaerobic transformation (-5.8±0.7‰). Therefore, we propose that the formation of TP2 causes the large carbon isotope fractionation during anaerobic transformation of SMX. The chemical reactions (e.g. photolysis and oxidation) are not selective like enzymatic reactions, cleavage at various positions undergoes simultaneously resulting in different degradation products, so that the observed ε_C values are derived from mixture of different mechanisms and depend on ratios of products,[46] which could explain the varying ε_C values observed during photolysis and oxidation and relatively lower ε_C values compared with that of anaerobic transformation.

This is the first study to report hydrogen isotope fractionation of SMX, as no hydrogen isotope data was available for SMX via HPLC-IRMS in previous studies.[38,40,46] No hydrogen atom is directly involved in the bond cleavage according to the proposed mechanism (**Figure 63**),[203] thus, the observed hydrogen isotope fractionation of SMX should be caused by secondary isotope kinetic effects. We assume that the substituted hydrogen atom at C_4 atom (mark red in **Figure 63**) contribute to the change of hydrogen isotope composition during formation of TP2 intermediate, as the three-membered-ring in TP2 intermediate increased the available oscillation space for above-mentioned hydrogen atom, and this circumstance is preferred by light hydrogen.[230] High uncertainties were observed in hydrogen isotope values with low concentrations of SMX, while we observed good correlation between hydrogen and carbon isotope compositions, which could confirm the observed hydrogen isotope fractionation during anaerobic transformation. This is also the first dual-element isotope fractionation study for SMX, there is no reported lambda value available from literature to compare with that obtained in our study. Dual-element isotope analysis of SMX provides more possibilities to characterize transformation processes, whereas previous studies by HPLC-IRMS[38] and HT-LC-IRMS

methods[183] are only capable to analyze carbon isotopes for sulfonamides, as analysis of other elements is limited by available efficient conversion steps. Isotope data for other elements are also crucial for investigating SMX transformation. For example, by screening photolysis products Willach found that apart from carbon[40] other atoms like N and S are also directly involved in bond cleavage for products formation, therefore, multiple element isotope analysis is essential. Nevertheless, in our study we show that dual-element analysis of SMX is feasible, and the lambda values of different processes could be used for assessment of SMX attenuation in field studies.

Table 14. Bulk enrichment factors ($\varepsilon_{C\,bulk}$), AKIE and Lambda values for the aerobic degradation of SMX by *Microbacterium* sp., anaerobic transformation of SMX by *D. vulgaris* Hildenborough and abiotic transformation of SMX including photolysis and oxidation.

Microbial and abiotic transformation of SMX	Initial concentration of SMX [µM]	ε_Cbulk [‰], (R^2)	AKIE C	ε_Hbulk [‰], (R^2)	AKIE H	ΛH/C , (R^2)	Reference
D. vulgaris Hildenborough	100	-5.8±0.7 (0.98)	1.029±0.003	-33.8±9.2 (0.81)	1.469±0.170	5.1±3.2 (0.77)	This study
Microbacterium sp. strain BR1	500	-0.6±0.1 (0.86)	1.006±0.001	N.D.	N.D.	N.D.	[38]
Direct photolysis at PH 7.4	1000	-2.0±0.1 (0.94)	1.021±0.002	N.D.	N.D.	N.D.	[38]
Direct photolysis at PH 5	1000	-3.0±0.1 (0.95)	1.031±0.004	N.D.	N.D.	N.D.	[38]
Direct photolysis at PH 3	790	0.8±0.1 (LP 254 nm), N.S. (MP, 200-600 nm), -4.8±0.1 (MP 310-600 nm), -1.9±0.1 (HP 220-500 nm)	N.D.	N.D.	N.D.	N.D.	[40]
Direct photolysis at PH 8	790	N.S. (LP 254 nm), N.S. (MP, 200-600 nm), -3.9±0.1 (MP 310-600 nm), -2.2±0.2 (HP 220-500 nm)	N.D.	N.D.	N.D.	N.D.	[40]
Oxidation at PH 3	790	-1.2±0.1 (O3), -2.2±0.1 (O3+DMSO), -0.8±0.1 (ClO2)	N.D.	N.D.	N.D.	N.D.	[46]
Oxidation at PH 8	790	N.S. (O3), N.S. (O3+DMSO), -1.3±0.1 (ClO2)	N.D.	N.D.	N.D.	N.D.	[46]

N.D. means not detected or not available in the related studies; N.S. means the isotope fractionation is not significant under these conditions; LP represents low pressure irradiation source, MP represents medium pressure irradiation source and HP represents high pressure irradiation source.

4.4.2 Apparent kinetic isotope effect (AKIE) in anaerobic transformation of SMX

According to the previously proposed anaerobic transformation mechanism,[203] the activation step is reductive cleavage and electron rearrangement of isoxazole ring. Anaerobic transformation of SMX is initiated by nucleophilic attack at N atom and the common intermediate is generated after cleavage of N-O bond, followed by electron rearrangement undergoing two different pathways (**Figure 63**). Therefore, the corresponding AKIE values for carbon and hydrogen ($AKIE_C$ and $AKIE_H$) were calculated based on the equations (7), (8) and (9) and compared with reported values from microbial aerobic degradation and chemical reactions in **Table 14**.

2 out of 10 carbon atoms are at the reactive positions

$$\delta_{reactive\ position}=\delta_{bulk} \times \frac{10}{2} \quad (7)$$

And 1 out of 11 hydrogen atoms is located at the reactive position

$$\delta_{reactive\ position}=\delta_{bulk} \times \frac{11}{1} \quad (8)$$

Based on mechanism in **Figure 63**, the number z is 1 for both carbon and hydrogen atoms during the formation of TP1 intermediate and TP2 intermediate.

$$AKIE=\frac{1}{1+1 \times \varepsilon_{\text{reactive position}}/1000} \quad (9)$$

The $AKIE_C$ value for anaerobic transformation by *D. vulgaris* was 1.029±0.003, which is significantly different from that of aerobic degradation by *Microbacterium* sp. strain BR1 as 1.006±0.001 (**Table 14**). Hence, the $AKIE_C$ values obtained in our study further support that anaerobic transformation utilizes different mechanism than that of aerobic degradation. The $AKIE_C$ value for aerobic degradation (upon *ipso*-hydroxylation) fits in the same range of aromatic ring hydroxylation of BTEX ($AKIE_C$ (benzene) =1.005±0.001, $AKIE_C$ (toluene) = 1.006±0.001)[173,231] and the theoretical range for epoxidation-like C=C bond cleavage ($AKIE_C$=1.00 to 1.01).[193] $AKIE_C$ (1.029±0.003) for anaerobic transformation is close to the reported value of anaerobic biodegradation of p-cresol by sulfate reducing bacteria ($AKIE_C$=1.028),[193,232] and also fits in the theoretical range of oxidation of C=C bonds with permanganate via dihydroxylation (1.025-0.028).[193,233] In this study, we also obtained $AKIE_H$

value for anaerobic transformation of SMX as 1.469±0.170, but there are no reported $AKIE_H$ values for SMX in literatures.

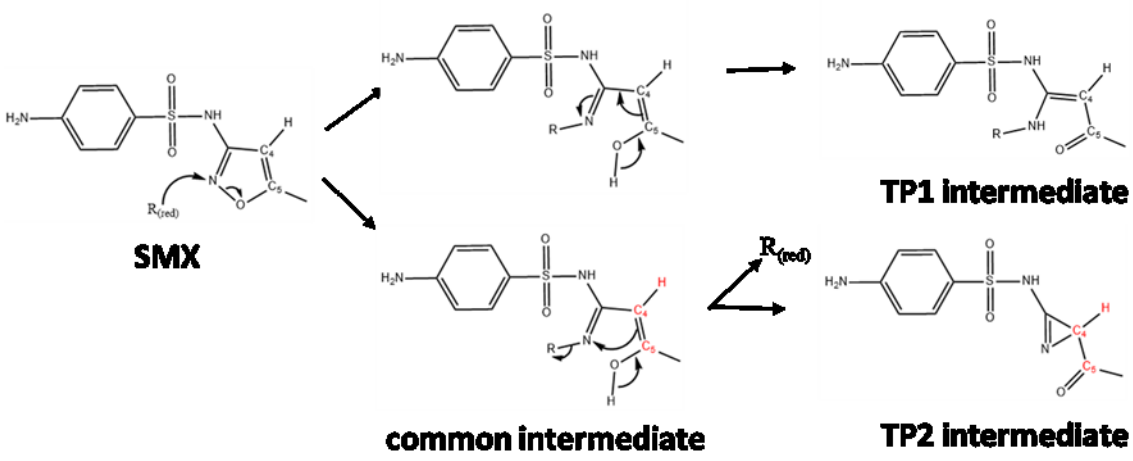

Figure 63. Initial reactions of anaerobic transformation of SMX by *D. vulgaris* Hildenborough activated by a reducing agent $R_{(red)}$. Elements in red represent atoms at the reactive positions.

4.4.3 Carbon isotope features of transformation products

We also tried to analyze the isotope features of transformation products to identify which pathway (TP1 pathway or TP2 pathway) triggers the carbon isotope fractionation. Peaks of TP1 and TP2 were not detected under hydrogen isotope analysis mode as the amounts of products were not sufficient. Only TP1 peak was detected under carbon isotope analysis mode and the structure of TP1 was confirmed by GC-MS (mass spectra not shown). We observed that the carbon isotope ratios of TP1 kept consistent during transformation of SMX (**Figure 64**). The fact indicates that the formation of TP1 did not contribute to the fractionation of SMX, which is in line with what we proposed in **Figure 63** that only the formation of TP2 induced carbon fractionation of SMX.

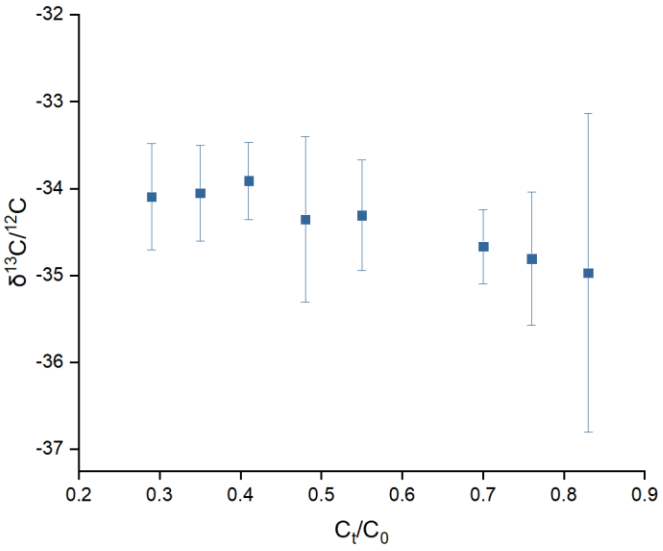

Figure 64. $\delta^{13}C/^{12}C$ value of TP1 during anaerobic transformation by *Desulfovibrio vulgaris* Hildenborough at different sampling points.

5 Conclusions and outlook

Conclusions

Key players for SMX degradation and transformation under aerobic and anaerobic conditions were identified in our study. In pig-farm impacted soil, we detected mineralization and assimilation of SMX under aerobic conditions. The complementary results from DNA- and protein-SIP revealed that the bacteria *Intrasporangiaceae* were the dominant players for SMX assimilation, indicating that non-cultivable bacteria may play a key role in SMX degradation in the real environment. In sediment and digester sludge, sulfate-reducing bacteria showed high activity in transformation of SMX. Transformation products in sulfate-reducing cultures were identified as reduced and isomerized form of the isoxazole moiety, showing less antibacterial activity than SMX. We revealed that anaerobic transformation of SMX by sulfate-reducing bacteria was a detoxification process. Population analysis indicated that *Desulfovibrio* as dominant bacteria in SMX-transforming cultures may act as key players, the assumption was then tested on pure strain *D. vulgaris* Hildenborough and the same transformation products were detected. Further experiments showed that anaerobic transformation of SMX by *D. vulgaris* was a cometabolic process, and addition of electron donor can promote the transformation. Besides, significant carbon and hydrogen isotope fractionations were observed during anaerobic transformation of SMX by *D. vulgaris*. In addition, our work also made progress in methodology. We developed protein-SIP method combined with metaproteomics database for soil microbiology, and revealed that protein-SIP was more sensitive than DNA-SIP in tracing incorporation of labeled atoms, while DNA-SIP was more precise in identifying phylogenetic information. Instead of HPLC-IRMS, we developed GC-IRMS method without derivatization for analyzing carbon and hydrogen isotope compositions of SMX, overcoming the limit of HPLC-IRMS on measurement of hydrogen isotope. The current work allowed a better understanding of microbial removal of SMX, and could enhance fate prediction of SMX in the environment and further contribute to the bioremediation of SMX.

Outlook

To further investigate the degradation capacity of the in-situ SMX-degraders, we can try to isolate and cultivate *Intrasporangiaceae* from the pig-farm impacted soil. However, the conventional enrichment cultivation in minimal salt medium with SMX as sole carbon source was already conducted in parallel with SIP experiment and we did not successfully enriched *Intrasporangiaceae*. Hence, we may need a novel cultivation method to isolate

Intrasporangiaceae, such as a recently reported culturing chip, which can facilitate culturing of uncultivable bacteria from aquatic environment.[234] In our SIP experiment, we incubated $^{13}C_6$-SMX with soil to identify key players, while the unlabeled carbon on the isoxazole ring was not traced, in this way, we could not trace bacteria attacking and assimilating the isoxazole ring of SMX, therefore, we can try to apply ^{13}C-fully labeled SMX for the SIP incubation in the future.

To reveal the transformation mechanism of *D. vulgaris* on the molecular basis, we can try to test the transformation activity of different protein fractions. The protein fractions can be obtained by different techniques including FPLC (fast protein liquid chromatography), ultrafiltration and Blue Native PAGE. In order to identify the functional proteins responsible for SMX transformation, the composition of active protein fractions can be analyzed by high resolution mass spectrometry.

Instead of cometabolic transformation of SMX by sulfate-reducing bacteria, we can try to enrich anaerobic cultures which can transform SMX metabolically. We assume that the aimed enrichment cultures can respire the sulfonamide group in SMX as electron acceptor for energy conservation, theoretically, the cultures could grow on a wide range of sulfonamide antibiotics, as the sulfonamide group is the essential and functional structure of these antibiotics. Besides, we can also test the SMX transformation activity of various groups of sulfate-reducing bacteria, to investigate whether reductive transformation is the common property of sulfate-reducing bacteria.

We can try to develop a GC-IRMS method to analyze the nitrogen isotope of SMX, as the initial attack of anaerobic transformation occurs on the N-O bond of the isoxazole ring. With the method we can study nitrogen isotope fractionation of SMX during different removal processes including aerobic degradation, anaerobic transformation or photolysis.

We could also scale up our results obtained from laboratory-scale cultivation, we can try to monitor the two transformation products by sulfate-reducing cultures in the real anaerobic environment, and monitor the carbon and hydrogen isotope compositions of SMX to estimate the removal extent of SMX.

Supporting information

Table S1. Number of shifted OTUs identified by comparing labeled and unlabeled samples for each fraction in a CsCl density gradient after ultracentrifugation. Buoyant density increased linearly from fraction 7 (lightest) to fraction 1 (heaviest). Among the significantly shifted OTUs, we define **enriched OTUs** as the ones which show higher relative abundance in labeled samples, and **diminished OTUs** as the ones which show lower relative abundance in labeled samples.

Fraction	Number of total OUTs in the ^{13}C-SMX treatment	Number of significantly shifted OTUs (significantly different population share between ^{12}C- and ^{13}C-SMX treatment)	Number of enriched OTUs* (higher population share in the ^{13}C than in the ^{12}C treatment)	Number of diminished OTUs* (higher population share in the ^{12}C than in the ^{13}C treatment)
7 (lightest)	12075	73	44 (60%)	29 (40%)
6	9467	7	3 (43%)	4 (57%)
5	11228	22	11 (50%)	11 (50%)
4	13401	20	18 (90%)	2 (10%)
3	19464	86	63 (73%)	23 (27%)
2	13906	34	28 (82%)	6 (18%)
1 (heaviest)	13359	19	17 (89%)	2 (11%)

Table S2. Quantification of SMX and transformation products in cultures shown in **Figure 20** including initial concentrations and concentrations after 14 months of incubation.

Nominal SMX conc. day 0	Measured SMX conc. day 0	Measured SMX conc. after 14 months	Calculated TP conc. after 14 months[1]	Transformation degree after 14 months	Measured SMX conc. NCC, day 0	Measured SMX conc. NCC, 14 months
100 µM	88 µM	10 µM	78 µM	89%	105 µM	116 µM
150 µM	160 µM	18 µM	142 µM	89%	170 µM	192 µM
250 µM	254 µM	21 µM	233 µM	92%	259 µM	267 µM
400 µM	410 µM	91 µM	319 µM	78%	433 µM	441 µM
600 µM	579 µM	377 µM	202 µM	35%	594 µM	602 µM
750 µM	724 µM	657 µM	67 µM	9%	760 µM	792 µM

[1]assumed to be equivalent to the concentration of transformed SMX. Abbreviations: conc – concentration, TP – transformation product, NCC – no cell control

Table S3 SMX and SMX transformation products in sulfate-reducing cultures detected by UPLC-MS/MS

	RT (min)	Precursor ion $[M+H]^+$ (*m/z*)	Fragment ions (*m/z*)	Difference to SMX	Molecular formula
SMX	8.02	254.06	92.05, 99.06, 108.04, 110.06, 156.01		$C_{10}H_{11}O_3N_3S$
TP1	6.16	256.07	92.05, 101.07, 108.04, 110.06, 156.01	+2H	$C_{10}H_{13}O_3N_3S$
TP2	6.96	254.06	92.05, 99.06, 108.04, 110.06, 156.01	--	$C_{10}H_{11}O_3N_3S$

Table S4. GC-MS signals of SMX and the corresponding by-products generated during the measurement

Injector temp. [°C]	Retention Time	Area	Compound	Percentage of compounds	Average Percentage of three measurements	Sum of by-products
180	33.0	3.01E+09	SMX	100	100	
	32.9	4.50E+09	SMX	100		
	32.9	4.27E+09	SMX	100		
200	28.4	7.15E+07	Sulfanilamide	1.54	1.89	2.52
	28.8	2.78E+07	4-aminothiophenol	0.6	0.63	
	33.0	4.51E+09	SMX	97.84	97.48	
	28.4	7.36E+07	Sulfanilamide	1.78		
	28.8	2.73E+07	4-aminothiophenol	0.66		
	33.0	4.03E+09	SMX	97.55		
	28.4	9.89E+07	Sulfanilamide	2.38		
	28.8	2.59E+07	4-aminothiophenol	0.62		
	33.0	4.02E+09	SMX	96.98		
220	28.4	2.48E+08	Sulfanilamide	4.95	4.94	5.4
	28.8	2.30E+07	4-aminothiophenol	0.45	0.46	
	33.0	4.74E+09	SMX	94.58	94.6	
	28.4	2.31E+08	Sulfanilamide	4.71		
	28.8	2.14E+07	4-aminothiophenol	0.43		
	33.0	4.64E+09	SMX	94.8		
	28.4	2.31E+08	Sulfanilamide	5.17		
	28.8	2.13E+07	4-aminothiophenol	0.47		
	33.0	4.21E+09	SMX	94.34		
240	28.4	2.76E+08	Sulfanilamide	7.34	4.95	5.37
	28.8	1.89E+07	4-aminothiophenol	0.5	0.42	
	32.9	3.47E+09	SMX	92.14	94.63	
	28.4	1.74E+08	Sulfanilamide	4.08		
	28.8	1.71E+07	4-aminothiophenol	0.4		
	32.9	4.06E+09	SMX	95.51		
	28.4	1.47E+08	Sulfanilamide	3.63		
	28.8	1.47E+07	4-aminothiophenol	0.36		
	32.9	3.89E+09	SMX	95.99		
260	28.4	1.56E+08	Sulfanilamide	3.74	2.15	2.38
	28.8	1.07E+07	4-aminothiophenol	0.25	0.23	
	32.9	4.00E+09	SMX	95.99	97.62	
	28.4	6.79E+07	Sulfanilamide	1.63		
	28.8	8.06E+06	4-aminothiophenol	0.19		
	32.9	4.09E+09	SMX	98.17		
	28.4	4.40E+07	Sulfanilamide	1.06		
	32.9	4.07E+09	SMX	98.93		

Reference

(1) Clardy, J.; Fischbach, M. A.; Currie, C. R., The natural history of antibiotics. *Curr. Biol.* **2009,** *19*, (11), R437-R441.
(2) Feinman, S. E.; Matheson, J. C., *Draft environmental impact statement: subtherapeutic antibacterial agents in animal feeds*. Department of Health, Education, and Welfare, Public Health Service: 1978.
(3) Zhang, Q. Q.; Ying, G. G.; Pan, C. G.; Liu, Y. S.; Zhao, J. L., Comprehensive evaluation of antibiotics emission and fate in the river basins of China: source analysis, multimedia modeling, and linkage to bacterial resistance. *Environ. Sci. Technol.* **2015,** *49*, (11), 6772-82.
(4) Sarmah, A. K.; Meyer, M. T.; Boxall, A. B., A global perspective on the use, sales, exposure pathways, occurrence, fate and effects of veterinary antibiotics (VAs) in the environment. *Chemosphere* **2006,** *65*, (5), 725-759.
(5) Van Boeckel, T. P.; Gandra, S.; Ashok, A.; Caudron, Q.; Grenfell, B. T.; Levin, S. A.; Laxminarayan, R., Global antibiotic consumption 2000 to 2010: an analysis of national pharmaceutical sales data. *Lancet Infect. Dis.* **2014,** *14*, (8), 742-750.
(6) Hooper, D. C., Emerging mechanisms of fluoroquinolone resistance. *Emerg. Infect. Dis.* **2001,** *7*, (2), 337.
(7) No time to wait: securing the future from drug-resistant infections. In World Health Organization Geneva, Switzerland: **2019**. https://www.who.int/antimicrobial-resistance/interagency-coordination-group/final-report/en/
(8) O'Neill, J., Antimicrobial resistance: tackling a crisis for the health and wealth of nations. HM Government **2014**. https://wellcomecollection.org/works/rdpck35v
(9) Baquero, F.; Martínez, J.-L.; Cantón, R., Antibiotics and antibiotic resistance in water environments. *Curr. Opin. Biotechnol.* **2008,** *19*, (3), 260-265.
(10) An, J.; Chen, H.; Wei, S.; Gu, J., Antibiotic contamination in animal manure, soil, and sewage sludge in Shenyang, northeast China. *Environ. Earth Sci.* **2015,** *74*, (6), 5077-5086.
(11) Karthikeyan, K.; Meyer, M. T., Occurrence of antibiotics in wastewater treatment facilities in Wisconsin, USA. *Sci. Total Environ.* **2006,** *361*, (1-3), 196-207.
(12) Li, W.; Shi, Y.; Gao, L.; Liu, J.; Cai, Y., Occurrence, distribution and potential affecting factors of antibiotics in sewage sludge of wastewater treatment plants in China. *Sci. Total Environ.* **2013,** *445*, 306-313.
(13) Zhao, L.; Dong, Y. H.; Wang, H., Residues of veterinary antibiotics in manures from feedlot livestock in eight provinces of China. *Sci. Total Environ.* **2010,** *408*, (5), 1069-1075.
(14) Bartelt-Hunt, S.; Snow, D. D.; Damon-Powell, T.; Miesbach, D., Occurrence of steroid hormones and antibiotics in shallow groundwater impacted by livestock waste control facilities. *J. Contam. Hydrol.* **2011,** *123*, (3-4), 94-103.
(15) Kümmerer, K., Antibiotics in the aquatic environment–a review–part I. *Chemosphere* **2009,** *75*, (4), 417-434.
(16) Lin, A. Y.-C.; Tsai, Y.-T., Occurrence of pharmaceuticals in Taiwan's surface waters: impact of waste streams from hospitals and pharmaceutical production facilities. *Sci. Total Environ.* **2009,** *407*, (12), 3793-3802.
(17) Thiele‐Bruhn, S., Pharmaceutical antibiotic compounds in soils–a review. *J. Soil Sci. Plant Nutr* **2003,** *166*, (2), 145-167.
(18) Zhu, Y.; Ouyang, W.; Wu, N.; Su, J.; Qiao, M., Antibiotic resistance: sources and mitigation. *Bulletin of the Chinese Academy of Sciences* **2015,** *30*, (4), 509-516.
(19) Pruden, A.; Pei, R.; Storteboom, H.; Carlson, K. H., Antibiotic resistance genes as emerging contaminants: studies in northern Colorado. *Environ. Sci. Technol.* **2006,** *40*, (23), 7445-7450.

(20) Ouyang, W.-Y.; Huang, F.-Y.; Zhao, Y.; Li, H.; Su, J.-Q., Increased levels of antibiotic resistance in urban stream of Jiulongjiang River, China. *Appl. Microbiol. Biotechnol.* **2015,** *99*, (13), 5697-5707.
(21) Su, J.-Q.; Wei, B.; Ou-Yang, W.-Y.; Huang, F.-Y.; Zhao, Y.; Xu, H.-J.; Zhu, Y.-G., Antibiotic resistome and its association with bacterial communities during sewage sludge composting. *Environ. Sci. Technol.* **2015,** *49*, (12), 7356-7363.
(22) Ghosh, S.; LaPara, T. M., The effects of subtherapeutic antibiotic use in farm animals on the proliferation and persistence of antibiotic resistance among soil bacteria. *ISME J.* **2007,** *1*, (3), 191-203.
(23) Forsberg, K. J.; Reyes, A.; Wang, B.; Selleck, E. M.; Sommer, M. O.; Dantas, G., The shared antibiotic resistome of soil bacteria and human pathogens. *Science* **2012,** *337*, (6098), 1107-1111.
(24) Christensen, A. M.; Ingerslev, F.; Baun, A., Ecotoxicity of mixtures of antibiotics used in aquacultures. *Environ. Toxicol. Chem.* **2006,** *25*, (8), 2208-2215.
(25) Cavallucci, S., Top 200: What's topping the charts in prescription drugs this year. *Pharmacy practice, Canadian Healthcare Network* **2007**.
(26) Hruska, K.; Franek, M., Sulfonamides in the environment: a review and a case report. *Vet. Med.* **2012,** *57*, (1), 1-35.
(27) Suzuki, S.; Ogo, M.; Miller, T. W.; Shimizu, A.; Takada, H.; Siringan, M. A., Who possesses drug resistance genes in the aquatic environment?: sulfamethoxazole (SMX) resistance genes among the bacterial community in water environment of Metro-Manila, Philippines. *Front. Microbiol.* **2013,** *4*, 102.
(28) Wei, R.; Ge, F.; Huang, S.; Chen, M.; Wang, R., Occurrence of veterinary antibiotics in animal wastewater and surface water around farms in Jiangsu Province, China. *Chemosphere* **2011,** *82*, (10), 1408-1414.
(29) Managaki, S.; Murata, A.; Takada, H.; Tuyen, B. C.; Chiem, N. H., Distribution of macrolides, sulfonamides, and trimethoprim in tropical waters: ubiquitous occurrence of veterinary antibiotics in the Mekong Delta. *Environ. Sci. Technol.* **2007,** *41*, (23), 8004-8010.
(30) Zhang, T.; Li, B., Occurrence, transformation, and fate of antibiotics in municipal wastewater treatment plants. *Crit. Rev. Environ. Sci. Technol.* **2011,** *41*, (11), 951-998.
(31) Benotti, M. J.; Brownawell, B. J., Microbial degradation of pharmaceuticals in estuarine and coastal seawater. *Env. Pollut.* **2009,** *157*, (3), 994-1002.
(32) Rubin, R. H.; Swartz, M. N., Trimethoprim-sulfamethoxazole. *N. Engl. J. Med.* **1980,** *303*, (8), 426-432.
(33) Göbel, A.; Thomsen, A.; McArdell, C. S.; Joss, A.; Giger, W., Occurrence and sorption behavior of sulfonamides, macrolides, and trimethoprim in activated sludge treatment. *Environ. Sci. Technol.* **2005,** *39*, (11), 3981-3989.
(34) Reemtsma, T.; Berger, U.; Arp, H. P. H.; Gallard, H.; Knepper, T. P.; Neumann, M.; Quintana, J. B.; Voogt, P. d., Mind the Gap: Persistent and Mobile Organic Compounds · Water Contaminants That Slip Through. *Environ. Sci. Technol.* **2016,** *50*, (19), 10308-10315.
(35) Spielmeyer, A.; Höper, H.; Hamscher, G., Long-term monitoring of sulfonamide leaching from manure amended soil into groundwater. *Chemosphere* **2017,** *177*, 232-238.
(36) Yang, S.-F.; Lin, C.-F.; Lin, A. Y.-C.; Hong, P.-K. A., Sorption and biodegradation of sulfonamide antibiotics by activated sludge: experimental assessment using batch data obtained under aerobic conditions. *Water Res.* **2011,** *45*, (11), 3389-3397.
(37) Alvarino, T.; Nastold, P.; Suarez, S.; Omil, F.; Corvini, P.; Bouju, H., Role of biotransformation, sorption and mineralization of 14C-labelled sulfamethoxazole under different redox conditions. *Sci. Total Environ.* **2016,** *542*, 706-715.
(38) Birkigt, J.; Gilevska, T.; Ricken, B.; Richnow, H.-H.; Vione, D.; Corvini, P. F.-X.; Nijenhuis, I.; Cichocka, D., Carbon stable isotope fractionation of sulfamethoxazole during

biodegradation by *Microbacterium* sp. strain BR1 and upon direct photolysis. *Environ. Sci. Technol.* **2015,** *49*, (10), 6029-6036.
(39) Boreen, A. L.; Arnold, W. A.; McNeill, K., Photochemical fate of sulfa drugs in the aquatic environment: sulfa drugs containing five-membered heterocyclic groups. *Environ. Sci. Technol.* **2004,** *38*, (14), 3933-3940.
(40) Willach, S.; Lutze, H. V.; Eckey, K.; Löppenberg, K.; Lüling, M.; Wolbert, J.-B.; Kujawinski, D. M.; Jochmann, M. A.; Karst, U.; Schmidt, T. C., Direct photolysis of sulfamethoxazole using various irradiation sources and wavelength ranges insights from degradation product analysis and compound-specific stable ssiotope analysis. *Environ. Sci. Technol.* **2018,** *52*, (3), 1225-1233.
(41) Niu, J.; Zhang, L.; Li, Y.; Zhao, J.; Lv, S.; Xiao, K., Effects of environmental factors on sulfamethoxazole photodegradation under simulated sunlight irradiation: kinetics and mechanism. *J. Environ. Sci.* **2013,** *25*, (6), 1098-1106.
(42) Trovó, A. G.; Nogueira, R. F.; Agüera, A.; Sirtori, C.; Fernández-Alba, A. R., Photodegradation of sulfamethoxazole in various aqueous media: persistence, toxicity and photoproducts assessment. *Chemosphere* **2009,** *77*, (10), 1292-1298.
(43) Trovó, A. G.; Nogueira, R. F.; Agüera, A.; Fernandez-Alba, A. R.; Sirtori, C.; Malato, S., Degradation of sulfamethoxazole in water by solar photo-Fenton. Chemical and toxicological evaluation. *Water Res.* **2009,** *43*, (16), 3922-3931.
(44) Ryan, C. C.; Tan, D. T.; Arnold, W. A., Direct and indirect photolysis of sulfamethoxazole and trimethoprim in wastewater treatment plant effluent. *Water Res.* **2011,** *45*, (3), 1280-1286.
(45) Ji, Y.; Ferronato, C.; Salvador, A.; Yang, X.; Chovelon, J.-M., Degradation of ciprofloxacin and sulfamethoxazole by ferrous-activated persulfate: implications for remediation of groundwater contaminated by antibiotics. *Sci. Total Environ.* **2014,** *472*, 800-808.
(46) Willach, S.; Lutze, H. V.; Eckey, K.; Löppenberg, K.; Lüling, M.; Terhalle, J.; Wolbert, J.-B.; Jochmann, M. A.; Karst, U.; Schmidt, T. C., Degradation of sulfamethoxazole using ozone and chlorine dioxide-Compound-specific stable isotope analysis, transformation product analysis and mechanistic aspects. *Water Res.* **2017,** *122*, 280-289.
(47) Marciocha, D.; Kalka, J.; Turek-Szytow, J.; Wiszniowski, J.; Surmacz-Górska, J., Oxidation of sulfamethoxazole by UVA radiation and modified Fenton reagent: toxicity and biodegradability of by-products. *Water Sci. Technol.* **2009,** *60*, (10), 2555-2562.
(48) Dodd, M. C.; Buffle, M.-O.; Von Gunten, U., Oxidation of antibacterial molecules by aqueous ozone: moiety-specific reaction kinetics and application to ozone-based wastewater treatment. *Environ. Sci. Technol.* **2006,** *40*, (6), 1969-1977.
(49) Yu, H.; Ge, P.; Chen, J.; Xie, H.; Luo, Y., The degradation mechanism of sulfamethoxazole under ozonation: a DFT study. *Environ. Sci. Process Impacts* **2017,** *19*, (3), 379-387.
(50) Yang, Y.; Lu, X.; Jiang, J.; Ma, J.; Liu, G.; Cao, Y.; Liu, W.; Li, J.; Pang, S.; Kong, X., Degradation of sulfamethoxazole by UV, UV/H2O2 and UV/persulfate (PDS): formation of oxidation products and effect of bicarbonate. *Water Res.* **2017,** *118*, 196-207.
(51) Dodd, M. C.; Huang, C.-H., Transformation of the antibacterial agent sulfamethoxazole in reactions with chlorine: kinetics, mechanisms, and pathways. *Environ. Sci. Technol.* **2004,** *38*, (21), 5607-5615.
(52) Deng, Y.; Li, B.; Zhang, T., Bacteria that make a meal of sulfonamide antibiotics: blind spots and emerging opportunities. *Environ. Sci. Technol.* **2018,** *52*, (7), 3854-3868.
(53) Gros, M.; Rodríguez-Mozaz, S.; Barceló, D., Rapid analysis of multiclass antibiotic residues and some of their metabolites in hospital, urban wastewater and river water by ultra-high-performance liquid chromatography coupled to quadrupole-linear ion trap tandem mass spectrometry. *J. Chromatogr. A* **2013,** *1292*, 173-188.

(54) Underwood, J. C.; Harvey, R. W.; Metge, D. W.; Repert, D. A.; Baumgartner, L. K.; Smith, R. L.; Roane, T. M.; Barber, L. B., Effects of the antimicrobial sulfamethoxazole on groundwater bacterial enrichment. *Environ. Sci. Technol.* **2011,** *45*, (7), 3096-3101.
(55) Kang, A. J.; Brown, A. K.; Wong, C. S.; Huang, Z.; Yuan, Q., Variation in bacterial community structure of aerobic granular and suspended activated sludge in the presence of the antibiotic sulfamethoxazole. *Bioresour. technol.* **2018,** *261*, 322-328.
(56) Demoling, L. A.; Bååth, E.; Greve, G.; Wouterse, M.; Schmitt, H., Effects of sulfamethoxazole on soil microbial communities after adding substrate. *Soil Biol. Biochem.* **2009,** *41*, (4), 840-848.
(57) Katipoglu-Yazan, T.; Merlin, C.; Pons, M.-N.; Ubay-Cokgor, E.; Orhon, D., Chronic impact of sulfamethoxazole on the metabolic activity and composition of enriched nitrifying microbial culture. *Water Res.* **2016,** *100*, 546-555.
(58) Zhang, Y.; Geng, J.; Ma, H.; Ren, H.; Xu, K.; Ding, L., Characterization of microbial community and antibiotic resistance genes in activated sludge under tetracycline and sulfamethoxazole selection pressure. *Sci. Total Environ.* **2016,** *571*, 479-486.
(59) Yan, W.; Bai, R.; Wang, S.; Tian, X.; Li, Y.; Wang, S.; Yang, F.; Xiao, Y.; Lu, X.; Zhao, F., Antibiotic resistance genes are increased by combined exposure to sulfamethoxazole and naproxen but relieved by low-salinity. *Environ. Int.* **2020,** *139*, 105742.
(60) Aydin, S.; Ince, B.; Ince, O., Development of antibiotic resistance genes in microbial communities during long-term operation of anaerobic reactors in the treatment of pharmaceutical wastewater. *Water Res.* **2015,** *83*, 337-344.
(61) Akiyama, T.; Savin, M. C., Populations of antibiotic-resistant coliform bacteria change rapidly in a wastewater effluent dominated stream. *Sci. Total Environ.* **2010,** *408*, (24), 6192-6201.
(62) Majewsky, M.; Wagner, D.; Delay, M.; Bräse, S.; Yargeau, V.; Horn, H., Antibacterial activity of sulfamethoxazole transformation products (TPs): general relevance for sulfonamide TPs modified at the para position. *Chem. Res. Toxicol.* **2014,** *27*, (10), 1821-1828.
(63) Majewsky, M.; Glauner, T.; Horn, H., Systematic suspect screening and identification of sulfonamide antibiotic transformation products in the aquatic environment. *Anal. Bioanal. Chem.* **2015,** *407*, (19), 5707-5717.
(64) Radke, M.; Lauwigi, C.; Heinkele, G.; Mürdter, T. E.; Letzel, M., Fate of the antibiotic sulfamethoxazole and its two major human metabolites in a water sediment test. *Environ. Sci. Technol.* **2009,** *43*, (9), 3135-3141.
(65) Larcher, S.; Yargeau, V., Biodegradation of sulfamethoxazole: current knowledge and perspectives. *Appl. Microbiol. Biotechnol.* **2012,** *96*, (2), 309-18.
(66) Achermann, S.; Bianco, V.; Mansfeldt, C. B.; Vogler, B.; Kolvenbach, B. A.; Corvini, P. F.; Fenner, K., Biotransformation of Sulfonamide Antibiotics in Activated Sludge: The Formation of Pterin-Conjugates Leads to Sustained Risk. *Environ. Sci. Technol.* **2018,** *52*, (11), 6265-6274.
(67) Liu, F.; Ying, G.-G.; Yang, J.-F.; Zhou, L.-J.; Tao, R.; Wang, L.; Zhang, L.-J.; Peng, P.-A., Dissipation of sulfamethoxazole, trimethoprim and tylosin in a soil under aerobic and anoxic conditions. *Environ. Chem.* **2010,** *7*, (4), 370-376.
(68) Wu, Y.; Williams, M.; Smith, L.; Chen, D.; Kookana, R., Dissipation of sulfamethoxazole and trimethoprim antibiotics from manure-amended soils. *J. Environ. Sci. Health B* **2012,** *47*, (4), 240-249.
(69) Lam, M. W.; Young, C. J.; Brain, R. A.; Johnson, D. J.; Hanson, M. A.; Wilson, C. J.; Richards, S. M.; Solomon, K. R.; Mabury, S. A., Aquatic persistence of eight pharmaceuticals in a microcosm study. *Environ. Toxicol. Chem.* **2004,** *23*, (6), 1431-1440.

(70) Göbel, A.; McArdell, C. S.; Joss, A.; Siegrist, H.; Giger, W., Fate of sulfonamides, macrolides, and trimethoprim in different wastewater treatment technologies. *Sci. Total Environ.* **2007,** *372*, (2-3), 361-371.
(71) Pérez, S.; Eichhorn, P.; Aga, D. S., Evaluating the biodegradability of sulfamethazine, sulfamethoxazole, sulfathiazole, and trimethoprim at different stages of sewage treatment. *Environ. Toxicol. Chem.* **2005,** *24*, (6), 1361-1367.
(72) Larcher, S.; Yargeau, V., Biodegradation of sulfamethoxazole by individual and mixed bacteria. *Appl. Microbiol. Biotechnol.* **2011,** *91*, (1), 211-8.
(73) Baumgarten, B.; Jaehrig, J.; Reemtsma, T.; Jekel, M., Long term laboratory column experiments to simulate bank filtration: factors controlling removal of sulfamethoxazole. *Water Res.* **2011,** *45*, (1), 211-220.
(74) Yang, C.-W.; Tsai, L.-L.; Chang, B.-V., Anaerobic degradation of sulfamethoxazole in mangrove sediments. *Sci. Total Environ.* **2018,** *643*, 1446-1455.
(75) Rodríguez-Escales, P.; Sanchez-Vila, X., Fate of sulfamethoxazole in groundwater: Conceptualizing and modeling metabolite formation under different redox conditions. *Water Res.* **2016,** *105*, 540-550.
(76) Poirier-Larabie, S.; Segura, P.; Gagnon, C., Degradation of the pharmaceuticals diclofenac and sulfamethoxazole and their transformation products under controlled environmental conditions. *Sci. Total Environ.* **2016,** *557*, 257-267.
(77) Drillia, P.; Dokianakis, S.; Fountoulakis, M.; Kornaros, M.; Stamatelatou, K.; Lyberatos, G., On the occasional biodegradation of pharmaceuticals in the activated sludge process: the example of the antibiotic sulfamethoxazole. *J. Hazard. Mater.* **2005,** *122*, (3), 259-265.
(78) Singh, S. N., *Microbial degradation of xenobiotics*. Springer: 2011.
(79) Jiang, B.; Li, A.; Cui, D.; Cai, R.; Ma, F.; Wang, Y., Biodegradation and metabolic pathway of sulfamethoxazole by *Pseudomonas psychrophila* HA-4, a newly isolated cold-adapted sulfamethoxazole-degrading bacterium. *Appl. Microbiol. Biotechnol.* **2014,** *98*, (10), 4671-81.
(80) Gauthier, H.; Yargeau, V.; Cooper, D. G., Biodegradation of pharmaceuticals by *Rhodococcus rhodochrous* and *Aspergillus niger* by co-metabolism. *Sci. Total Environ.* **2010,** *408*, (7), 1701-1706.
(81) Kassotaki, E.; Buttiglieri, G.; Ferrando-Climent, L.; Rodriguez-Roda, I.; Pijuan, M., Enhanced sulfamethoxazole degradation through ammonia oxidizing bacteria co-metabolism and fate of transformation products. *Water Res.* **2016,** *94*, 111-119.
(82) Banzhaf, S.; Nödler, K.; Licha, T.; Krein, A.; Scheytt, T., Redox-sensitivity and mobility of selected pharmaceutical compounds in a low flow column experiment. *Sci. Total Environ.* **2012,** *438*, 113-121.
(83) Xu, B.; Mao, D.; Luo, Y.; Xu, L., Sulfamethoxazole biodegradation and biotransformation in the water–sediment system of a natural river. *Bioresour. technol.* **2011,** *102*, (14), 7069-7076.
(84) Adrian, L.; Szewzyk, U.; Wecke, J.; Görisch, H., Bacterial dehalorespiration with chlorinated benzenes. *Nature* **2000,** *408*, (6812), 580-583.
(85) Hazen, T. C., Cometabolic bioremediation. **2010**.
(86) Rodríguez-Nava, O.; Ramírez-Saad, H.; Loera, O.; González, I., Evaluation of the simultaneous removal of recalcitrant drugs (bezafibrate, gemfibrozil, indomethacin and sulfamethoxazole) and biodegradable organic matter from synthetic wastewater by electro-oxidation coupled with a biological system. *Environ. Technol.* **2016,** *37*, (23), 2964-2974.
(87) OECD Guidelines for testing of chemicals. 301 D Closed bottletest adopted by the council on 17th July 1992. . In Paris, France, 1992.
(88) OECD Guideline for testing of chemicals. In Paris, France, 2005; pp 1-13.
(89) Gartiser, S.; Urich, E.; Alexy, R.; Kümmerer, K., Anaerobic inhibition and biodegradation of antibiotics in ISO test schemes. *Chemosphere* **2007,** *66*, (10), 1839-1848.

(90) Al-Ahmad, A.; Daschner, F.; Kümmerer, K., Biodegradability of cefotiam, ciprofloxacin, meropenem, penicillin G, and sulfamethoxazole and inhibition of waste water bacteria. *Arch. Environ. Contam. Toxicol.* **1999,** *37*, (2), 158-163.
(91) Alexy, R.; Kümpel, T.; Kümmerer, K., Assessment of degradation of 18 antibiotics in the closed bottle test. *Chemosphere* **2004,** *57*, (6), 505-512.
(92) Ingerslev, F.; Halling‐Sørensen, B., Biodegradability properties of sulfonamides in activated sludge. *Environ. Toxicol. Chem.* **2000,** *19*, (10), 2467-2473.
(93) Bouju, H.; Ricken, B.; Beffa, T.; Corvini, P. F.; Kolvenbach, B. A., Isolation of bacterial strains capable of sulfamethoxazole mineralization from an acclimated membrane bioreactor. *Appl. Environ. Microbiol.* **2012,** *78*, (1), 277-9.
(94) Wang, S.; Wang, J., Biodegradation and metabolic pathway of sulfamethoxazole by a novel strain *Acinetobacter* sp. *Appl. Microbiol. Biotechnol.* **2018,** *102*, (1), 425-432.
(95) Reis, P. J.; Reis, A. C.; Ricken, B.; Kolvenbach, B. A.; Manaia, C. M.; Corvini, P. F.; Nunes, O. C., Biodegradation of sulfamethoxazole and other sulfonamides by *Achromobacter denitrificans* PR1. *J. Hazard. Mater.* **2014,** *280*, 741-9.
(96) Herzog, B.; Lemmer, H.; Horn, H.; Müller, E., Characterization of pure cultures isolated from sulfamethoxazole-acclimated activated sludge with respect to taxonomic identification and sulfamethoxazole biodegradation potential. *BMC Microbiol.* **2013,** *13*, (1), 276.
(97) Mao, F.; Liu, X.; Wu, K.; Zhou, C.; Si, Y., Biodegradation of sulfonamides by *Shewanella oneidensis* MR-1 and *Shewanella* sp. strain MR-4. *Biodegradation* **2018,** *29*, (2), 129-140.
(98) Yan, N.; Xia, S.; Xu, L.; Zhu, J.; Zhang, Y.; Rittmann, B. E., Internal loop photobiodegradation reactor (ILPBR) for accelerated degradation of sulfamethoxazole (SMX). *Appl. Microbiol. Biotechnol.* **2012,** *94*, (2), 527-535.
(99) Yang, C.-W.; Hsiao, W.-C.; Fan, C.-H.; Chang, B.-V., Bacterial communities associated with sulfonamide antibiotics degradation in sludge-amended soil. *Environ. Sci. Pollution Res.* **2016,** *23*, (19), 19754-19763.
(100) Ricken, B.; Corvini, P. F.; Cichocka, D.; Parisi, M.; Lenz, M.; Wyss, D.; Martínez-Lavanchy, P. M.; Müller, J. A.; Shahgaldian, P.; Tulli, L. G., Ipso-hydroxylation and subsequent fragmentation: a novel microbial strategy to eliminate sulfonamide antibiotics. *Appl. Environ. Microbiol.* **2013,** *79*, (18), 5550-5558.
(101) Deng, Y.; Mao, Y.; Li, B.; Yang, C.; Zhang, T., Aerobic degradation of sulfadiazine by *Arthrobacter* spp.: kinetics, pathways, and genomic characterization. *Environ. Sci. Technol.* **2016,** *50*, (17), 9566-9575.
(102) Kim, D.-W.; Thawng, C. N.; Lee, K.; Wellington, E. M.; Cha, C.-J., A novel sulfonamide resistance mechanism by two-component flavin-dependent monooxygenase system in sulfonamide-degrading actinobacteria. *Environ. Int.* **2019,** *127*, 206-215.
(103) Ricken, B.; Kolvenbach, B. A.; Bergesch, C.; Benndorf, D.; Kroll, K.; Strnad, H.; Vlček, Č.; Adaixo, R.; Hammes, F.; Shahgaldian, P.; Schäffer, A.; Kohler, H.-P. E.; Corvini, P. F. X., FMNH2-dependent monooxygenases initiate catabolism of sulfonamides in *Microbacterium* sp. strain BR1 subsisting on sulfonamide antibiotics. *Sci. Rep.* **2017,** *7*, (1), 15783.
(104) Ghattas, A.-K.; Fischer, F.; Wick, A.; Ternes, T. A., Anaerobic biodegradation of (emerging) organic contaminants in the aquatic environment. *Water Res.* **2017,** *116*, 268-295.
(105) Schaffer, M.; Kröger, K. F.; Nödler, K.; Ayora, C.; Carrera, J.; Hernández, M.; Licha, T., Influence of a compost layer on the attenuation of 28 selected organic micropollutants under realistic soil aquifer treatment conditions: Insights from a large scale column experiment. *Water Res.* **2015,** *74*, 110-121.
(106) Grünheid, S.; Amy, G.; Jekel, M., Removal of bulk dissolved organic carbon (DOC) and trace organic compounds by bank filtration and artificial recharge. *Water Res.* **2005,** *39*, (14), 3219-3228.

(107) Heberer, T.; Massmann, G.; Fanck, B.; Taute, T.; Dünnbier, U., Behaviour and redox sensitivity of antimicrobial residues during bank filtration. *Chemosphere* **2008,** *73*, (4), 451-460.
(108) Schmidt, C. K.; Lange, F. T.; Brauch, H.-J. In *Assessing the impact of different redox conditions and residence times on the fate of organic micropollutants during riverbank filtration*, 4th International Conference on Pharmaceuticals and Endocrine Disrupting Chemicals in Water, 2004; 2004; p 2004.
(109) Barbieri, M.; Carrera, J.; Ayora, C.; Sanchez-Vila, X.; Licha, T.; Nödler, K.; Osorio, V.; Pérez, S.; Köck-Schulmeyer, M.; de Alda, M. L., Formation of diclofenac and sulfamethoxazole reversible transformation products in aquifer material under denitrifying conditions: batch experiments. *Sci. Total Environ.* **2012,** *426*, 256-263.
(110) Nödler, K.; Licha, T.; Barbieri, M.; Pérez, S., Evidence for the microbially mediated abiotic formation of reversible and non-reversible sulfamethoxazole transformation products during denitrification. *Water Res.* **2012,** *46*, (7), 2131-2139.
(111) Mohatt, J. L.; Hu, L.; Finneran, K. T.; Strathmann, T. J., Microbially mediated abiotic transformation of the antimicrobial agent sulfamethoxazole under iron-reducing soil conditions. *Environ. Sci. Technol.* **2011,** *45*, (11), 4793-4801.
(112) Jia, Y.; Khanal, S. K.; Zhang, H.; Chen, G.-H.; Lu, H., Sulfamethoxazole degradation in anaerobic sulfate-reducing bacteria sludge system. *Water Res.* **2017,** *119*, 12-20.
(113) Hem, J. D., *Study and interpretation of the chemical characteristics of natural water*. Department of the Interior, US Geological Survey: 1985; Vol. 2254.
(114) Fauque, G. D., Ecology of sulfate-reducing bacteria. In *Sulfate-Reducing Bacteria*, Springer: 1995; pp 217-241.
(115) Muyzer, G.; Stams, A. J., The ecology and biotechnology of sulphate-reducing bacteria. *Nat. Rev. Microbiol.* **2008,** *6*, (6), 441-454.
(116) Ollivier, B.; Cayol, J.-L.; Fauque, G., Sulphate-reducing bacteria from oil field environments and deep-sea hydrothermal vents. In *Sulphate-Reducing Bacteria: Environmental and Engineered Systems*, 2007; pp 305-328.
(117) Lovley, D. R.; Klug, M. J., Model for the distribution of sulfate reduction and methanogenesis in freshwater sediments. *Geochim. Cosmochim. Acta* **1986,** *50*, (1), 11-18.
(118) Kaksonen, A. H.; Plumb, J. J.; Franzmann, P. D.; Puhakka, J. A., Simple organic electron donors support diverse sulfate-reducing communities in fluidized-bed reactors treating acidic metal-and sulfate-containing wastewater. *FEMS Microbiol. Ecol.* **2004,** *47*, (3), 279-289.
(119) Santos, A. A.; Venceslau, S. S.; Grein, F.; Leavitt, W. D.; Dahl, C.; Johnston, D. T.; Pereira, I. A., A protein trisulfide couples dissimilatory sulfate reduction to energy conservation. *Science* **2015,** *350*, (6267), 1541-1545.
(120) Lizama, H. M.; Wilkins, L. A.; Scott, T. C., Dibenzothiophene sulfur can serve as the sole electron acceptor during growth by sulfate-reducing bacteria. *Biotechnol. Lett.* **1995,** *17*, (1), 113-116.
(121) Marietou, A., Nitrate reduction in sulfate-reducing bacteria. *FEMS Microbiol. Lett.* **2016,** *363*, (15), fnw155.
(122) da Silva, S. M.; Voordouw, J.; Leitao, C.; Martins, M.; Voordouw, G.; Pereira, I. s. A., Function of formate dehydrogenases in *Desulfovibrio vulgaris* Hildenborough energy metabolism. *Microbiology* **2013,** *159*, (Pt_8), 1760-1769.
(123) Liamleam, W.; Annachhatre, A. P., Electron donors for biological sulfate reduction. *Biotechnol. Adv.* **2007,** *25*, (5), 452-463.
(124) Barton, L. L.; Fauque, G. D., Biochemistry, physiology and biotechnology of sulfate‐reducing bacteria. *Adv. Appl. Microbiol.* **2009,** *68*, 41-98.
(125) Poehlein, A.; Daniel, R.; Schink, B.; Simeonova, D. D., Life based on phosphite: a genome-guided analysis of Desulfotignum phosphitoxidans. *BMC Genom.* **2013,** *14*, (1), 1-14.

(126) Bak, F.; Cypionka, H., A novel type of energy metabolism involving fermentation of inorganic sulphur compounds. *Nature* **1987,** *326*, (6116), 891-892.
(127) Heidelberg, J. F.; Seshadri, R.; Haveman, S. A.; Hemme, C. L.; Paulsen, I. T.; Kolonay, J. F.; Eisen, J. A.; Ward, N.; Methe, B.; Brinkac, L. M., The genome sequence of the anaerobic, sulfate-reducing bacterium *Desulfovibrio vulgaris* Hildenborough. *Nat. Biotechnol.* **2004,** *22*, (5), 554.
(128) Vita, N.; Valette, O.; Brasseur, G.; Lignon, S.; Denis, Y.; Ansaldi, M.; Dolla, A.; Pieulle, L., The primary pathway for lactate oxidation in Desulfovibrio vulgaris. *Front. Microbiol.* **2015,** *6*, 606.
(129) Pereira, P. M.; He, Q.; Valente, F. M.; Xavier, A. V.; Zhou, J.; Pereira, I. A.; Louro, R. O., Energy metabolism in *Desulfovibrio vulgaris* Hildenborough: insights from transcriptome analysis. *Antonie Van Leeuwenhoek* **2008,** *93*, (4), 347-362.
(130) Flowers, J. J.; Richards, M. A.; Baliga, N.; Meyer, B.; Stahl, D. A., Constraint‐based modelling captures the metabolic versatility of Desulfovibrio vulgaris. *Environ. Microbiol. Rep.* **2018,** *10*, (2), 190-201.
(131) Aubert, C.; Brugna, M.; Dolla, A.; Bruschi, M.; Giudici-Orticoni, M.-T., A sequential electron transfer from hydrogenases to cytochromes in sulfate-reducing bacteria. *Biochim. Biophys. Acta* **2000,** *1476*, (1), 85-92.
(132) Lovley, D. R.; Roden, E. E.; Phillips, E.; Woodward, J., Enzymatic iron and uranium reduction by sulfate-reducing bacteria. *Mar. Geol.* **1993,** *113*, (1-2), 41-53.
(133) Ganesh, R.; Robinson, K. G.; Chu, L.; Kucsmas, D.; Reed, G. D., Reductive precipitation of uranium by *Desulfovibrio desulfuricans*: evaluation of cocontaminant effects and selective removal. *Water Res.* **1999,** *33*, (16), 3447-3458.
(134) Chardin, B.; Giudici-Orticoni, M.-T.; De Luca, G.; Guigliarelli, B., and; Bruschi, M., Hydrogenases in sulfate-reducing bacteria function as chromium reductase. *Appl. Microbiol. Biotechnol.* **2003,** *63*, (3), 315-321.
(135) Abu Laban, N.; Selesi, D.; Jobelius, C.; Meckenstock, R. U., Anaerobic benzene degradation by Gram-positive sulfate-reducing bacteria. *FEMS Microbiol. Ecol.* **2009,** *68*, (3), 300-311.
(136) Musat, F.; Widdel, F., Anaerobic degradation of benzene by a marine sulfate‐reducing enrichment culture, and cell hybridization of the dominant phylotype. *Environ. Microbiol.* **2008,** *10*, (1), 10-19.
(137) Bergmann, F. D.; Selesi, D.; Meckenstock, R. U., Identification of new enzymes potentially involved in anaerobic naphthalene degradation by the sulfate-reducing enrichment culture N47. *Arch. Microbiol.* **2011,** *193*, (4), 241-250.
(138) Ramsay, J. A.; Li, H.; Brown, R.; Ramsay, B. A., Naphthalene and anthracene mineralization linked to oxygen, nitrate, Fe (III) and sulphate reduction in a mixed microbial population. *Biodegradation* **2003,** *14*, (5), 321-329.
(139) Kniemeyer, O.; Musat, F.; Sievert, S. M.; Knittel, K.; Wilkes, H.; Blumenberg, M.; Michaelis, W.; Classen, A.; Bolm, C.; Joye, S. B., Anaerobic oxidation of short-chain hydrocarbons by marine sulphate-reducing bacteria. *Nature* **2007,** *449*, (7164), 898-901.
(140) Bian, X.-Y.; Mbadinga, S. M.; Liu, Y.-F.; Yang, S.-Z.; Liu, J.-F.; Ye, R.-Q.; Gu, J.-D.; Mu, B.-Z., Insights into the anaerobic biodegradation pathway of n-alkanes in oil reservoirs by detection of signature metabolites. *Sci. Rep.* **2015,** *5*, 9801.
(141) Ulrich, A. C.; Edwards, E. A., Physiological and molecular characterization of anaerobic benzene‐degrading mixed cultures. *Environ. Microbiol.* **2003,** *5*, (2), 92-102.
(142) Safinowski, M.; Meckenstock, R. U., Methylation is the initial reaction in anaerobic naphthalene degradation by a sulfate‐reducing enrichment culture. *Environ. Microbiol.* **2006,** *8*, (2), 347-352.

(143) Badea, S.-L.; Vogt, C.; Weber, S.; Danet, A.-F.; Richnow, H.-H., Stable isotope fractionation of γ-hexachlorocyclohexane (lindane) during reductive dechlorination by two strains of sulfate-reducing bacteria. *Environ. Sci. Technol.* **2009,** *43*, (9), 3155-3161.
(144) Yoo, E.; Libra, J.; Wiesmann, U., Reduction of azo dyes by *Desulfovibrio desulfuricans*. *Water Sci. Technol.* **2000,** *41*, (12), 15-22.
(145) Hockin, S. L.; Gadd, G. M.; Barton, L.; Hamilton, W., Bioremediation of metals and metalloids by precipitation and cellular binding. In *Sulphate-reducing bacteria*, 2007; pp 405-434.
(146) Newman, D. K.; Kennedy, E. K.; Coates, J. D.; Ahmann, D.; Ellis, D. J.; Lovley, D. R.; Morel, F. M., Dissimilatory arsenate and sulfate reduction in *Desulfotomaculum auripigmentum* sp. nov. *Arch. Microbiol.* **1997,** *168*, (5), 380-388.
(147) Lovley, D. R.; Phillips, E., Reduction of uranium by *Desulfovibrio desulfuricans*. *Appl. Environ. Microbiol.* **1992,** *58*, (3), 850-856.
(148) Wang, Y.-T.; Shen, H., Modelling Cr (VI) reduction by pure bacterial cultures. *Water Res.* **1997,** *31*, (4), 727-732.
(149) Lovley, D. R.; Phillips, E. J., Reduction of chromate by *Desulfovibrio vulgaris* and its c3 cytochrome. *Appl. Environ. Microbiol.* **1994,** *60*, (2), 726-728.
(150) Huang, S.; Jaffé, P. R., Characterization of incubation experiments and development of an enrichment culture capable of ammonium oxidation under iron-reducing conditions. *Biogeosciences* **2015,** *12*, (3), 769-779.
(151) Bodor, A.; Bounedjoum, N.; Vincze, G. E.; Kis, Á. E.; Laczi, K.; Bende, G.; Szilágyi, Á.; Kovács, T.; Perei, K.; Rákhely, G., Challenges of unculturable bacteria: environmental perspectives. *Rev. Environ. Sci. Biotechnol.* **2020**, 1-22.
(152) Dorival-García, N.; Zafra-Gómez, A.; Navalón, A.; González-López, J.; Hontoria, E.; Vílchez, J., Removal and degradation characteristics of quinolone antibiotics in laboratory-scale activated sludge reactors under aerobic, nitrifying and anoxic conditions. *J. Environ. Manage.* **2013,** *120*, 75-83.
(153) Ding, C.; Enyi, F. O.; Adrian, L., Anaerobic ammonium oxidation (anammox) with planktonic cells in a redox-stable semicontinuous stirred-tank reactor. *Environ. Sci. Technol.* **2018,** *52*, (10), 5671-5681.
(154) Chamchoi, N.; Nitisoravut, S., Anammox enrichment from different conventional sludges. *Chemosphere* **2007,** *66*, (11), 2225-2232.
(155) Tracy, B. P.; Gaida, S. M.; Papoutsakis, E. T., Flow cytometry for bacteria: enabling metabolic engineering, synthetic biology and the elucidation of complex phenotypes. *Curr. Opin. Biotechnol.* **2010,** *21*, (1), 85-99.
(156) Fantner, G. E.; Barbero, R. J.; Gray, D. S.; Belcher, A. M., Kinetics of antimicrobial peptide activity measured on individual bacterial cells using high-speed atomic force microscopy. *Nat. Nanotechnol.* **2010,** *5*, (4), 280-285.
(157) Eyice, Ö.; Namura, M.; Chen, Y.; Mead, A.; Samavedam, S.; Schäfer, H., SIP metagenomics identifies uncultivated *Methylophilaceae* as dimethylsulphide degrading bacteria in soil and lake sediment. *ISME J.* **2015,** *9*, 2336-2348.
(158) Jehmlich, N.; Schmidt, F.; von Bergen, M.; Richnow, H.-H.; Vogt, C., Protein-based stable isotope probing (Protein-SIP) reveals active species within anoxic mixed cultures. *ISME J.* **2008,** *2*, (11), 1122-1133.
(159) Neufeld, J. D.; Vohra, J.; Dumont, M. G.; Lueders, T.; Manefield, M.; Friedrich, M. W.; Murrell, J. C., DNA stable-isotope probing. *Nat. Protocols* **2007,** *2*, (4), 860-866.
(160) Manefield, M.; Whiteley, A. S.; Griffiths, R. I.; Bailey, M. J., RNA stable isotope probing, a novel means of linking microbial community function to phylogeny. *Appl. Environ. Microbiol.* **2002,** *68*, (11), 5367-5373.

(161) Adrian, L.; Marco-Urrea, E., Isotopes in geobiochemistry: tracing metabolic pathways in microorganisms of environmental relevance with stable isotopes. *Curr. Opin. Biotechnol.* **2016,** *41*, 19-25.
(162) Jehmlich, N.; Vogt, C.; Lünsmann, V.; Richnow, H. H.; von Bergen, M., Protein-SIP in environmental studies. *Curr. Opin. Biotechnol.* **2016,** *41*, 26-33.
(163) Coplen, T. B., Guidelines and recommended terms for expression of stable-isotope-ratio and gas-ratio measurement results. *Rapid Commun. Mass Spectrom.* **2011,** *25*, (17), 2538-2560.
(164) Sachsenberg, T.; Herbst, F.-A.; Taubert, M.; Kermer, R.; Jehmlich, N.; von Bergen, M.; Seifert, J.; Kohlbacher, O., MetaProSIP: automated inference of stable isotope incorporation rates in proteins for functional metaproteomics. *J. Proteome Res.* **2014,** *14*, (2), 619-627.
(165) Grob, C.; Taubert, M.; Howat, A. M.; Burns, O. J.; Dixon, J. L.; Richnow, H. H.; Jehmlich, N.; von Bergen, M.; Chen, Y.; Murrell, J. C., Combining metagenomics with metaproteomics and stable isotope probing reveals metabolic pathways used by a naturally occurring marine methylotroph. *Environ. Microbiol.* **2015,** *17*, (10), 4007-4018.
(166) Marco-Urrea, E.; Seifert, J.; Von Bergen, M.; Adrian, L., Stable isotope peptide mass spectrometry to decipher amino acid metabolism in *Dehalococcoides* strain CBDB1. *J. Bacteriol.* **2012,** *194*, (16), 4169-4177.
(167) Von Bergen, M.; Jehmlich, N.; Taubert, M.; Vogt, C.; Bastida, F.; Herbst, F.-A.; Schmidt, F.; Richnow, H.-H.; Seifert, J., Insights from quantitative metaproteomics and protein-stable isotope probing into microbial ecology. *ISME J.* **2013,** *7*, (10), 1877.
(168) Hettich, R. L.; Pan, C.; Chourey, K.; Giannone, R. J., Metaproteomics: harnessing the power of high performance mass spectrometry to identify the suite of proteins that control metabolic activities in microbial communities. *Anal. Chem* **2013,** *9*, 4203-4214.
(169) Kublik, A.; Deobald, D.; Hartwig, S.; Schiffmann, C. L.; Andrades, A.; Bergen, M.; Sawers, R. G.; Adrian, L., Identification of a multi‐protein reductive dehalogenase complex in Dehalococcoides mccartyi strain CBDB1 suggests a protein‐dependent respiratory electron transport chain obviating quinone involvement. *Environ. Microbiol.* **2016,** *18*, (9), 3044-3056.
(170) Hartzog, P. E.; Sladek, M.; Kelly, J. J.; Larkin, D. J., Bottle effects alter taxonomic composition of wetland soil bacterial communities during the denitrification enzyme activity assay. *Soil Biol. Biochem.* **2017,** *110*, 87-94.
(171) Hunkeler, D.; Meckenstock, R. U.; Sherwood Lollar, B.; Schmidt, T. C.; Wilson, J.; Schmidt, T.; Wilson, J., A guide for assessing biodegradation and source identification of organic ground water contaminants using compound specific isotope analysis (CSIA). In US EPA: Oklahoma, USA,, 2008.
(172) Liu, Y.; Wu, L.; Kohli, P.; Kumar, R.; Stryhanyuk, H.; Nijenhuis, I.; Lal, R.; Richnow, H.-H., Enantiomer and carbon isotope fractionation of α-hexachlorocyclohexane by Sphingobium indicum strain B90A and the corresponding enzymes. *Environ. Sci. Technol.* **2019,** *53*, (15), 8715-8724.
(173) Vogt, C.; Cyrus, E.; Herklotz, I.; Schlosser, D.; Bahr, A.; Herrmann, S.; Richnow, H.-H.; Fischer, A., Evaluation of toluene degradation pathways by two-dimensional stable isotope fractionation. *Environ. Sci. Technol.* **2008,** *42*, (21), 7793-7800.
(174) Kümmel, S.; Starke, R.; Chen, G.; Musat, F.; Richnow, H. H.; Vogt, C., Hydrogen isotope fractionation as a tool to identify aerobic and anaerobic PAH biodegradation. *Environ. Sci. Technol.* **2016,** *50*, (6), 3091-3100.
(175) Griebler, C.; Adrian, L.; Meckenstock, R.; Richnow, H., Stable carbon isotope fractionation during aerobic and anaerobic transformation of trichlorobenzene. *FEMS Microbiol. Ecol.* **2004,** *48*, (3), 313-321.
(176) Chevallier, M. L.; Cooper, M.; Kümmel, S.; Barbance, A.; Le Paslier, D.; Richnow, H. H.; Saaidi, P.-L.; Adrian, L., Distinct carbon isotope fractionation signatures during biotic and

abiotic reductive transformation of chlordecone. *Environ. Sci. Technol.* **2018,** *52*, (6), 3615-3624.
(177) Knossow, N.; Siebner, H.; Bernstein, A., Isotope Fractionation (δ13C, δ15N) in the Microbial Degradation of Bromoxynil by Aerobic and Anaerobic Soil Enrichment Cultures. *J. Agric. Food. Chem.* **2020,** *68*, (6), 1546-1554.
(178) Zwank, L.; Berg, M.; Elsner, M.; Schmidt, T. C.; Schwarzenbach, R. P.; Haderlein, S. B., New evaluation scheme for two-dimensional isotope analysis to decipher biodegradation processes: Application to groundwater contamination by MTBE. *Environ. Sci. Technol.* **2005,** *39*, (4), 1018-1029.
(179) Thullner, M.; Fischer, A.; Richnow, H.-H.; Wick, L. Y., Influence of mass transfer on stable isotope fractionation. *Appl. Microbiol. Biotechnol.* **2013,** *97*, (2), 441-452.
(180) Renpenning, J.; Rapp, I.; Nijenhuis, I., Substrate hydrophobicity and cell composition influence the extent of rate limitation and masking of isotope fractionation during microbial reductive dehalogenation of chlorinated ethenes. *Environ. Sci. Technol.* **2015,** *49*, (7), 4293-4301.
(181) Vogt, C.; Dorer, C.; Musat, F.; Richnow, H.-H., Multi-element isotope fractionation concepts to characterize the biodegradation of hydrocarbons—from enzymes to the environment. *Curr. Opin. Biotechnol.* **2016,** *41*, 90-98.
(182) Kuder, T.; Wilson, J. T.; Kaiser, P.; Kolhatkar, R.; Philp, P.; Allen, J., Enrichment of stable carbon and hydrogen isotopes during anaerobic biodegradation of MTBE: microcosm and field evidence. *Environ. Sci. Technol.* **2005,** *39*, (1), 213-220.
(183) Kujawinski, D. M.; Zhang, L.; Schmidt, T. C.; Jochmann, M. A., When other separation techniques fail: compound-specific carbon isotope ratio analysis of sulfonamide containing pharmaceuticals by high-temperature-liquid chromatography-isotope ratio mass spectrometry. *Anal. Chem.* **2012,** *84*, (18), 7656-7663.
(184) Liu, L.; Liu, Y.-h.; Wang, Z.; Liu, C.-x.; Huang, X.; Zhu, G.-f., Behavior of tetracycline and sulfamethazine with corresponding resistance genes from swine wastewater in pilot-scale constructed wetlands. *J. Hazard. Mater.* **2014,** *278*, 304-310.
(185) Marco-Urrea, E.; Nijenhuis, I.; Adrian, L., Transformation and carbon isotope fractionation of tetra-and trichloroethene to trans-dichloroethene by *Dehalococcoides* sp. strain CBDB1. *Environ. Sci. Technol.* **2011,** *45*, (4), 1555-1562.
(186) Widdel, F. Anaerober Abbau yon Fettsäuren und Benzoesäure durch neu isolierte Arten Sulfat-reduzierender Bakterien. 1980.
(187) Krsek, M.; Wellington, E., Comparison of different methods for the isolation and purification of total community DNA from soil. *J. Microbiol. Methods* **1999,** *39*, (1), 1-16.
(188) Fierer, N.; Hamady, M.; Lauber, C. L.; Knight, R., The influence of sex, handedness, and washing on the diversity of hand surface bacteria. *Proc. Natl. Acad. Sci. USA* **2008,** *105*, (46), 17994-17999.
(189) Caporaso, J. G.; Kuczynski, J.; Stombaugh, J.; Bittinger, K.; Bushman, F. D.; Costello, E. K.; Fierer, N.; Peña, A. G.; Goodrich, J. K.; Gordon, J. I., QIIME allows analysis of high-throughput community sequencing data. *Nat. Methods* **2010,** *7*, (5), 335-336.
(190) Meyer, F.; Paarmann, D.; D'Souza, M.; Olson, R.; Glass, E. M.; Kubal, M.; Paczian, T.; Rodriguez, A.; Stevens, R.; Wilke, A., The metagenomics RAST server–a public resource for the automatic phylogenetic and functional analysis of metagenomes. *BMC Bioinf.* **2008,** *9*, (1), 386-393.
(191) Renpenning, J.; Kümmel, S.; Hitzfeld, K. L.; Schimmelmann, A.; Gehre, M., Compound-specific hydrogen isotope analysis of heteroatom-bearing compounds via gas chromatography–chromium-based high-temperature conversion (Cr/HTC)–isotope ratio mass spectrometry. *Anal. Chem.* **2015,** *87*, (18), 9443-9450.

(192) Gilevska, T.; Gehre, M.; Richnow, H. H., Multidimensional isotope analysis of carbon, hydrogen and oxygen as tool for identification of the origin of ibuprofen. *Journal of pharmaceutical and biomedical analysis* **2015,** *115*, 410-417.
(193) Elsner, M.; Zwank, L.; Hunkeler, D.; Schwarzenbach, R. P., A new concept linking observable stable isotope fractionation to transformation pathways of organic pollutants. *Environ. Sci. Technol.* **2005,** *39*, (18), 6896-6916.
(194) Cord-Ruwisch, R., A quick method for the determination of dissolved and precipitated sulfides in cultures of sulfate-reducing bacteria. *J. Microbiol. Methods* **1985,** *4*, (1), 33-36.
(195) Zhu, Y.-G.; Zhao, Y.; Li, B.; Huang, C.-L.; Zhang, S.-Y.; Yu, S.; Chen, Y.-S.; Zhang, T.; Gillings, M. R.; Su, J.-Q., Continental-scale pollution of estuaries with antibiotic resistance genes. *Nat. Microbiol.* **2017,** *2*, 16270.
(196) Marco-Urrea, E.; Paul, S.; Khodaverdi, V.; Seifert, J.; von Bergen, M.; Kretzschmar, U.; Adrian, L., Identification and characterization of a *Re*-citrate synthase in *Dehalococcoides* strain CBDB1. *J. Bacteriol.* **2011,** *193*, (19), 5171-5178.
(197) Karcı, A.; Balcıoğlu, I. A., Investigation of the tetracycline, sulfonamide, and fluoroquinolone antimicrobial compounds in animal manure and agricultural soils in Turkey. *Sci. Total Environ.* **2009,** *407*, (16), 4652-4664.
(198) Andrews, J. M., Determination of minimum inhibitory concentrations. *J. Antimicrob. Chemotherapy* **2001,** *48*, 5-16.
(199) Jones, R. C.; Chatterley, A.; Marty, R.; Owton, W. M.; Elsegood, M. R., Isoxazole to oxazole: a mild and unexpected transformation. *Chem. Commun.* **2015,** *51*, (6), 1112-1115.
(200) L'abbé, G., Molecular rearrangements of five-membered ring heteromonocycles. *J. Heterocyclic. Chem.* **1984,** *21*, (3), 627-638.
(201) Klagkou, K.; Pullen, F.; Harrison, M.; Organ, A.; Firth, A.; Langley, G. J., Fragmentation pathways of sulphonamides under electrospray tandem mass spectrometric conditions. *Rapid Commun. Mass Spectrom.* **2003,** *17*, (21), 2373-2379.
(202) Neill, G. P.; Davies, N. W.; McLean, S., Automated screening procedure using gas chromatography—mass spectrometry for identification of drugs after their extraction from biological samples. *J. Chromatogr. B Biomed. Sci. Appl.* **1991,** *565*, (1-2), 207-224.
(203) Ouyang, W.-Y.; Birkigt, J.; Richnow, H. H.; Adrian, L., Anaerobic Transformation and Detoxification of Sulfamethoxazole by Sulfate-Reducing Enrichments and *Desulfovibrio vulgaris*. *Environ. Sci. Technol.* **2021,** *55*, (1), 271-282.
(204) Liu, H.; Wang, H.; Wang, G., *Intrasporangium chromatireducens* sp. nov., a chromate-reducing *Actinobacterium* isolated from manganese mining soil, and emended description of the genus *Intrasporangium*. *Int J Syst Evol Microbiol.* **2012,** *62*, (2), 403-408.
(205) Alvarez, A.; Saez, J. M.; Costa, J. S. D.; Colin, V. L.; Fuentes, M. S.; Cuozzo, S. A.; Benimeli, C. S.; Polti, M. A.; Amoroso, M. J., *Actinobacteria*: Current research and perspectives for bioremediation of pesticides and heavy metals. *Chemosphere* **2017,** *166*, 41-62.
(206) Kitagawa, W.; Tamura, T., Three types of antibiotics produced from *Rhodococcus erythropolis* strains. *Microbes Environ.* **2008,** *23*, (2), 167-171.
(207) Iwatsuki, M.; Uchida, R.; Takakusagi, Y.; Matsumoto, A.; Jiang, C.-L.; Takahashi, Y.; Arai, M.; Kobayashi, S.; Matsumoto, M.; Inokoshi, J., Lariatins, novel anti-mycobacterial peptides with a lasso structure, produced by *Rhodococcus jostii* K01-B0171. *J. Antibiot.* **2007,** *60*, (6), 357.
(208) Baltz, R. H., Antimicrobials from *Actinomycetes*: back to the future. *Microbe* **2007,** *2*, (3), 125.
(209) Thompson, C.; Ward, J.; Hopwood, D., DNA cloning in *Streptomyces*: resistance genes from antibiotic-producing species. *Nature* **1980,** *286*, (5772), 525.

(210) Andersen, S. J.; Quan, S.; Gowan, B.; Dabbs, E. R., Monooxygenase-like sequence of a *Rhodococcus equi* gene conferring increased resistance to rifampin by inactivating this antibiotic. *Antimicrob. Agents Chemother.* **1997,** *41*, (1), 218-221.
(211) McLeod, M. P.; Warren, R. L.; Hsiao, W. W.; Araki, N.; Myhre, M.; Fernandes, C.; Miyazawa, D.; Wong, W.; Lillquist, A. L.; Wang, D., The complete genome of *Rhodococcus* sp. RHA1 provides insights into a catabolic powerhouse. *Proc. Natl. Acad. Sci. USA* **2006,** *103*, (42), 15582-15587.
(212) Taubert, M.; Vogt, C.; Wubet, T.; Kleinsteuber, S.; Tarkka, M. T.; Harms, H.; Buscot, F.; Richnow, H.-H.; Von Bergen, M.; Seifert, J., Protein-SIP enables time-resolved analysis of the carbon flux in a sulfate-reducing, benzene-degrading microbial consortium. *ISME J.* **2012,** *6*, (12), 2291-2301.
(213) Herbst, F. A.; Bahr, A.; Duarte, M.; Pieper, D. H.; Richnow, H. H.; Bergen, M.; Seifert, J.; Bombach, P., Elucidation of in situ polycyclic aromatic hydrocarbon degradation by functional metaproteomics (protein-SIP). *Proteomics* **2013,** *13*, (18-19), 2910-2920.
(214) Crofts, T. S.; Wang, B.; Spivak, A.; Gianoulis, T. A.; Forsberg, K. J.; Gibson, M. K.; Johnsky, L. A.; Broomall, S. M.; Rosenzweig, C. N.; Skowronski, E. W., Shared strategies for β-lactam catabolism in the soil microbiome. *Nat. Chem. Biol.* **2018,** *14*, (6), 556.
(215) Hungate, B. A.; Mau, R. L.; Schwartz, E.; Caporaso, J. G.; Dijkstra, P.; van Gestel, N.; Koch, B. J.; Liu, C. M.; McHugh, T. A.; Marks, J. C., Quantitative microbial ecology through stable isotope probing. *Appl. Environ. Microbiol.* **2015,** *81*, (21), 7570-7581.
(216) Dumont, M. G.; Murrell, J. C., Stable isotope probing—linking microbial identity to function. *Nat. Rev. Microbiol.* **2005,** *3*, (6), 499.
(217) Jones, M. D.; Crandell, D. W.; Singleton, D. R.; Aitken, M. D., Stable-isotope probing of the polycyclic aromatic hydrocarbon-degrading bacterial guild in a contaminated soil. *Environ. Microbiol.* **2011,** *13*, (10), 2623-2632.
(218) Albuquerque, L.; França, L.; Rainey, F. A.; Schumann, P.; Nobre, M. F.; da Costa, M. S., *Gaiella occulta* gen. nov., sp. nov., a novel representative of a deep branching phylogenetic lineage within the class *Actinobacteria* and proposal of *Gaiellaceae* fam. nov. and *Gaiellales* ord. nov. *Syst. Appl. Microbiol.* **2011,** *34*, (8), 595-599.
(219) Grünanger, P.; Vita-Finzi, P., *Isoxazoles*. John Wiley & Sons: 2009; Vol. 168.
(220) Xu, W.; Zhang, G.; Li, X.; Zou, S.; Li, P.; Hu, Z.; Li, J., Occurrence and elimination of antibiotics at four sewage treatment plants in the Pearl River Delta (PRD), South China. *Water Res.* **2007,** *41*, (19), 4526-4534.
(221) Kumar, S.; Pandey, A. K., Chemistry and biological activities of flavonoids: an overview. *Sci. World J.* **2013,** *2013*.
(222) Gallemi, C. F.; Arnal, C. L.; Serrat, A. F.; Ruiz, J. C.; Bono, I. M.; Lopez, D. B.; Roca, C. S.; Mesa, N. T.; Garcia, A. F. Substituted isoxazoles and their use as antibiotics. 2005.
(223) Achari, A.; Somers, D. O.; Champness, J. N.; Bryant, P. K.; Rosemond, J.; Stammers, D. K., Crystal structure of the anti-bacterial sulfonamide drug target dihydropteroate synthase. *Nat. Struct. Biol.* **1997,** *4*, (6), 490-497.
(224) Wood Jr, W. B., Studies on the antibacterial action of the sulfonamide drugs: the relation of p-aminobenzoic acid to the mechanism of bacteriostasis. *J. Exp. Med.* **1942,** *75*, (4), 369.
(225) Esnault, G.; Caumette, P.; Garcia, J.-L., Characterization of Desulfovibrio giganteus sp. nov., a sulfate-reducing bacterium isolated from a brackish coastal lagoon. *Syst. Appl. Microbiol.* **1988,** *10*, (2), 147-151.
(226) Pereira, I. A.; Romão, C. V.; Xavier, A. V.; LeGall, J.; Teixeira, M., Electron transfer between hydrogenases and mono-and multiheme cytochromes in *Desulfovibrio* ssp. *J. Biol. Inorg. Chem.* **1998,** *3*, (5), 494-498.

(227) Pereira, P. M.; Teixeira, M.; Xavier, A. V.; Louro, R. O.; Pereira, I. A., The Tmc complex from *Desulfovibrio vulgaris* Hildenborough is involved in transmembrane electron transfer from periplasmic hydrogen oxidation. *Biochemistry* **2006,** *45*, (34), 10359-10367.
(228) Pagán, R.; Mackey, B., Relationship between membrane damage and cell death in pressure-treated *Escherichia coli* cells: differences between exponential-and stationary-phase cells and variation among strains. *Appl. Environ. Microbiol.* **2000,** *66*, (7), 2829-2834.
(229) Ricken, B.; Fellmann, O.; Kohler, H. P.; Schaffer, A.; Corvini, P. F.; Kolvenbach, B. A., Degradation of sulfonamide antibiotics by Microbacterium sp. strain BR1 - elucidating the downstream pathway. *N. Biotechnol.* **2015,** *32*, (6), 710-5.
(230) Aelion, C. M.; Höhener, P.; Hunkeler, D.; Aravena, R., *Environmental isotopes in biodegradation and bioremediation*. CRC Press: 2009.
(231) Fischer, A.; Herklotz, I.; Herrmann, S.; Thullner, M.; Weelink, S. A.; Stams, A. J.; Schlömann, M.; Richnow, H.-H.; Vogt, C., Combined carbon and hydrogen isotope fractionation investigations for elucidating benzene biodegradation pathways. *Environ. Sci. Technol.* **2008,** *42*, (12), 4356-4363.
(232) Morasch, B.; Richnow, H. H.; Vieth, A.; Schink, B.; Meckenstock, R. U., Stable isotope fractionation caused by glycyl radical enzymes during bacterial degradation of aromatic compounds. *Appl. Environ. Microbiol.* **2004,** *70*, (5), 2935-2940.
(233) DelMonte, A. J.; Haller, J.; Houk, K.; Sharpless, K. B.; Singleton, D. A.; Strassner, T.; Thomas, A. A., Experimental and theoretical kinetic isotope effects for asymmetric dihydroxylation. Evidence supporting a rate-limiting "(3+ 2)" cycloaddition. *J. Am. Chem. Soc.* **1997,** *119*, (41), 9907-9908.
(234) Lodhi, A. F.; Zhang, Y.; Adil, M.; Deng, Y., A novel culturing chip (cChip) can facilitate culturing of unculturable bacteria from aquatic environment. **2020**.DOI: 10.21203/rs.3.rs-91678/v1